RMZ – MATERIALS AND GEOENVIRONMENT

PERIODICAL FOR MINING, METALLURGY AND GEOLOGY

RMZ – MATERIALI IN GEOOKOLJE

REVIJA ZA RUDARSTVO, METALURGIJO IN GEOLOGIJO

Historical Rewiev

More than 80 years have passed since in 1919 the University Ljubljana in Slovenia was founded. Technical fields were joint in the School of Engineering that included the Geologic and Mining Division while the Metallurgy Division was established in 1939 only. Today the Departments of Geology, Mining and Geotechnology, Materials and Metallurgy are part of the Faculty of Natural Sciences and Engineering, University of Ljubljana.

Before War II the members of the Mining Section together with the Association of Yugoslav Mining and Metallurgy Engineers began to publish the summaries of their research and studies in their technical periodical Rudarski zbornik (Mining Proceedings). Three volumes of Rudarski zbornik (1937, 1938 and 1939) were published. The War interrupted the publication and not untill 1952 the first number of the new journal Rudarsko-metalurški zbornik - RMZ (Mining and Metallurgy Quarterly) has been published by the Division of Mining and Metallurgy, University of Ljubljana. Later the journal has been regularly published quarterly by the Departments of Geology, Mining and Geotechnology, Materials and Metallurgy, and the Institute for Mining, Geotechnology and Environment.

On the meeting of the Advisory and the Editorial Board on May 22nd 1998 Rudarsko-metalurški zbornik has been renamed into "RMZ - Materials and Geoenvironment (RMZ -Materiali in Geookolje)" or shortly RMZ - M&G.

RMZ - M&G is managed by an international advisory and editorial board and is exchanged with other world-known periodicals. All the papers are reviewed by the corresponding professionals and experts.

RMZ - M&G is the only scientific and professional periodical in Slovenia, which is published in the same form nearly 50 years. It incorporates the scientific and professional topics in geology, mining, and geotechnology, in materials and in metallurgy.

The wide range of topics inside the geosciences are wellcome to be published in the RMZ -Materials and Geoenvironment. Research results in geology, hydrogeology, mining, geotechnology, materials, metallurgy, natural and antropogenic pollution of environment, biogeochemistry are proposed fields of work which the journal will handle. RMZ - M&G is co-issued and co-financed by the Faculty of Natural Sciences and Engineering Ljubljana, and the Institute for Mining, Geotechnology and Environment Ljubljana. In addition it is financially supported also by the Ministry of Higher Education, Science and Technology of Republic of Slovenia.

<div align="right">Editor in chief</div>

Table of Contents – Kazalo

Quasicrystal-strengthened cast Al-alloys

Aluminijeve livne zlitine, utrjene s kvazikristali

Franc Zupanič[1, *], Tonica Bončina[1], Niko Rozman[1], Boštjan Markoli[2]

[1]University of Maribor, Faculty of Mechanical Engineering, Smetanova 17, SI-2000 Maribor, Slovenia, franc.zupanic@uni-mb.si
[2]University of Ljubljana, Faculty of Natural Sciences and Engineering, Aškerčeva cesta 12, SI-1000, Ljubljana, Slovenia

*Corresponding author. E-mail: franc.zupanic@uni-mb.si

Abstract: Modern engineering materials must be able to carry high load and simultaneously possess high reliability. Among convenient materials, aluminium alloys still play an important role, in spite of the rapid development of lighter magnesium alloys and different types of composites. In Al-Si casting alloys alloyed with different additions (e.g. AlSi12CuNiMg) tensile strengths up to 400 MPa can be attained, and the elongations around 5 %. In order to increase strength, dislocation mobility should be impeded or hindered. The effect of microstructure on fracture toughness is rather complex. Nonetheless, by the presence of only coherent precipitates strain localization can occur leading to rather low ductility and fracture toughness. Therefore, the presence of incoherent precipitates is desirable. Larger particles of secondary phases often impart ductility and toughness, especially when they grow in the form of needles and/or plates. They can serve as crack nucleation sites, and when they fracture, also as crack propagation paths.

The increase in strength normally results in decrease of ductility and toughness. A lot of work had been and still is directed to obtain appropriate combination of strength and ductility for particular application. This is possible by obtaining a hierarchical microstructure consisting of constituents of different sizes to produce various types of strengthening, but also to make the propagation of cracks more difficult. It was found that quasicrystals possess the ability

Original scientific paper

to strengthen an aluminium matrix, and make more difficult crack formation and growth. Recently, some Al-alloys were found to have rather high quasicrystalline forming ability. This means that the icosahedral quasicrystalline phase (i-phase) can form during rather slow cooling, at cooling rates typical for solidification in metallic dies (cooling rates are estimated to be between 100 K/s and 1000 K/s). In some alloys, almost ideal two-phase microstructure consisting of α-Al and i-phase will form having convenient combination of strength and toughness. So in this contribution, some alloys of this type developed over the last few years will be presented.

Izvleček: Od sodobnih tehničnih materialov zahtevamo, da imajo veliko trdnost, hkrati pa morajo biti zanesljivi in varni. Med njimi imajo Al-zlitine še vedno velik pomen kljub hitremu razvoju še lažjih magnezijevih zlitin in različnih vrst kompozitnih materialov. V livnih zlitinah na osnovi Al-Si, ki vsebujejo različne zlitinske elemente (npr. AlSi12CuNiMg), se dosežejo natezne trdnosti do 400 MPa, medtem ko je razteznost le do 5-odstotna. Za povečanje trdnosti kovin je treba zmanjšati gibljivost dislokacij. Vpliv mikrostrukture na lomno žilavost je bolj zapleten. Ob navzočnosti koherentnih izločkov se lahko zmanjša žilavost zaradi lokalizacije deformacije, zato je navzočnost nekoherentnih izločkov koristna. Veliki delci sekundarnih faz (čisti elementi – Si, binarne spojine Al_3Fe ali kompleksne intermetalne faze) imajo negativen vpliv na žilavost in duktilnost, še posebej, če rastejo v obliki iglic ali ploščic. Na njih lahko nastanejo razpoke, lahko pa so tudi prednostna mesta za rast razpok.

Povečanje trdnosti je navadno povezano z zmanjšanjem žilavosti, zato je veliko raziskav usmerjenih k cilju, kako doseči primerno kombinacijo trdnosti in žilavosti za določeno aplikacijo. To je mogoče, če dosežemo mikrostrukturno hierarhijo, ki vsebuje mikrostrukturne sestavine različnih velikosti in lahko povzroči raznovrstno utrjanje, hkrati pa oteži napredovanje razpok. V zadnjem obdobju je bilo veliko raziskav namenjenih razvoju aluminijevih zlitin, utrjenih s kvazikristali. Za ikozaedrično kvazikristalno fazo (i-fazo) velja, da povzroči močno utrjanje aluminijeve osnove, hkrati pa oteži nastanek in napredovanje razpok. Šele pred kratkim so bile razvite zlitine, pri katerih nastane i-faza tudi pri sorazmerno počasnem ohlajanju, kot je npr. pri litju v kovinske kokile, kjer je hitrost

ohlajanja 100−1000 K s⁻¹. Znani so primeri, da imajo skoraj idealno dvofazno mikrostrukturo ter ustrezno razmerje trdnosti in žilavosti. V tem prispevku predstavljamo nekaj zlitin, ki so bile razvite v zadnjih letih.

Key words: aluminium, quasicrystal, strengthening, mechanical properties

Ključne besede: aluminij, kvazikristal, utrjanje, mehanske lastnosti

INTRODUCTION

Aluminium alloys belong to the most important engineering materials. They can find their application in the most demanding areas, such as automotive and aerospace industries. Al-alloys with properties tailored for particular requirements can be utilized for the most critical constructional elements. This was made possible by exploiting the highly sophisticated casting technologies, such as SOPHIA and the latest methods of die-casting.[1] The building of aeroplanes normally requires the highest possible strengths, whereas car building demands the highest values of elongations, that can be attained at the lowest costs.[2] Very frequently, the convenient combination of strength and elongation (or ductility) is required. This can be expressed by the alloy index Q:

$$Q = R_m + d \cdot \lg(a)$$

where R_m stands for tensile strength, A is elongation at fracture, and d is an empirical constant. [3]

Table 1. Basic data regarding high-strength Al-cast alloys [4]

alloy	numerical designation	condition	yield strength $R_{p0,2}$/MPa	tensile strength R_m/MPa	elongation A/%
AlSi12CuNiMg	48 000	die cast / T6	320–390	350–400	0,5–2,5
AlSi5Cu3Mg	45 100	die cast / T6	310–380	420–450	2–7
AlSi9Mg1		die cast / F	240–310	320–400	2–4
AlCu4TiMg	21 000	die cast / T6	260–380	360–440	3–18
AlCu4MgAgTi		die cast / T6	410–460	460–510	5–8
AlCu4Ti	21100	die cast / T6	310–400	420–475	7–16

Tensi and Högerl[2] have shown that the strengthening of Al-alloys based on the Al-Si system can be considered as a combination of several hardening mechanisms:

- solid-solution strengthening (alloying with elements soluble in Al, having rather different atomic sizes than Al)
- grain boundary strengthening caused by the decreasing grain size of the matrix that can be caused through grain refinement and controlling the casting parameters
- texture hardening obtained by directional solidification
- particle hardening
- large particles, e.g. Si-phase in the eutectic (modification, casting parameters)
- dispersion hardening (uniformly distributed incoherent particles)
- precipitation hardening (coherent particles, heat-treatment).

In metals and alloys, the mobility of dislocations should be hindered in order to achieve hardening. Consequently, the stress for transition from elastic to plastic deformation is increased. On the other hand, elongation (ductility) can be increased by preventing the formation and propagation of cracks.

The highest yield strength, R_{p02}, that can be obtained in Al-Si alloys is slightly below 400 MPa, whereas the limiting value for the tensile strength, R_m, is approximately 450 MPa. However, this strength levels cause decrease in elongation at fracture to only few percents. Table 1 indicates that the highest strengths can be obtained in precipitation-hardened alloys. Nevertheless, the properties of these alloys are strongly influenced by the inherent properties of silicon. Silicon is a semimetal; it is brittle, having low fracture toughness and hardness around 1000 HV. It can be expected that the replacement of silicon with a harder, but at the same time tougher phase, may provide alloys with both higher strength and toughness. Many of the intermetallic phases found in the Al-alloys possess similar or even higher hardness than that of silicon, but, unfortunately, their fracture toughness is even lower. In addition, they are prone to grow in the form of needles or plates, which makes the resistance of an alloy against the crack propagation even inferior.

There is a strong interest in the automotive and aerospace industries for the application of alloys having better combinations of strength and elongation than alloys currently in use. In this respect, activities are carried to improve the properties of existing alloys, as well as to develop completely new alloys, such as those strengthened by quasicrystals.

Measures for attaining the highest strengths

Limiting strengths of Al-alloys can be calculated based on the aluminium modulus of elasticity, $E = 70$ GPa, and shear modulus, $G = 26$ GPa. Thus, the theoretical shear strength τ_t could be $G/15 \approx 1700$ MPa. This is a stress, at which elastic-to-plastic transition would take place in aluminium in the absence of dislocations. The cohesive strength of materials, σ_t, is approximately $E/15$. This is theoretical rupture strength of a material in the absence of cracks and/or other defects causing local stress peaks. It is known, that the real strengths can only approach to this theoretical values. They can be achieved most likely when the sample sizes decrease to micro- or even in the nanoregion (e.g. in whiskers), but they cannot be expected in castings for e.g. aerospace and automotive industries.

In »Inoue Superliquid Glass Project«, lead by Prof. Inoue on Tohoku University, Sendai, Japan, a range of novel aluminium alloys containing quasicrystals was developed.[5] They reported that by using powder metallurgy methods (gas atomisation of melt, densification with warm extrusion or pressing) it was possible to attain a wide range of properties of aluminium alloys that cannot be achieved by conventional methods (Figure 1). They have developed several alloys with combined high-strength and ductility (Al-Mn-M, Al-Cr-M and Al-Cr-Mn-M where M

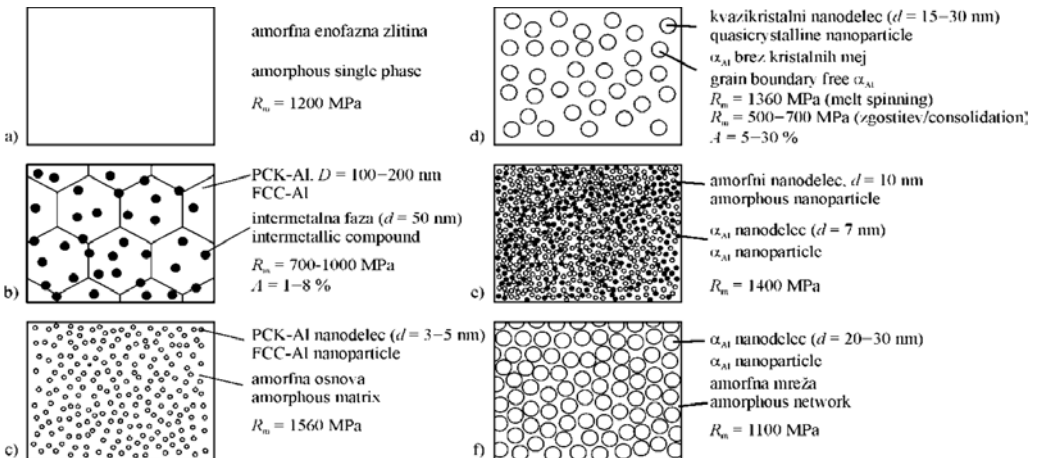**Figure 1.** Microstructures formed during rapid solidification of special Al-alloys developed be Inoue and Kimura.[5] Using conventional casting technologies one can obtain a microstructure shown in d), however the particles would be much coarser.

stands for one or several alloying elements: Cu, Ni, Fe, Ti or Zr). Chromium and manganese were responsible for the formation of icosahedral quasicrystals on rapid solidification, whilst other elements provided either solid solution or precipitation hardening (Cu). Among the above-mentioned alloys, the alloys arising from the Al-Mn-Cu system possessed comparable strength to commercial high-strength aluminium alloys (500–600 MPa), but with much better ductility (elongation >20 %). The appropriate microstructure, consisting of aluminium solid solution and nanoscale i-phase particles, was achieved in the smallest particles only (Figure 2d). In these alloys, the i-phase did not form during slower cooling.

So far, there is no information regarding the practical applications of these alloys. Perhaps oxide layers formed during powder processing prevented adequate sintering, and thus achieving of designed – theoretically accessible – properties.

Casting alloys strengthened by quasicrystals

In order to increase the strength the dislocation mobility should be impeded. This can be achieved through interaction with atoms (solid solution strengthening); the effect is proportional to the differences in atomic sizes between aluminium and alloying elements. The effect is limited because only a small number of elements (Cu, Mg and Zn) have a considerable solubility in aluminium. In some aluminium alloys (Al-Cu, Al-Zn, Al-Mg-Si) coherent precipitates form during natural or artificial aging causing considerable hardening. In alloys containing chromium and manganese, complex incoherent precipitates form after faster cooling and additional aging. They do not contribute much to the hardening, but they prevent grain growth and softening due to recrystallization. Larger secondary phases that are often present in Al-alloys do not cause considerable hardening; their effect on properties can be calculated by using a simple rule of mixtures. The effect of microstructure on fracture toughness, on the other hand, is rather complex. Nonetheless, the presence of only coherent precipitates can cause strain localization leading to rather low ductility and fracture toughness. Therefore, the presence of incoherent precipitates is desirable. Larger particles of secondary phases (pure elements – Si, binary compounds – Al_3Fe or complex intermetallic phases) often have an adverse effect on ductility and toughness, especially when they grow in the form of needles and plates. They can serve as crack nucleation sites, and when they fracture, as crack propagation paths.
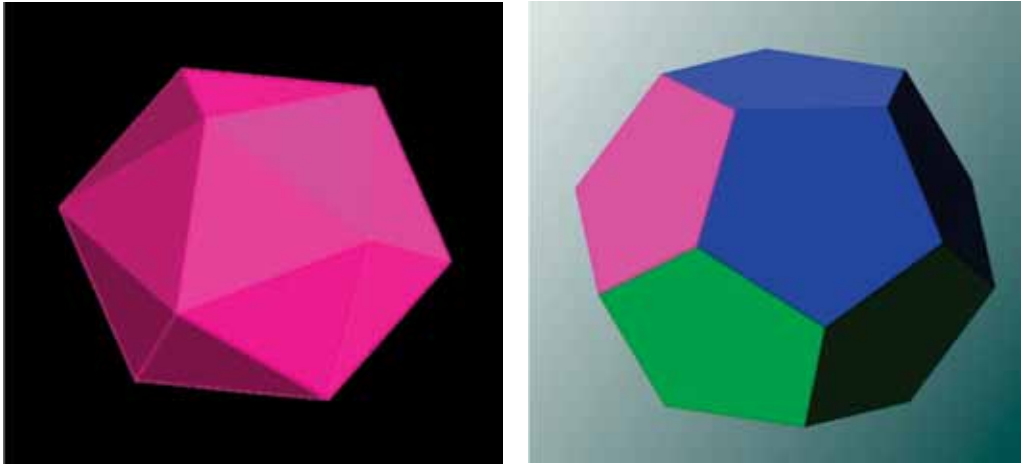
Figure 2. Possible shapes of quasicrystals with icosahedral symmetry:
a) icosahedron, b) pentagonal dodecahedron.

The increase in strength normally results in decrease of ductility and toughness. A lot of work is directed to obtain appropriate combination of strength and ductility for particular application. The idea is to obtain hierarchical microstructure consisting of microstructural constituents of different sizes to produce various types of strengthening, but also to make the propagation of cracks more difficult. It would be of the utmost importance for particles to form in-situ during solidification or solid-state reactions because the interface strength is much higher in this case.

Icosahedral quasicrystalline phase (i-phase) belongs to the quasiperiodic crystals that were first discovered at the beginning of nineteen eighties by Shechtman et al. in Al-Mn system.[6] This phase has an orientational long-range order, but it lacks periodicity. That was rather revolutionary discovery at the time because of strong belief that the solids can only have periodic crystalline or glassy (amorphous) structure. Also, quasicrystals possess some unusual mechanical, magnetic and electrical properties, e.g. strain softening because of quasiperiodicity.

This can be shown in an icosahedron (Figure 2a), which has very high symmetry. Namely, it possesses six five-fold, ten threefold and fifteen twofold rotational axes.[7] Therefore, it can attain several different orientations with other phases. It is even possible to attain epitaxy on almost all interfaces. Small mismatches can be adapted by dislocations.[8] On this ground, it is rather safely to state that i-phase represents almost ideal strengthening

phase for the Al-alloys. It was discovered that threefold directions present predominant growth directions, thus i-phase could in general grow in twenty different directions. During faceted growth, i-phase often adopts a shape of pentagonal dodecahedron (Figure 2b). It is of utmost importance that even during dendritic growth the spherical shape is attained, because of a strong tendency to equiaxed growth. In addition, this shape causes the smallest stress concentrations, thus making it more difficult for crack to form and grow.

In aluminium alloys stable and metastable icosahedral quasicrystal (i-phase) can be formed. The trouble with the stable i-phase is that it is not present in the equilibrium with α-Al phase (Al-rich solid solution, which is ductile and tough), which is the case in Mg-alloys from the system Mg-Zn-Y.[9] Contrary, the i-phase field of existence is surrounded by brittle intermetallic phases[10] (Figure 3a), making these materials inconvenient for structural applications. On the other hand metastable i-phase can be present in α-Al, however it can only be formed at higher cooling rates (during melt-spinning or melt atomization at cooling rates of 10^6 K/s) [6], because it is not a part of the equilibrium binary phase diagram (Figure 3b).[11]

Schurack et al.[12, 13] wanted to improve properties of aluminium alloys by applying strengthening with the quasicrystalline phases. Alloys were produced by melt spinning, mechanical alloying and conventional casting. They reported that mechanical alloying of stable AlCuFe-quasicrystals and aluminium powders did not give the required
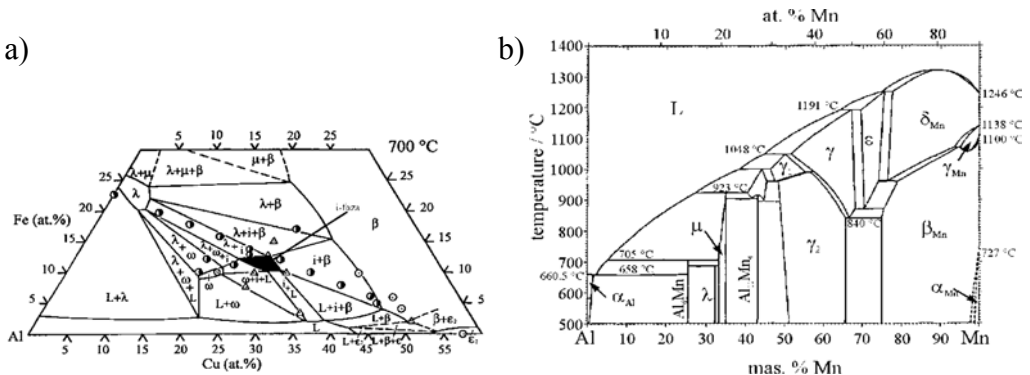

Figure 3. a) Isothermal section through the Al-Cu-Fe system at 700 °C. Near i-phase several intermetallic phases exist.[10] b) Phase diagram Al-Mn in Al-corner, where no i-phase region is. Thus, i-phase and other quasicrystalline phases can form by rapid solidification only.[11]

combination of strength and ductility. However, Ce-addition to Al-Mn-alloys improved the quasicrystalline forming ability, presumably due to stabilisation of the icosahedral structure in the melt. This allowed direct formation of icosahedral quasicrystals during continuous cooling of the melt. The milled and extruded melt-spun ribbons of the alloy $Al_{92}Mn_6Ce_2$ attained strength of approximately 800 MPa and elongation ≈25 %, but the conventionally cast rods had strength around 500 MPa and elongation ≈20 % only. It could be inferred that cerium represented an effective addition element to Al-Mn alloys, but it is unlikely, due it its high cost and reactivity to produce the Ce-containing alloys in an economic sound way.

Song et al.[14] found out that the addition of beryllium strongly reduced the critical cooling rate for the formation of quasicrystals and optimized the required Mn-content in Al-Mn alloys. They established that quasicrystals also formed using conventional casting methods, e.g. die-casting. However, in their alloys additional intermetallic phases (hexagonal approximants) were always present. Additional intermetallic phases besides i-phase were also discovered in other investigations (Table 2). Typical microstructures of alloy with several intermetallic phases and almost ideal two-phase (α-Al + i-phase) microstructure are shown in Figure 4.

Jun et al.[23] used »Mischmetal« instead of cerium. Mischmetal is much cheaper and commercially available. They attained almost two-phase microstructure α-Al + i-phase. Similar achievement was attained by Zupanic et al.[16] in a four-component Al-Mn-Be-Cu alloy (Figure 5a). Figure 5b shows microstructu-
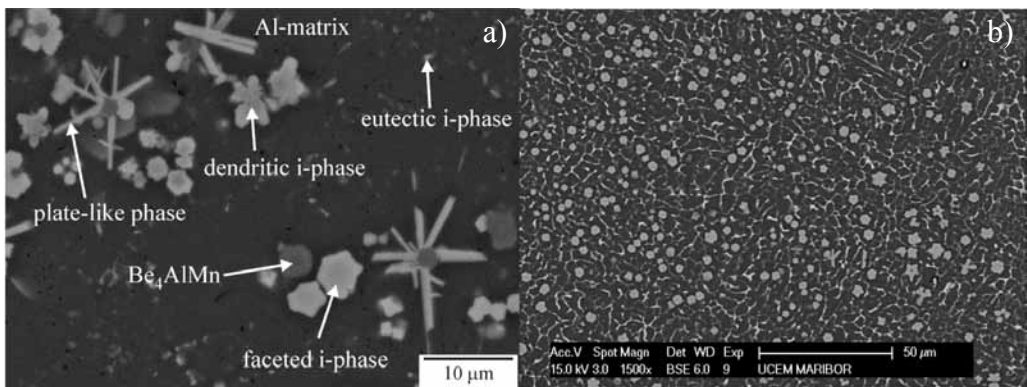

Figure 4. Microstructures of Al-alloys containing quasicrystalline phase: a) $Al_{84}Mn_5Be_{11}$ alloy[15] and b) $Al_{94}Mn_2Be_2Cu_2$ alloy[16]

Table 2. Phase composition of cast Al-alloys in which i-phase was observed

alloy	casting method	phase composition	reference
$Al_{91}Mn_7Fe_2$ $Al_{92}Mn_6Ce_2$ $Al_{80}Pd_{15}Mn_5$, $Al_{90}Pd_8Mn_2$	centrifugal casting	α-Al, i-phase, Al_6Mn $Al_{10}Mn_7Ce_2$, Al_6Mn, Al_4Ce, α-Al, i-phase α-Al, i-phase, Al_3Pd	[13]
$Al_{92}Fe_3Cr_2Mn_3$	wedge casting centrifugal casting	$Al_{75.7}Cr_{8.2}Mn_{8.4}Fe_{7.7}$ $Al_{75.7}Cr_{8.2}Mn_{8.4}Fe_{7.7}$ α-Al, Al_6Mn, $Al_{12}(Cr,Mn)$	[17]
$Al_{93}Fe_3Cr_2Ti_2$	suction casting	α-Al, Al_{13}(Fe, Cr), Al_3Ti, i-phase	[18]
$Al_{90}Mn_{2.5}Be_{7.5}$, $Al_{79.9}Mn_{13.5}Be_{6.6}$, $Al_{93}Mn_{2.5}Be_{4.5}$, $Al_{80}Mn_{13.5}Be_{6.5}$ $Al_{83}Mn_6Be_{11}$	conventional casting injection moulding cone shape die	α-Al, i-phase, hexagonal approximants	[14, 15, 19-21]
$Al_{79.9}Mn_{13}SiBe_6$	conventional casting	α-Al, i-phase, α-Al-Mn-Si 1/1 cubic approximant	[22]
$Al_{94}Mn_2Be_2Cu_2$	conventional casting	α-Al + i-phase	[16]
$Al_{92}Mn_6Mm_2$ $Al_{90}Mn_6Mm_4$ $Al_{88}Mn_6Mm_6$	conventional casting	α-Al + i-phase	[23]

Table 3. Possible aluminium alloys containing quasicrystals

alloying elements required for formation of i-phase	alloying elements reducing critical cooling rate	alloying element enabling precipitation hardening
Mn, Cr, (V)	Ce, Be, Si, Cu, Fe, B, Mm (Mischmetall)	Cu, Zn, (Si + Mg)

re after compressive test, when the logarithmic deformation was 0.7. No cracks can be observed near i-phase particles, whereas the hexagonal phase has fractured. Also at Al_2Cu-particles, micropores have formed that can represents initiation sites for formation of microcracks.

Figure 6 shows characteristic tensile diagrams of the alloys Al-Mn-Mm [23]. It can be seen that very high strength is achieved in the as-cast condition, and a rather high elongation is retained. Addition of 6 % Mn is too high, because the alloy became too brittle.
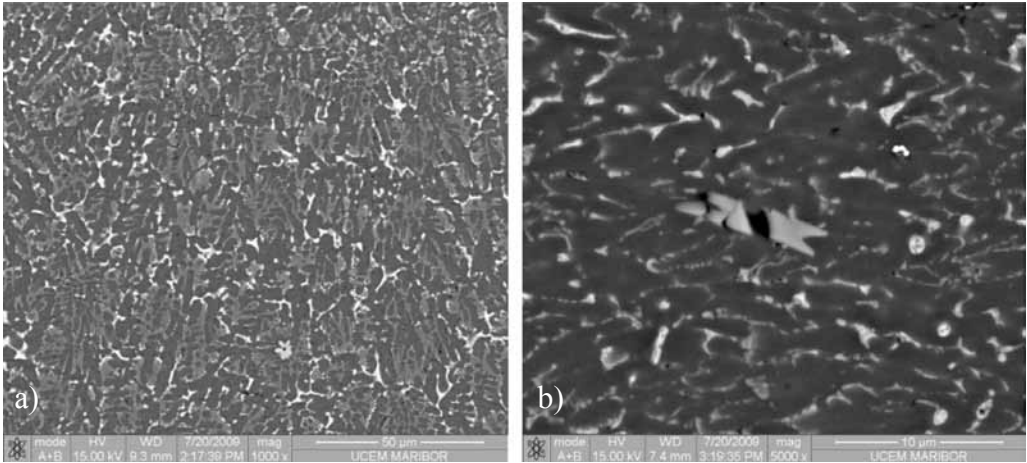
Figure 5. a) Microstructure of predominantly two-phase alloy i-phase + α-Al in the as-cast condition (mould diameter was 2 mm). i-phase has a shape of primary particles with a dendritic morphology, and it is present as a part of a binary eutectic (α-Al + i-phase). b) Microstructure after compressive test, logarithmic deformation was 0.7. No cracks can be observed near i-phase particles, whereas the hexagonal phase has fractured. At Al_2Cu-particles, micro-pores are formed that was found to form microcracks that can cause fracture.

Figure 6. Tensile diagrams of alloys based on the Al-Mn-Mn system [23]

Further perspectives of quasicrystal-strengthened Al-alloys

The main requirements for the quasicrystal-strengthened Al-alloys are:

- predominant two-phase microstructure consisting of α-Al + i--phase in the casting with higher wall thickness (the initial goal should be 10 mm)
- i-phase must be stable enough to survive required heat or thermomechanical treatment
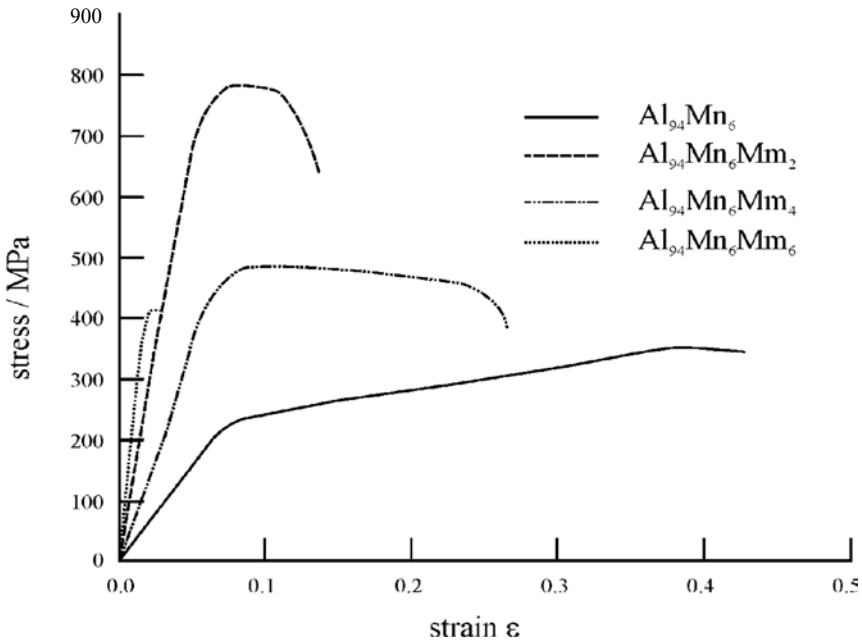- precipitation hardening is possible, in order to attain required combination of strength and elongation
- it is possible to attain microstructural hierarchy that allows several hardening mechanisms to be simultaneously active (using microstructural engineering)
- rupture strength should be higher than 400 MPa, and elongation at fracture larger than 10 %
- the liquidus temperature should be lower than 750 °C.

One of the main goals is the optimisation of chemical composition. The alloying elements can be divided according to their main effect (Table 3). It is necessary to take into account both positive and negative effects arising from interactions between different alloying elements. Most of them cannot be predicted because all of these alloys are or should be multicomponent. This means that fundamental researches will also be necessary, because not all ternary phase diagrams in question are available.

For further improvements, it is also necessary to stimulate development of new innovative casting technologies that will enable faster cooling rates. In this regard, it would be necessary to determine experimentally the critical cooling rates for the formation of the i-phase. By application of solidification simulations, it will then be possible to predict where in the casting will the required microstructure form itself.

Conclusions

According to the literature survey and our own experimental results, it could be stated that casting Al-alloys strengthened by quasicrystals possess a potential for becoming a new generation of alloys for special applications.

Nevertheless, for attaining this goal several obstacles should be overcome. Thus several fundamental investigations are required (determination of corresponding stable and metastable phase diagrams), as well as more applicative and development work (improvement of casting technologies, determination of critical cooling rates).

Acknowledgement

REFERENCES

[1] TIRYAKIOGLU, M., CAMPBELL, J., ALEXOPOULOS, N. D. (2009): Quality Indices for Aluminum Alloy Castings: A Critical Review. *Metall. Mater. Trans. B-Proc. Metall. Mater. Proc. Sci.*, Vol. 40, pp. 802–811.

[2] TENSI, H. M., HOGERL, J. (1994): Metallographic investigation of microstructure for quality assurance of alsi-castings. *Metall*, Vol. 48, pp. 776–781.

[3] Alexopoulos, N. D., Pantelakis, S. G. (2004): A new quality index for characterizing aluminum cast alloys with regard to aircraft structure design requirements. *Metall. Mater. Trans. A-Phys. Metall. Mater. Sci.*, Vol. 35A, pp. 301–308.

[4] Alurheinfelden [online]: last accessed: 19. 10. 2010, Dostopno na svetovnem spletu: http://www.alurheinfelden.com/web/guest/alloytoy.

[5] INOUE, A., KIMURA, H. (2001): Fabrication and mechanical properties of bulk amorphous, nanocrystalline, nanoquasicrystalline alloys and aluminium-based system. *J Light Metals*, Vol. 1, pp. 31–41.

[6] SHECHTMAN, D., BLECH, I., GRATIAS, D., CAHN, J. W. (1984): Metallic phase with long-range orientational order and no translational symmetry. *Physical Review Letters*, Vol. 53, pp. 1951–1953.

[7] CHATTOPADHYAY, K., RAVISHANKAR, N., GOSWAMI, R. (1997): Shapes of quasicrystals. *Progress in Crystal Growth and Characterization of Materials*, Vol. 34, pp. 237–249.

[8] SINGH, A., SOMEKAWA, H., TSAI, A. P. (2008): Interfaces made by tin with icosahedral phase matrix. *Scr. Mater.*, Vol. 59, pp. 699–702.

[9] YI, S., PARK, E. S., OK, J. B., KIM, W. T., KIM, D. H. (2001): (Icosahedral phase + alpha-Mg) two phase microstructures in the Mg-Zn-Y ternary system. *Mater. Sci. Eng. A-Struct. Mater. Prop. Microstruct. Process.*, Vol. 300, pp. 312–315.

[10] ZHANG, L. M., LUCK, R. (2003): Phase diagram of the Al-Cu-Fe quasicrystal-forming alloy system - III. Isothermal sections. *Z. Metallk.*, Vol. 94, pp. 108–115.

[11] MCALISTER, A., MURRAY, J. (1990): Al-Mn (Aluminum-Manganese), ASM International, (1990).

[12] SCHURACK, F., ECKERT, J., SCHULTZ, L. (2000): Quasicrystalline Al-alloys with high strength and good ductility. *Mater. Sci. Eng. A-Struct. Mater. Prop. Microstruct. Process.*, Vol. 294, pp. 164–167.

[13] SCHURACK, F., ECKERT, J., SCHULTZ, L. (2001): Synthesis and mechanical properties of cast quasicrystal-reinforced Al-alloys. *Acta Mater.*, Vol. 49, pp. 1351–1361.

[14] Song, G. S., Fleury, E., Kim, S. H., Kim, W. T., Kim, D. H. (2002): Enhancement of the quasicrystal-forming ability in Al-based alloys by Be-addition. *J. Alloy. Compd.*, Vol. 342, pp. 251–255.

[15] Boncina, T., Markoli, B., Zupanic, F. (2009): Characterization of cast Al86Mn3Be11 alloy. *J. Microsc.-Oxf.*, Vol. 233, pp. 364–371.

[16] Zupanic, F., Boncina, T., Rozman, N., Anzel, I., Grogger, W., Gspan, C., Hofer, F., Markoli, B. (2008): Development of an Al-Mn-Be-Cu alloy with improved quasicrystalline forming ability. *Z. Kristall.*, Vol. 223, pp. 735–738.

[17] Rios, C. T., Bolfarini, C., Botta, W. J., Kiminami, C. S. (2007): Rapidly solidified Al92Fe3Cr2Mn3 alloy. *Mater. Sci. Eng. A-Struct. Mater. Prop. Microstruct. Process.*, Vol. 449, pp. 1057–1061.

[18] Kim, K. B., Xu, W., Tomut, M., Stoica, M., Calin, M., Yi, S., Lee, W. H., Eckert, J. (2007): Formation of icosahedral phase in an Al-93Fe3Cr2Ti2 bulk alloy. *J. Alloy. Compd.*, Vol. 436, pp. L1–L4.

[19] Kim, S. H., Song, G. S., Fleury, E., Chattopadhyay, K., Kim, W. T., Kim, D. H. (2002): Icosahedral quasicrystalline and hexagonal approximant phases in the Al-Mn-Be alloy system. *Philosophical Magazine a-Physics of Condensed Matter Structure Defects and Mechanical Properties*, Vol. 82, pp. 1495–1508.

[20] Chang, H. J., Fleury, E., Song, G. S., Kim, W. T., Kim, D. H. (2004): Formation of quasicrystalline phases in Al-rich Al-Mn-Be alloys. *J. Non-Cryst. Solids*, Vol. 334, pp. 12–16.

[21] Song, G. S., Fleury, E., Kim, S. H., Kim, W. T., Kim, D. H. (2002): Formation and stability of quasicrystalline and hexagonal approximant phases in an Al-Mn-Be alloy. *J. Mater. Res.*, Vol. 17, pp. 1671–1677.

[22] Chang, H. J., Fleury, E., Song, G. S., Lee, M. H., Kim, W. T., Kim, D. H. (2004): Microstructure modification and quasicrystalline phase formation in Al-Mn-Si-Be cast alloys. *Mater. Sci. Eng. A-Struct. Mater. Prop. Microstruct. Process.*, Vol. 375, No. 77, pp. 992–997.

[23] Jun, I. H., Kim, J. M., Kim, K. T., Jung, W. J. (2007): Fabrication and mechanical properties of quasicrystal-reinforced Al-Mn-Mm alloys. *Mater. Sci. Eng. A-Struct. Mater. Prop. Microstruct. Process.*, Vol. 449, pp. 979–982.

Wear level influence on chip segmentation and vibrations of the cutting tool

Vpliv stopnje obrabe na segmentacijo odrezka in vibracije rezalnega orodja

Aco Antić[1, *], Dušan Kovačević[1], Milan Zeljković[1], Borut Kosec[2], Jozef Novak-Marcinčin[3]

[1]University of Novi Sad, Faculty of Technical Sciences, Trg D. Obradovića 6, 21000 Novi Sad, Serbia
[2]University of Ljubljana, Faculty of Natural Sciences and Engineering, Aškerčeva cesta 12, SI-1000 Ljubljana, Slovenia
[3]Technical University in Košice, Faculty of Manufacturing Technologies in Prešov, Bayerova 1, 080 01 Prešov, Slovakia

*Corresponding authors. E-mail: antica@uns.ac.rs

Abstract: The paper presents the experimental research on wear level influence on chip formation mechanisms, chip segmentation morphology and tool vibration in turning. Based on the direct microscopic analysis of chip samples, the correlation has been established between tool wear condition and chip cross-sections. During the processing, the tool girder vibrations in the zone close to the cutting area have been registered. On the basis of the comparative analysis of experimental results (electronic microscope) and vibration signals registered in the machining operation, the correlation between tool wear level and the variation in chip segmentation form and type has been defined, as well as the frequency characteristics of the vibration. The aim of the research described in this paper is to contribute to the better understanding of chip segmentation mechanism, typology and morphology, in the sense of more qualitative definitions of input information for development of the system for tool wear condition classification.

Original scientific paper

Povzetek: V prispevku je prikazana eksperimentalna raziskava vpliva stopnje obrabe orodja na mehanizem nastanka in tip segmentacije odrezka ter vibracije orodja pri struženju. Na osnovi direktne mikroskopske analize odrezkov je formulirana korelacija med stanjem obrabe orodja in obliko prečnega prereza odrezka. Med procesom struženja so bile merjene vibracije nosilca orodja v neposredni bližini cone rezanja. Na osnovi vzporedne analize eksperimentalnih rezultatov (SEM-mikroskop) in signalov vibracij, merjenih med procesom struženja, je bila definirana korelacija med stopnjo obrabe orodja s spremembo oblike in tipom segmentacije odrezka, kot tudi frekvenčne karakteristike vibracij. Cilj raziskav, opisanih v tem delu, je prispevek k boljšemu razumevanju mehanizmov, tipov in oblik segmentacije odrezkov v smislu kvalitetne definicije vhodnih podatkov za razvoj sistema za vrednotenje obrabe orodij.

Key words: Tool wear, chip morphology, chip segmentation, vibration spectre

Ključne besede: obraba orodja, morfologija odrezka, segmentacija odrezka, vibracijski spekter

Introduction

The understanding of the correlations between chip formation mechanisms and tool wear in machining operations has a significant role in determining the influences on tool vibration, on attrition in the contact point between tool and chip in the cutting process, as well as on determining the optimal machining conditions. Based on the analysis on the cross-section type and morphology of the formed chip, it is possible to determine the following parameters: dimensions, shape and frequency of the chip lamella segmentation.[1] Thermal and chemical processes in the cutting zone at the contact point between the chip and the front tool surface cause the appearance of the diverse mechanisms and forms of tool wear. The most common forms are crater wear on the front tool surface, flank wear on the rear surface and cutting edge wear.[2] The chip formed in the condition of the increased cutting velocity and supplementary movement at the contact point between the tool and the chip induces the increased pressure on front tool surface and directly influences the velocity of the increasing wear, i.e. crater wear. Except for the better understanding of the chip formation mechanisms, chip morphology can be utilized as a tool wear condition indicator in unfavourable machining conditions. The forma-

tion mechanism, shape and direction of a chip on a front tool surface have a significant impact on wearing and the quality of the product's machining surface. In their papers, OZCATALBAS[3] and DUTTA[2] analysed of the formed chip shape depending on the tool wear level. One of the important sources of tool vibrations in the machining process is the formation of chip segments. In material cutting, during the segment formation, the segmented chip induces the force impulses that generate vibrations of the tool itself. In that sense, SUN[4] researched the frequencies of chip lamella formation depending on the dynamic component variation of the cutting forces. Likewise, the research directed towards the registration of the dynamic parameters in chip lamella formation processes during turning includes the application of diverse sensors and experimental research techniques. PETROVIC[5], ANTIC[6, 7] and KLANCNIK[8] used acceleration gauges for monitoring diverse dynamic parameters in the chip formation process as a basis for the development of fuzzy systems for tool wear monitoring. Furthermore, besides the stated indirect methods, COTTERELL & BYRNE[9] used in their research direct methods and techniques based on the high resolution cameras and high sampling rate in order to determine types and parameters of formed chips in turning, for the usage in real industrial cutting regimes.

Chip formation mechanism and its classification can be determined on the basis of the following: material microstructure, cutting speed, supplementary movement speed, cutting depth, shear angle, etc. The result of the common classification in chip morphology, type and form in turning is the classification into: continual, segmented and strip chips. Figure 1 presents the typical appearance of a continual segmentation chip with no variations in cross section structure, where the loose chip surface is flat and with no clearly distinctive lamella teeth.

Figure 2 presents a discontinual segmented chip with very distinctive lamella peaks on the loose chip end. This is the dominant form of the chip originating from the machining of the material with the increased hardness (Titanium alloy and the like). Likewise, the segmented chip is the consequence of the machining of the thermally improved materials in higher cutting speed regimes.

Discontinual type chip is the result of machining the material with dominant thermo-plastic instability. Inside the primary cutting zone, the action of shear forces and cutting forces leads to the material sliding as a consequence of thermal softening, and the discontinuity on the loose chip end is formed. The outcome of these
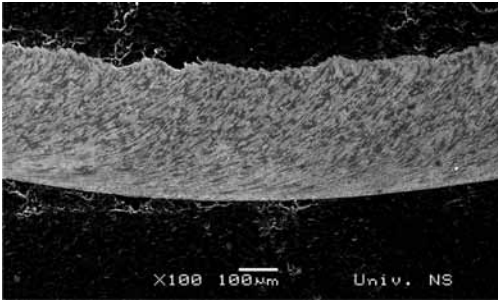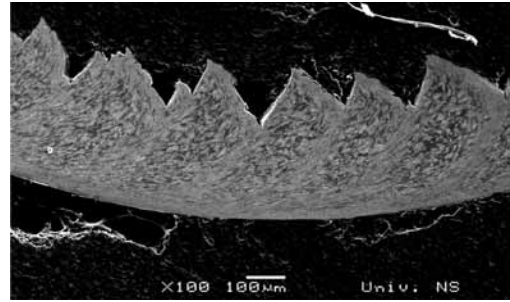
Figure 1. Continual chip

Figure 2. Segmented chip

actions is chip formation based on the adiabatic shear mechanism and discontinual type chip formation with clearly defined intensive shear zones which spreads inside the material structure. Barry & Gerald[10] considered chip formation mechanisms in machining hardened steel and concluded that the cause of the intensive shear appearance inside the primary zone is the adiabatic type of chip formation resulting in the saw-like form of the chip. Inside the primary cutting zone, i.e. the narrow strip with highly distinctive shear, the dominant is the shear stresses aiding at the material movement of the formed segment towards the loose chip surface. The increase in material hardness, cutting velocity, cutting depth and negative front angle, in the combination with the increase in tool wear, leads to a saw-like chip type. Furthermore, it is experimentally determined that the deformed part of the chip cross section reduces with the increase in cutting speed.

The objective of the research presented in this paper is to characterize chip lamella formation in turning depending on tool wear level and based on the direct microscopic analysis of the formed chip. The comparative analysis of frequency of vibration, chip lamella formation frequency and direct microscopic analysis results can present the formulation for the correlation between tool wear level and chip formation type, with the possibility of defining the robust indicator for tool wear monitoring.

Chip formation mechanism

A great number of researches in the area of real industrial production have had a goal to classify chip formation in dependence to the material micro structure, cutting speed, supplementary movement speed, cutting depth, shear angle, etc. Chip formation mechanism in high cutting speed circumstances differs from those in conventional machining process.[11, 12] Namely, the chip

generated in machining hard and improved materials in most cases is either a continual chip or a saw-like chip, as presented in Figures 1 and 2. According to available literature information, saw-like chip formation is in most cases the consequence of the adiabatic lamella shear. Geometric characteristics of a segment are as follows: tooth height, tooth span, undeformed tooth surface length ($L_{undeformed}$), tooth machined surface length ($L_{machined}$), and shearing angle (Φ_{seg}), as presented in Figure 3.
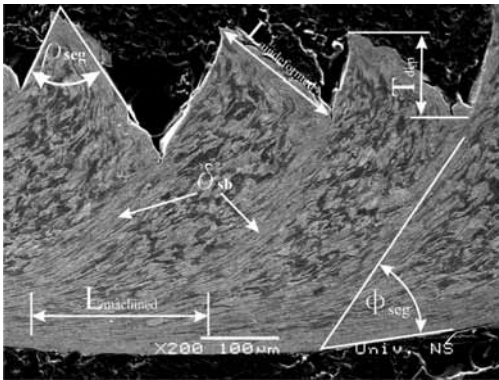

Figure 3. Chip segmentation parameters

Geometric ratio between a tooth undeformed surface length and a tooth machined surface length is presented by the expression (1).[4]

$$r = \frac{L_{udeformed}}{L_{machined}} \qquad (1)$$

In the case of ideal continual chip, this geometric ratio is $r = 1$ due to the fact that both undeformed and machined surface on the formed chip have the same length. If $r < 1$, the newly formed segment is pushed along the sliding plane ahead, due to which a crease is formed on the loose chip surface, and the machined segment surface is elongated along the front tool surface due to sliding attrition. If $r > 1$, the newly formed segment is pressed along the sliding plane forward towards the loose chip surface and it is realised from the tool peak action, forming a shorter machined surface due to less segment pressure and attrition on the front tool surface. Due to the increase in cutting speed, the continual (constant) shear gradually disappears and the chip presents the appearance of the periodical segmentation in rather distinctive zones where the material sliding is under the shearing angle from 30° to 45°. Material deformation is distinctive in the shearing zone δ_{sb}, while the material deformation in the segment is very small, as can be observed in Figure 3. It is important to mention that, due to such intensive material sliding, crack can also appear, and they can be observed together with the shear band in all cutting velocities.

SURVEY OF EXPERIMENTAL RESULTS

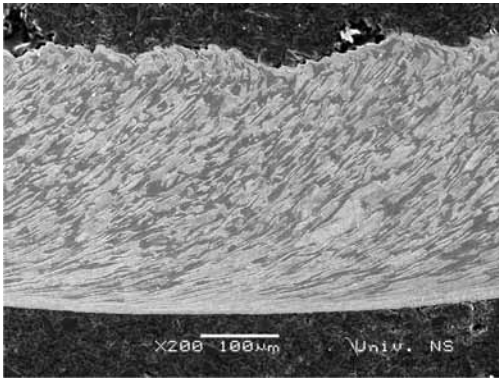The experimental research with direct measurement on an electronic micro-
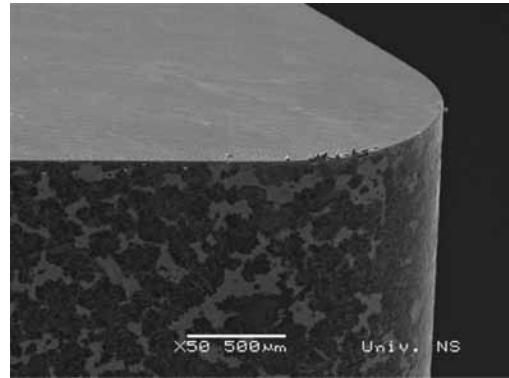
Figure 4. Continual chip segmentation

Figure 5. Tool wear condition in generating a continual chip

scope, presented in the paper, provides a good insight into the characteristics and shape of chip lamellas depending on the tool wear level. The variation in tool wear level has a direct impact on the variation of the type and form of chip formation, which is the result of the analysis on cross-sections and loose chip surface.

Continual chip formation

Continual chip is formed by material shear in the primary cutting zone with no clearly defined segment boundaries in cross-section and no distinctive bumps on the loose chip surface. Chip formation frequency is one order larger than in the case of saw-like chip[13]. A significant influence on the lamella mechanism and shear mode in creating a certain type of a chip is related to the ratio of feed and cutting speed.

The loose surface of the formed chip in machining with a new tool (continual chip) has no clearly distinctive difference in the height of the formed lamellas. The experiments do not show a direct link between chip type variation and chip thickness variation. With continual chips, the segment height on the loose chip surface is very low and corresponding to the width of an individual segment. With the formation of the discontinual type segment, the segment width is the same order as the cutting depth and it is approximately 50 % of the cutting depth.

Figure 4 presents a chip cross section formed by continual segmentation. The upper chip zone presents a loose surface of a continual chip with the mildly wavy shape and tiny indications of the beginning of lamella formation. The samples of the presented chip have been obtained by an orthogonal cutting
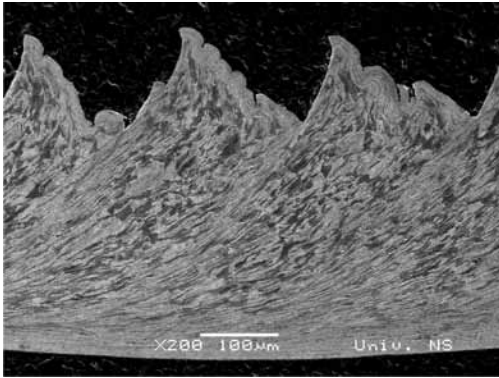
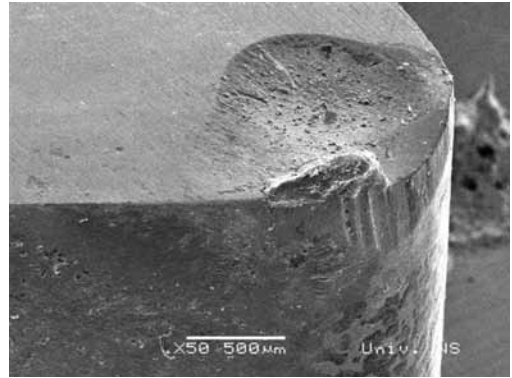**Figure 6.** Saw-like type of chip segmentation

Figure 7. Tool wear condition at the time of generating a discontinual chip form

process of low alloyed tool steel with the hardness of 45 HRC. Machining parameters are the following: cutting speed is 200 m/min and feed is $f = 0.2$ mm/r. Figure 5 presents the cutting tool wear condition in generating a continual chip.

DISCONTINUAL CHIP FORMATION

On a loose surface of a discontinual chip, presented in Figure 5, one can clearly observe the intensive shear zone on the boundaries of formed segments. Figure 6 shows a microscopic view of a chip generated on the thermally treated low alloy carbon steel, with the hardness of 45 HRC and the cutting speed 200 m/min. The increase in the wearing band and wearing crater on the front tool surface, i.e. the increase in the degradation level of the cutting geometry, Figure 7, leads to

the variation in the type of the formed chip. It is evident that formed segments originated in the cycle process of segment creation beginning with the first segment all the way to the last one. After a certain period of machining, due to variations in tool wear level, the chip type also began altering. Microscopically observing, chip form becomes flatter with more distinctive material sliding on the main plane. Rear chip surface becomes wavy and uneven in comparison to the one obtained after new tool machining process.

Grain extension in material structure appears as linear in the narrow band, i.e. primary shearing zone, and it is visible in the cross section of the formed chip, as in Figure 8. Instead of creating an initial crack and break spreading downwards through the primary sliding zone, the generated deformation band is localised as a band formed due
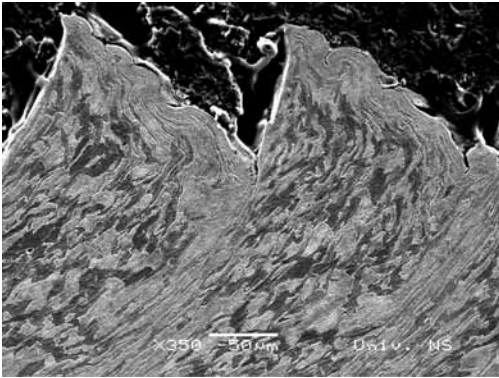
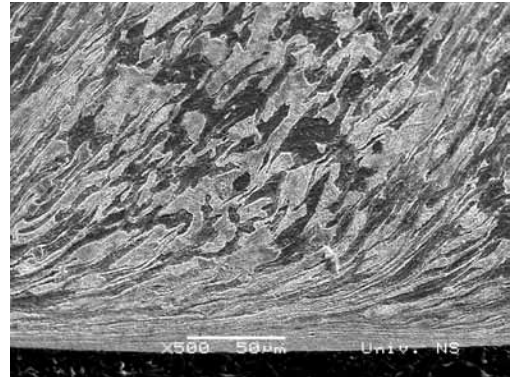**Figure 8.** Discontinual form of chip segmentation

Figure 9. Merging of the intensive shearing zones on rear chip side

to adiabatic material shear. The lack in the appearance of an initial crack and distinctive material separation among segments in the upper part of the primary shearing zone demonstrates the existence of stress deformation and relaxation due to the influence of thermal softening of the main material in the narrow zone. This conclusion is based on the fact that the appearance of the very pronounced shear zone and its width is related to the sampling material, tool geometry and shape, presenting a shear initialization due to the action of cutting forces and tool's cutting edge.

The material band along the rear chip edge, which leads over the front tool surface, creates an additional shear along the edge of the chip formed due to secondary cutting zone action. The elongated zone of the rather distinctive material shear formed in the narrow zone of the rear chip side transfers to the distinctive

shear band within the primary sliding zone creating individual chip segments, as it can be observed in Figure 9.

The machining conditions, in which the discontinual type chip is generated, with the very distinctive segment ends on the loose chip surface, are identical in everything to the ones in machining in which the continual chip is generated, except in the case of tool wear level. Within the observed chip segments, one can clearly identify the variations in the chip formation mechanism within the primary shear zone and the formation of the individual segment peaks on the loose chip end. It is believed that this chip shape is the consequence of s in machining conditions due to variations in cutting tool wedge geometry due to wearing. The variation in the chip morphology reflects on vibrations, processed surface quality and energy loss for material splits removal.

VIBRATIONS AND FREQUENCY OF CHIP SEGMENTATION

One of the main parameters defining the character of vibrations in the cutting process is the frequency of lamella formation. COTTERELL & BYRNE[9] determined the frequency of lamella formation in their researches used f_{seg} analyses of video surveillance of lamella formation. The frequency of forming chip lamellas has a linear increase with the increase in the cutting speed, and has a decrease with the increase in the cutting depth. Frequency of creating a lamella chip has the range between 3.8 kHz and 250 kHz in processing hardened materials.[14] This range of chip segmentation frequencies also causes great force variations on the tool cutting edge.

The frequency of chip lamella formation can be calculated on the basis of the following: steps in the formation of lamellas p_c, cutting depth (width of the undeformed chip segment) h, height of the undeformed chip segment h_{ch} and cutting speed v_c, on applying the following expression:

$$f_{lam} = \frac{v_c \cdot h_{ch}}{h \cdot p_c} = \frac{v_c}{\lambda \cdot p_c} \qquad (2)$$

The vibrations in the cutting tool during machining appear due to attrition on the front and flank tool surface, wear on the tool cutting edge, bumpiness of the processed surface, etc. The basic tool vibration frequency is the resonant system frequency caused by attrition and cutting forces on the cutting edge. Since the cutting tool vibrations are high frequency vibrations (over 1 kHz), the tool vibration acceleration is selected as a parameter for tool wear monitoring.[15, 16] Vibration acceleration signal is directly in correlation to the cutting process, and also with other vibration sources due to the interaction with the tool and machining system. These researches began with the assumption that in a certain segment of the frequency spectre there is a distortion and masking of the information content which is of interest, yet it appears in such an amount that, with the application of adequate procedures, there is a possibility for extracting the information content which will aid in undoubted recognition of the current wear condition of the tool cutting edge. Monitoring the wearing process and evaluating the tool wear condition that enables a normal cutting process provides conditions for fulfilling the set quality in shapes and micro-geometry of the formed surface.

Figure 10 presents the dependency between lamella segmentation and tool wear level. It can be observed that the increase in tool wear decreases the segmentation frequency for constant cutting conditions. The research in chip segmentation explains the mechanism of chip lamella formation.
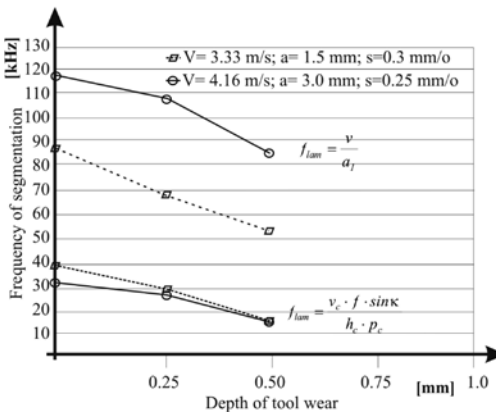
Figure 10. Dependency between lamella formation frequency and tool wear level

VIBRATION CHARACTER IN CHIP FORMATION PROCESS

The formation of initial crack inside the primary shearing zone and individual chip segments during the appearance of discontinual chip results in the increased level of energy release and vibration amplitude in comparison to the continual chip. The result of discontinual chip formation is the increase in deformation energy, the appearance of adiabatic material shearing, the variations in vibrations and the appearance of self-induced vibrations. This assumption provides the connection between vibrations and cutting depth during the continual chip formation. Chip formation induces a significant level of vibrations and acoustic emission (AE) regardless the chip shape and type. If the chip width

is small enough, the extension of initial crack and spreading towards the front tool surface is such that stresses and energy can be measured. The conducted researches indicate that the high-frequency segment of vibration features measured on the handle of the turning knife in the zone close to the cutting zone presents a good indicator in the variation of chip mechanism and formation type induced by cutting tool wear condition variation, i.e. degradation of its cutting edge by wearing. In the range between 1 kHz and 50 kHz the majority of tool's own vibrations is situated, so certain resonance appearances due to self-induced forces appear after chip segmentation. The formation of segmented chip can be observed as a process of discrete self-induction of the processed system with a set of impulses whose frequency can be determined with an acceptable error. Vibrations emerging during machining can be recognized in the processing system, especially on the cutting tool handle. From the analysis of experimental research results, it is concluded that the processing system outcome is different when the self-induction is induced by continual chip formation. Inside any chip segment formation cycle, the cutting identification is also destabilized by the very primary shearing zone, resulting in energy release and stress formation. As already stated, the frequency of segment formation
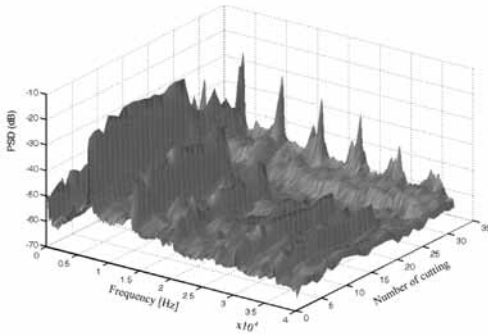
Figure 11. Signal energy distribution on frequency axis depending on the tool wear level
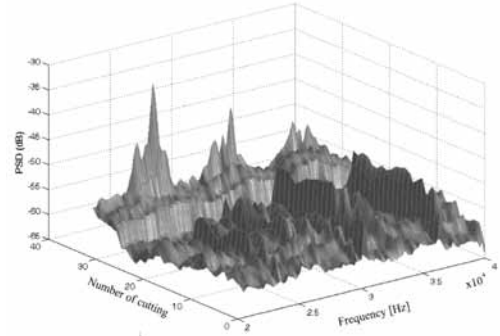

Figure 12. Signal energy distribution on frequency axis depending on tool wear level

is usually larger than 10 kHz, which is above the measuring performances level of typical acceleration gauges. The more distinctive appearance of peaks in vibration signals is observed on releasing the lamella shearing energy after generating the discontinual chip shape. Figure 11 illustrates these cases.

The analysis of the results in these experiments can provide the conclusion that the dominant influence on the type of the formed chip in the cutting process does not only have the condition and characteristics of materials and cutting conditions, but also has wear condition of the tool insert, i.e. tool geometry. Furthermore, it is determined that in maintaining constant cutting conditions (speed, feed, cutting depth, material characteristics), due to variations in tool wear level, there

appears the variation in the chip type. The variation in chip type is induced by the variation in cutting geometry which alters with the tool wear level. The variation in cutting geometry, and hence chip type, directly influences the observed parameters in the analysed high-frequency segment of the vibration spectre.

Figure 12 presents signal energy spectres (in [dB]) for diverse tool wear levels processed with the following parameters: window = 2048; noverlap = 512; pwelch (data_N(:,1), window, noverlap,[], Fs).

Frequency spectre is limited to 50 kHz. The used equipment provides measuring accuracy even for a wider frequency range (up to 100 kHz), which has not been done due to limitations of the available acceleration gauge.

Conclusion

The research analysed the variation in the mechanism of chip formation process in dependence to tool wear level. The formed chip in the initial machining phase (new tool) has a flat shape with smooth rear part which is in contact with the front tool surface, while the chip loose surface has no distinctive lamella segment teeth. Cutting tool is new, sharp and without any indications of crater formation on the front surface. After the increase in wear band and crater tool wear, the chip varies the shape, and becomes more bumpy, wavy and cracked on its ends, while the segmentation type varies into the discontinual one with very distinctive teeth on the chip loose surface. The increase in flank wear increases the chip segmentation while the lamella formation frequency decreases, as it can be observed in Figure 10. The plastic material deformation in the primary cutting zone becomes more distinctive with the clear boundary between formed segments. The cross section of the created chip has very distinctive roughness on the chip loose surface in diverse zones of material deformation in the cutting process: zones with distinctive attrition next to the tool edge, primary shearing zones, zones with distinctive initial crack, and zones with decreased material deformation. It indicates the combined action of the stress toughening and heat softening, i.e. the existence of the combined action in chip formation. The formation of the discontinual type of the chip is characterized by thermal and plastic deformation due to tool and cutting force action. The zone of thermal and plastic instability dominates until the beginning of segment formation and formed shear zone. Thus, in that segment, the cutting is conducted by "adiabatic theory" of shear. Vibration response is variable, with distinctive peaks in individual frequencies overlapping with the chip segmentation frequency. The variation in chip type causes the appearance of new frequency components (harmonics) which are close to lamella formation frequency, with the occasional appearance of self-induced vibrations in the moments when the tool is at the end of its life span.

Acknowledgments

REFERENCES

[1] BARRY, J., BYRNE, G., LENNON, D. (2001): Observations on chip formation and acoustic emission in machining Ti–6Al–4V alloy. *International Journal of Machine Tools & Manufacture;* Vol. 41, pp. 1055–1070.

[2] DUTTA, A. K., CHATTOPADHYAYA, A. B., RAYC, K. K. (2006): Progressive flank wear and machining performance of silver toughened alumina cutting tool inserts. *Wear*; Vol. 261, pp. 885–895.

[3] OZCATALBAS Y. (2003): Chip and built-up edge formation in the machining of in situ Al4C3–Al composite, *Materials and Design;* Vol. 24, pp. 215–221.

[4] SUN, S., BRANDT, M., DARGUSCH, M. S. (2010): The Effect of a Laser Beam on Chip Formation during Machining of Ti6Al4V Alloy. *Metallurgical and Materials Transactions A;* Vol. 41A, pp. 1573–1581.

[5] PETROVIC, B. P., JAKOVLJEVIC, Z., MILACIC, V. R. (2009): Context sensitive recognition of abrupt changes in cutting process. *Expert Systems with Applications;* Vol. 37, pp. 3721–3729.

[6] ANTIC, A., ZELJKOVIC, M., PETROVIC, P. (2010): Development of the Tool Wear Condition Classification System Model in Turning. *Machine Design*; pp. 207–212.

[7] ANTIC, A., ZELJKO, M., HODOLIC, J., ZIVKOVIC, A. (2010): Model of Classification System of Tool Wear Condition While Machining by Turning. *Journal of Production Engineering*; Vol. 12, No. 1, pp. 1–4.

[8] KLANCNIK, S., BALIC, J., CUS, F. (2010): Intelligent prediction of milling strategy using neural networks. *Control Cybern.*; Vol. 39, No. 1, pp. 9–22.

[9] COTTERELL, M., BYRNE, G. (2008): Dynamics of chip formation during orthogonal cutting of titanium alloy Ti–6Al–4V. *CIRP Annals - Manufacturing Technolo*gy; Vol. 57, pp. 93–96.

[10] BARRY, J., GERALD, B. (2002): The mechanisms of chip formation in machining hardened steels. *Transactions of the ASME, Journal of Manufacturing Science and Engineering*; Vol. 124, No. 3, pp. 528–535.

[11] DAYMI, A., BOUJELBENE, M., BEN SALEM, S., HADJ SASSI, B., TORBATY, S. (2009): Effect of the cutting speed on the chip morphology and the cutting forces. *Archives of Computational Materials Science and Surface Engineering*; 1/2, pp 77–83.

[12] MURCINKOVA, Z., KOMPIS, V., STIAVNICKY, M. (2008): Trefftz functions for 3D stress concentration problems. *Computer Assisted Mechanics and Engineering Sciences;* Vol. 15, No. 3–4, pp. 305–318.

[13] KOPAC, J., SOKOVIC, M., DOLINSEK, S. (2001): Tribology of coated tools in conventional and HSC machin-

ing. *Journal of Materials Processing Technology;* Vol. 118, pp. 377–384.

[14] Ekinovic, S., Dolinsek, S., Jawahir, I. S. (2004): Some observations of the chip formation process and the white layer formation in high speed milling of hardened steel. *Journal of Machining Science and Technology;* Vol. 8, pp. 327–340.

[15] Kociusko, M., Janak, M. (2008): Creation Method of Visual Disassembly Procedure. *Journal CA Systems in Production Planning;* Vol. 9, No. 1, pp. 37–39.

[16] Marcincin, J. N. (2008): Design of Milling Toll Cutting Strategy for CNC Manufacturing Operations. *Engineering Review;* Vol. 28, No. 1, pp. 93–97.

Soft annealing productivity optimization

Optimiranje produktivnosti mehkega žarjenja

Miha Kovačič[1, 2, *], Božidar Šarler[2]

[1]ŠTORE STEEL, d. o. o., Štore, Slovenia
[2]University of Nova Gorica, Laboratory for Multiphase Processes,
Nova Gorica, Slovenia

*Corresponding author. E-mail: miha.kovacic@store-steel.si

Abstract: The optimal thermo-mechanical processing in steel industry is difficult because of the multi-constituent and multiphase character of the commercial steels, variety of multi-constituent the possible processing paths, and plant specific equipment characteristics. This paper shows successful implementation of the genetic programming approach for increasing the furnace conveyor speed and consequently productivity of the heat treatment furnace in the soft annealing process. The data (222 samples covering 24 different steel grades) on a furnace conveyor speed, chemical composition of steel (weight percent of C, Cr, Mo, Ni and V) and Brinell hardness before and after the soft annealing were collected during daily production. On the basis of the monitored data a mathematical model for the hardness after the soft annealing was developed by genetic programming. According to the modeled influences on the hardness, the higher furnace conveyor speed was attempted in practice. The experimental results of the hardness after the soft annealing with the increased conveyor speed and the predictions of the mathematical model were compared within the agreement of 3.24 %. The productivity of the soft annealing process increased (from the furnace conveyor speed 3.2 m/h to 7 m/h) as a consequence of the used computational intelligence approach.

Izvleček: Zaradi težko določljivih lastnosti komercialnih jekel, razno-likosti tehnoloških poti in specifične opreme je optimalno termo-mehansko procesiranje v jeklarstvu izredno problematično. V

Original scientific paper

članku je predstavljena uporaba genetskega pogramiranja z name-
nom povečati hitrost transportnega traku žarilne peči in posledično
produktivnost žarilne peči in procesa žarjenja samega. Med tipično
proizvodnjo so bili zbrani podatki (222 vzorcev, 24 kvalitet jekla)
o hitrosti peči, kemijski sestavi jekla (masni deleži C, Cr, Mo, Ni
in V) ter trdota po Brinellu pred mehkim žarjenju in po njem. Na
podlagi zbranih podatkov je bil izdelan matematični model trdote
po mehkem žarjenju z metodo genetskega programiranja. Glede
na izračunane vplive na trdoto po mehkem žarjenju smo povečali
hitrost žarjenja. Po povečanju hitrosti žarjenja se izmerjene trdote
materiala ujemajo z izračunanimi v povprečju 3,24-odstotno. Pro-
duktivnost mehkega žarjenja se je povečala iz 3,2 m/h na 7 m/h kot
posledica umetne inteligence.

Key words: steel, soft annealing, productivity, hardness, genetic pro-
gramming, modeling
Ključne besede: jeklo, mehko žarjenje, produktivnost, trdota, genetsko
programiranje, modeliranje

Introduction

There is a strong trend in steel indus-
try for enhanced productivity, safety,
and environmental friendliness of the
involved processes, in parallel with the
enhanced product variety and quality.
In the last two decades, the thermo-
mechanical physical models are in-
creasingly developed for casting, roll-
ing, and heat treatment operations.[1]
However, the current state-of-the-art in
physical modeling does not permit to
quantitatively model the whole range
of steel behavior neither from the mi-
croscopic materials science point of
view, nor from the macroscopic process
level. This is probably due to the multi-
constituent and multi-phase character

of the steel as well as due to the fact
that the important physical processes
took place over a huge range of length
scales from the nano up to 100 m. The
physical modeling is thus increasingly
connected with the intelligent algo-
rithms (such as for example artificial
neural networks, evolutionary com-
putation, swarm intelligence, artificial
immune systems, and fuzzy systems)
[2] which complement or replace the
physical models in solving realistic in-
dustrial problems. An example of such
symbiosis[3] is the continuous casting
physical modeling with the evolution-
ary algorithm for searching the opti-
mum casting conditions. The purpose
of the heat treatment of the steels is to
cause the desired changes in the met-

allurgical structure and thus material properties.[4] Soft annealing represents heat treatment wherein a material is altered, causing changes in its ductility and hardness. Several attempts have been made to attain the control of the above mentioned material properties at the soft annealing treatment.[5–9] The aim of the present research is to find out the possibilities of increasing the furnace productivity (speed of the furnace conveyor) at the soft annealing process. The genetic programming method is used in the present paper to establish the relations between the chemical composition of the principal alloying elements (carbon, chromium, molybdenum, nickel and vanadium), the principal process parameters (such as the speed of the furnace conveyor), and the principal material property (hardness after the soft annealing treatment). Having this relations set, more optimal conveyor speed could be easily determined with respect to the process parameter constraints, i.e. maximum possible speed of the conveyor, and product properties constraints, i.e. maximum hardness.

Genetic programming is one of the methods of the evolutionary computation.[10, 11] In the genetic programming, organisms which are more or less complicated computer programs, are subject to adaptation. The computer programs are in fact models for prediction

of the hardness after the soft annealing in the present study. Many different prediction models, differing in the quality of prediction and the complexity of the structure, were obtained during the simulated evolution. Only one model out of many is discussed in the present paper.

THE HEAT TREATMENT FURNACE DESIGN AND THE EXPERIMENTAL DATA

All experimental data, used in the present paper, have been obtained from the pusher-type furnace of Štore Steel steelworks - Slovenia, one of the major spring-steel producers in Europe. The scheme of the furnace is depicted in Figure 1. The hardness after the annealing process depends on the chemical composition of the steel and the furnace process parameters. The main methodological constraint of the present paper is, according to production pace, that the production lining parameters could only be monitored and not allowed to vary. The experimental data have been thus obtained directly from the undisturbed production. The principal seven adjustable furnace process parameters are the six different temperatures of the heat treatment zones and the time of the annealing (inversely proportional to the speed of the furnace conveyor). The principal two fixed construction parameters of the furnace are the maxi-
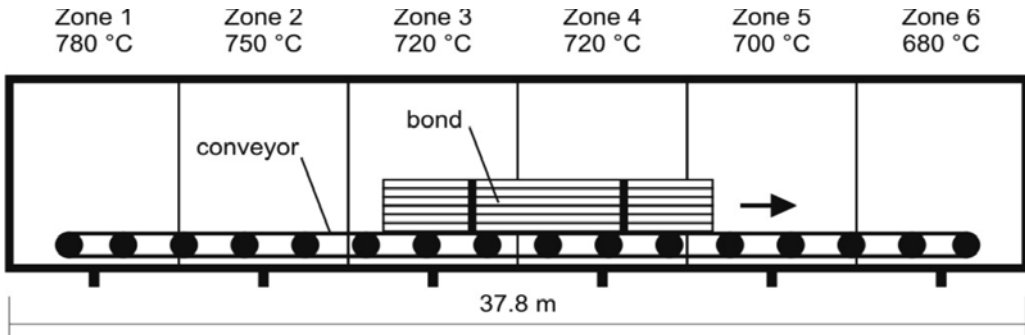
Figure 1. Heat treatment furnace with its six equidistant temperature zones

Table 1. The number of steel grade specimens and the average chemical composition

	Composition, *w*/%		C	Cr	Mo	Ni	V
#	Steel grade	Number of specimens					
1	15CrNi6	1	0.14	1.56	0.04	1.53	0
2	16MnCr5	1	0.19	1.03	0.02	0.09	0
3	17CrNiMo6	2	0.18	1.65	0.28	1.50	0
4	18 CrNi 8	1	0.19	1.95	0.02	2.01	0
5	18CrNiMo7-6	15	0.17	1.64	0.29	1.53	0.001
6	18CrNiMo7-6 HH	2	0.19	1.69	0.29	1.53	0
7	23MnNiCrMo5-2-A	12	0.22	0.49	0.21	0.47	0
8	25CrMo4	4	0.24	1.01	0.20	0.10	0
9	34CrNiMo6	28	0.36	1.61	0.22	1.60	0.003
10	41Cr4	7	0.42	1.08	0.03	0.11	0
11	42CrMo4	33	0.42	1.07	0.22	0.11	0
12	42CrMoS4	8	0.43	1.03	0.21	0.11	0
13	50CrMoS4	14	0.51	1.04	0.22	0.13	0
14	50CrV4	34	0.50	1.05	0.04	0.11	0.156
15	51CrMoV4	1	0.54	1.06	0.18	0.09	0.11
16	51CrV4	11	0.51	1.08	0.04	0.11	0.1555
17	51CrV4 HH	3	0.51	1.08	0.04	0.12	0.170
18	52CrMoV4	6	0.54	1.05	0.18	0.10	0.113
19	55Si7	16	0.57	0.29	0.04	0.12	0
20	70MnVS4	20	0.70	0.15	0.03	0.08	0.113
21	25CrMo4	1	0.24	1.05	0.21	0.14	0
22	42CrMo4	2	0.43	1.03	0.21	0.11	0
SUM		222					

mum bond specific weight 2.5 t/m and the maximum conveyor speed 7 m/h. The cross-sections of the round and flat bars in the bond varied from 43.28 mm² to 5676.40 mm². The temperature of the six heat treatment zones was kept constant in all cases (see data in Figure 1). The only influential heat treatment

Table 2. Part of the monitored data set

#	Conveyor speed [m/h]	Hardness before the soft annealing [HB]	$w(C)$/%	$w(Cr)$/%	$w(Mo)$/%	$w(Ni)$/%	$w(V)$/%	Hardness after the soft annealing [HB]
1	3.2	298	0.51	1.09	0.22	0.19	0	219
2	3.2	248	0.43	1.08	0.02	0.1	0	191
3	3.2	313	0.69	0.14	0.02	0.08	0.11	229
4	3.2	309	0.70	0.13	0.02	0.08	0.12	215
5	3.2	290	0.55	0.28	0.04	0.12	0	229
6	3.2	290	0.59	0.36	0.05	0.12	0	229
…	…	…	…	…	…	…	…	…
220	3.2	298	0.17	1.64	0.29	1.53	0	198
221	3.2	290	0.40	1.04	0.22	0.08	0	207
222	3.2	333	0.52	1.14	0.05	0.11	0.15	229

productivity process parameter was the speed of the furnace conveyor. The speed of the furnace conveyor was kept steady during the heat treatment of the individual bond. The required hardness of the annealed steel has to be below 260 HB before the bond steel bars are subsequently saw-cut.

The number of each steel grade specimens and the average chemical composition (mass fractions w/% of C, Cr, Mo, N and V) is represented in Table 1.

According to actual production technology only two furnace conveyor speeds of 2.5 m/h and 3.2 m/h were used for soft annealing. Brinell hardness for each data set before and after soft annealing was measured at the bar centre at the three positions per bond: once from the bar taken from the bond surface and twice from the bar taken from the middle of the bond. Then the average hardness per bond was calculated and used for modeling. Only a part of the respective monitored data set is shown in Table 2.

GENETIC PROGRAMMING MODELING OF THE HARDNESS AFTER THE SOFT ANNEALING

Genetic programming is probably the most general evolutionary optimization method.[11] The organisms that undergo adaptation are in fact mathematical expressions (models) for the hardness after the soft annealing in the present work. The prediction consists of the available function genes (i.e., basic arithmetical functions) and terminal genes (i.e., independent input parameters, and random floating-point constants). In the present case the mod-

els consist of the following function genes: addition (+), subtraction (−), multiplication (*) and division (/), and the following terminal genes: furnace conveyor speed (speed), measured v/ (m/h), hardness before soft annealing (HB), measured in Brinell units, and chemical composition of the principal alloying elements: carbon (C), chromium (Cr), molybdenum (Mo), nickel (Ni) and vanadium (V), measured in mass fractions, w/%.One of the randomly generated mathematical models is schematically represented in Figure 2 as a program tree with included function genes (*, + , /) and terminal genes (Mo, speed, V, C, and a real number constant 5.1).

The following evolutionary parameters were selected for the process of simu-

lated evolutions: 500 for the size of the population of organisms, 100 for the maximum number of generations, 0.4 for the reproduction probability, 0.6 for the crossover probability, 6 for the maximum permissible depth in the creation of the population, 10 for the maximum permissible depth after the operation of crossover of two organisms, and 2 for the smallest permissible depth of organisms in generating new organisms. Genetic operations of reproduction and crossover were used. For selection of organisms the tournament method with tournament size 7 was used. 100 independent civilizations of mathematical models for prediction of the hardness after the soft annealing have been developed.

The best obtained model for the hardness after the soft annealing is:

$$
\begin{aligned}
&127.132 + 19.309\,\mathrm{Cr} + \frac{V\left(3.436 + Mo + 4.117\,Ni - \frac{V}{Mo}\right)}{-2.234\,Mo + 2\,Ni + \frac{1}{speed} + V} + \frac{\left(C + \frac{1+Cr}{V}\right)V}{Ni\left(-1.234\,Mo - 1.234\,Ni + 2.845\,speed - \frac{V}{Mo}\right)} + \\[2ex]
&C\left(136.993 + 6.298\,Mo + 38.664\,Ni + 6.117\,V - \frac{6\,V}{Mo} - \frac{V}{Ni} + \frac{-2.234\,Mo + Ni + V}{Ni} - \frac{-2.234\,Mo + Ni + 2\,V}{Mo}\right) + \\[2ex]
&Mo\left(-2.234 - 2.234\,Mo\left(4.117 + C + \frac{Cr}{Mo} - 2\,V\right) + V + \frac{\left(C + \frac{1}{V}\right)V}{Ni\,speed}\right)\left(\frac{Cr}{Mo} - \frac{(0.2429 + C)(-2.234\,Mo + Ni + 2\,V)}{speed}\right) + \\[2ex]
&0.021\left(HB + Mo + \frac{2 + 2\,Mo + 5.117\,Ni + \frac{speed\left(2\,C + \frac{1}{CrV}\right)}{Cr} + V - \frac{V}{Ni}}{-1 + 19.075\,Mo + 6.117\,Ni - \frac{4.117V}{Mo} - \frac{\left(C + \frac{Cr}{Mo}\right)V}{speed} - \frac{V}{Ni+V}}\right) + \\[2ex]
&2.845\left(speed + V\left(19.309\,Cr - 1.234\,Mo + \frac{\frac{C + \frac{Cr}{Ni}}{speed} + \frac{C + \frac{Cr}{V}}{speed}}{19.309\,Mo + 5.117\,Ni + 4.117\,V - \frac{V}{Mo}} - \frac{4.117\,Ni + \frac{\frac{Cr}{V} + C\,(4.117 + 4.117V)}{speed}}{-2.234 + 20.309\,Mo + 2\,Ni + V - \frac{2\,V}{Mo}}\right)\right)
\end{aligned}
$$

with the average percentage deviation of 3.24 %.

SOFT ANNEALING PRODUCTIVITY OPTIMIZATION

The maximum furnace conveyor speed, declared from the furnace producer, is 7 m/h. As previously mentioned, the required hardness of the cutting material should be below 260 HB in order to satisfy the product quality requirement.

The previously mentioned results and behavior regarding the sensitivity of the furnace conveyor speed in the soft annealing process allows us to carefully (in several steps) increasing the conveyor speed up to 5 m/h and at last for 7 m/h in industrial practice. The ex-perimental results of hardness for 13 specimens are shown in Table 3, compared with the calculated values from the computational intelligence model.

CONCLUSION

In this paper the possibility of the productivity enhancement of the heat treatment furnace for the soft annealing of the round and the flat steel bars in Štore Steel company was studied. The Brinell hardness after the process was measured for 24 different steel grades as a function of the furnace process parameters and steel composition.

Table 3. Measured and calculated hardness after the soft annealing

#	Conveyor Speed v/(m/h)	Hardness before softannealing	C $w(C)$/%	Cr $w(Cr)$/%	Mo $w(Mo)$/%	Ni $w(Ni)$/%	V $w(V)$/%	Hardness after the soft annealing (monitored) [HB]	Hardness after the soft annealing (genetic programming model) [HB]	Percentage deviation
	5.0	298.0	0.59	0.28	0.05	0.13	0.00	229	237.089	3.53 %
	5.0	464.0	0.34	1.51	0.20	1.50	0.01	229	235.528	2.85 %
3	5.0	335.0	0.53	1.13	0.05	0.19	0.14	229	236.332	3.20 %
4	5.0	438.0	0.36	1.64	0.23	1.64	0.01	229	241.571	5.49 %
5	5.0	438.0	0.34	1.51	0.20	1.50	0.01	229	234.982	2.61 %
6	5.0	339.0	0.43	1.18	0.22	0.15	0.00	215	224.551	4.44 %
7	5.0	339.0	0.43	1.18	0.22	0.15	0.00	215	224.551	4.44 %
8	5.0	309.0	0.7	0.12	0.02	0.07	0.11	215	216.467	0.68 %
9	5.0	309.0	0.7	0.12	0.02	0.07	0.11	215	216.467	0.68 %
10	5.0	309.0	0.7	0.13	0.02	0.08	0.12	215	214.519	0.22 %
11	7.0	335.0	0.55	1.14	0.03	0.12	0.15	249	237.717	4.53 %
12	7.0	313.0	0.53	1.13	0.03	0.10	0.15	239	235.34	1.53 %
13	7.0	361.0	0.54	1.08	0.17	0.09	0.12	249	250.438	0.58 %
									Average percentage deviation	2.68 %

This established an experimental data base for development of 100 models, deduced through the genetic programming methodology. Genetic programming predicts the hardness after the soft annealing with the average percentage deviation of only 3.24 %. The best genetically developed model was closely analyzed and it was established that the furnace conveyer speed is not a sensitive parameter for influencing the hardness after the soft annealing. These findings lead to the changes of the maximum furnace conveyor speed from 3.2 m/h up to 7 m/h in the production practice. The substantially higher conveyor speed did not influence the hardness of the steel after the soft annealing as expected from the model prediction. The hardness after the soft annealing was below the required hardness of 260 HB also in the case of the enhanced conveyor speed in all 13 tested cases. The agreement between the tested and the calculated data is 2.68 %. The results of the research were practically applied.

References

[1]   Verlinden, B., Driver, J., Samajdar, I., Doherty, R. D. (2007): *Thermomechanical Processing of Metallic Materials*; Elsevier, Amsterdam.

[2]   Engelbrecht, A. P. (2007): *Computational Intelligence – An Introduction*; J.Willey & Sons, Chichester.

[3]   Šarler, B., Filipič, B., Raudensky, M., Horsky, J. (2000): An interdisciplinary approach towards optimum continuous casting of steel. *Materials Processing in the Computer Age III*; TMS, Warrendale.

[4]   Totten, G. E., Howes, M. A. H. (1997): *Steel Treatment Handbook*; Marcel Dekker, New York.

[5]   Zeytin, H. K., Aydin, C. K. H. (2008): Investigation of dual phase transformation of commercial low alloy steels: Effect of holding time at low inter-critical annealing temperatures. *Materials Letters*; Vol. 62, No. 17–18, pp. 2651–2653.

[6]   Kain, V., Gupta, V., Pranab, K. (2008): Embrittlement cracking of a stabilized stainless steel wire mesh in an ammonia converter. *Environment-Induced Cracking of Materials*; Elsevier, Amsterdam.

[7]   Broughton, J. S., Mahfouf, M., Linkens, D. A. (2007): Paradigm for the scheduling of a continuous walking beam reheat furnace using a modified genetic algorithm. *Materials and Manufacturing Processes*; Vol. 22, pp. 607–614.

[8]   Sahay, S. S., Mehta, R., Krishnan, K. (2007): Genetic-algorithm-based optimization of an industrial age-hardening operation for packed bundles of aluminum rods. *Materials and Manufacturing Processes*; Vol. 22, pp. 615–622.

[9]   Mehta, R., Sahay, S. S., Datta, A., Chodha, A. (2008): Neural network models for industrial batch annealing operation. *Materials and Manufacturing Processes*;

Vol. 23, pp. 204–209.

[10] Chakraborti, N., Deb, K., Jha, A. (2000): A genetic algorithm based heat transfer analysis of a bloom re-heating furnace. *Steel Research*; Vol. 71, pp. 396–402.

[11] Koza, J., R. (1999): *Genetic programming III*.; Morgan Kaufmann, San Francisco.

[12] Kovačič, M., Uratnik, P., Brezočnik, M., Turk, R. (2007): Prediction of the bending capability of rolled metal sheet by genetic programming. *Materials and manufacturing processes*; Vol. 22, pp. 634–640.

Cell for electrochemical and electrophysiological measurements in peripheral nerves

Celica za elektrokemijske in elektrofiziološke meritve na perifernih živcih

Polona Pečlin[1], Samo Ribarič[2, 3], Janez Rozman[1, *]

[1]Centre for Implantable Technology and Sensors, ITIS, d. o. o., Ljubljana, Lepi pot 11, SI-1102 Ljubljana, Slovenia
[2]Laboratory for Movement Disorders, Dept. of Neurology, University Clinical Centre Ljubljana, Zaloška 2, SI-1000 Ljubljana, Slovenia
[3]Institute of Pathophysiology, Zaloška 4, Medical Faculty, University of Ljubljana, Republic of Slovenia, SI-1000 Ljubljana, Slovenia

*Corresponding author. E-mail: jnzrzmn6@gmail.com

Abstract: The aim of the work was to develop the cell to be used in electrochemical and electrophysiological measurements in peripheral nerves, when electrical stimulating pulses are selectively applied to preselected locations along the nerve. The main part of the cell is the silicone spiral cuff system, including spiral matrix of ninety-nine platinum electrodes, arranged in eleven longitudinal spiral electrode configurations of nine electrodes for establishing electrical contact with specific sites on the peripheral nerve. To maximize the fatigue life of lead wires connected to the electrodes, which should sustain frequent bending, a high frequency miniature and highly flexible, multi-stranded and enameled copper wire, was used. The cell is made of Plexiglas and is instrumented with the precision temperature probe, Ag/AgCl reference electrode, 3D micro-manipulator positioning system and custom designed force transducers to measure stretching and radial pressure that could be applied on nerve segment during measurements.

Izvleček: Namen dela je bil razviti celico za izvajanje elektrokemijskih in elektrofizioloških meritev na perifernih živcih v času selektivnega dovajanja stimulacijskih impulzov na predhodno izbrana mesta

Original scientific paper

vzdolž živca. Najpomembnejši del celice je spiralna silikonska objemka, ki vključuje spiralno matriko devetindevedesetih elektrod, razporejenih v enajst longitudinalnih skupin po devet elektrod za vzpostavitev stika s posameznimi mesti na perifernem živcu. Za čim daljšo trajnostno dobo žic, povezanih z elektrodami, ki morajo vzdržati pogosto upogibanje, je bila izbrana visokofrekvenčna, drobna in zelo upogljiva ter lakirana bakrena pletenica. Sama celica je izdelana iz pleksi stekla in opremljena s precizijsko temperaturno sondo, referenčno elektrodo Ag/AgCl, z mikromanipulatorjem za 3D pozicioniranje in s posebej izdelanimi senzorji sile za merjenje natega in radialnega tlaka, ki mu bo med meritvami izpostavljen vzorec živca.

Key words: platinum, stimulating electrode, peripheral nerve, electrophysiology, electrochemistry

Ključne besede: platina, stimulacijska elektroda, periferni živec, elektrofiziologija, elektrokemija

INTRODUCTION

One of the greatest problems in nonselective vagus nerve stimulation used worldwide as a potentially useful therapy for treating various heart conditions and certain types of intractable epilepsy and major depression is nonselective stimulation of particular superficial regions as well as non-selective stimulation of fibers innervating a targeting organ.[1, 2, 3, 4, 5, 6]

The result is the occurrence of undesirable side effects such as: an intermittent decrease in respiratory flow during sleep, disordered breathing, loud snoring, obstructive sleep aponea, alteration of voice, coughing, pharyngitis, throat pain, hoarseness, frank laryngeal muscle spasm, headache, nausea, vomiting, dyspepsia, dyspnea and paresthesia. To alleviate the above-defined problems, the research was aimed at developing a new model and multielectrode system that selectively and safely stimulates a certain group of fibers in a nerve trunk without excitation of other fibers. For the purpose of performing electrochemical and electrophysiological measurements in functional peripheral nerves an appropriate cell simulating physiological environment needs to be developed.

MATERIALS AND METHODS

The cell was designed taking into consideration the results of histological

examination of the left vagus nerve of a pig, the model of selective electrical stimulation of particular superficial regions of the nerve and the model of selective stimulation of nerve fibers with different diameters.[7, 8, 9] The entire cell was machined out from Plexiglas, using CNC milling machine. The cuff however, was designed taking into consideration the model of selective stimulation of particular superficial regions of the nerve and different types of nerve fibers as well as numerical solution of the 3D current density and electrical field distribution in the superficial region of the nerve, generated by a particular group of electrodes.[10]

Accordingly, the cuff was made by bonding two 0.1 mm thick silicone sheets together. One sheet, stretched and fixed in that position, was covered with a layer of adhesive (MED-1511, NuSil, Carpinteria, CA, USA). A second un-stretched sheet was placed on the adhesive and the composite was compressed to a thickness of 0.3 mm until the whole curing process was completed. When released, the composite curled into a spiral tube as the stretched sheet contracted to its natural length.[11, 12, 13] The composite is self-sizing and flexible, minimizing mechanical trauma when installed onto the nerve. Ninety-nine rectangular electrodes with a width of 0.5 mm and length of 2 mm made of 45 μm thick annealed platinum ribbon (99.99 % purity) connected/soldered to the insulated multi-stranded wire, were then mounted on the third silicone sheet with a thickness of 0.05 mm.

As shown in Figure 1, the electrodes having a flat geometric surface of 1 mm^2 were arranged in a matrix of nine parallel groups each containing eleven electrodes with a distance of 0.5 mm between them, while the distance between the groups was 2 mm. Since it is necessary to activate nerve fibers located at a certain distance from the electrode, the electrode should be able to inject enough charge without causing irreversible electrochemical reactions damaging both, the neural tissue and to the electrode itself.[14] Platinum as an electrode material has the advantage of decreasing impedance with increasing frequency. The contact area (0.5 × 2) mm resulted in a relatively low impedance of about 2.5 kΩ measured »in vivo«. However, in case when thick fatty tissue around the nerve is present, significantly higher impedance could be expected.

To maximize the fatigue life of lead wires shown in Figure 2, high frequency miniature and highly flexible insulated, multi-stranded and enamelled copper wire (CU-LACKDRAHT DIN 46 435, NENN Φ (12 × 0.04) mm, ELEKTRISOLA, Dr. Gerd Schildbach

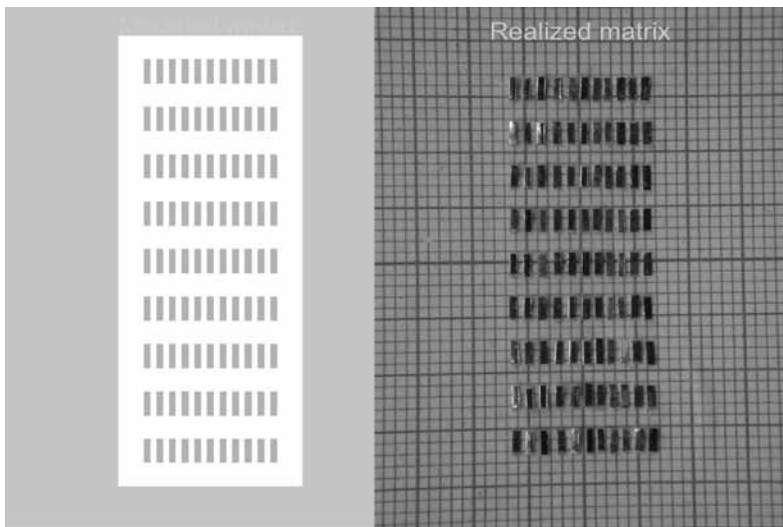**Figure 1.** Modeled and realized matrix of 99 platinum electrodes
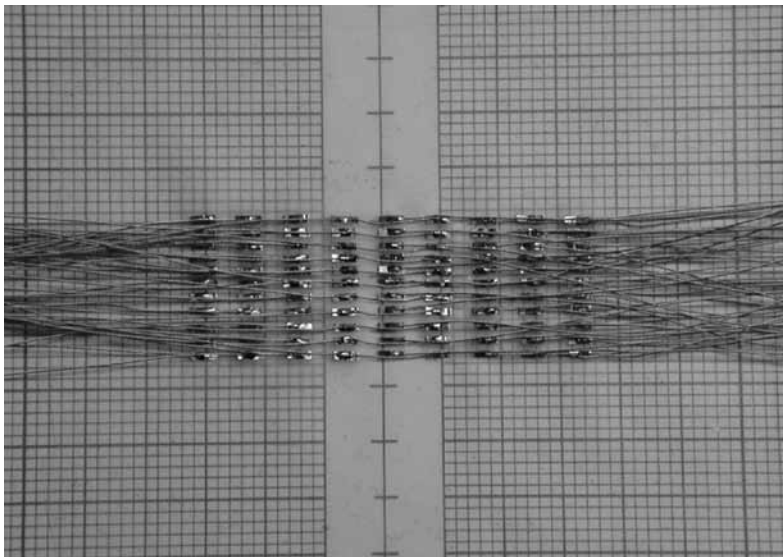

Figure 2. Multi-stranded copper wires, soldered on platinum electrodes within the matrix

GmbH & Co. KG, Hüttenwiese 2-4, D-51580 Reichshof-Eckenhagen, Germany, Tel: +49(0)2265 12 0, Fax: +49 (0)2265 9436, e-mail: sales@elektri- sola.de), was used.[15] In the wire drawing process, the finest copper wire with diameter of 0.04 mm is drawn through a series of dies. Before enameling pro-

cess, the bare wire is annealed in annealing oven to achieve necessary softness of the copper. The multi-stranded wire was used since it has the same average fatigue life as their individual constituent strands but the variance of that life is smaller. However, to maximize service life it was suggested that wire strands should be manufactured at the smallest diameter possible (without introducing structural flaws).

Stretching force that could be applied to the nerve could be adjusted in fine increments, using especially designed micrometer mechanism. Stretching force is transmitted via the surgical suture, attached serially to the nerve to the custom designed miniature force transducer, which is an integrating part of the experimental cell.

To measure a length of the neural segment stretching, a voltage divider realized by using precision linear potentiometer attached to sliding elements of a mechanical micrometer stretching system, was used (Spectrol, 20 kΩ).

Radial pressure applied onto the nerve when the cuff is installed, could be adjusted at different values in fine increments. For this purpose, especially designed precise mechanism containing a miniature custom designed force transducer, which was an integrating part of the experimental cell, was used. Namely, the cuff will be subjected to a proce-

dure of defining the pressure which appears when the cuff is installed on the nerve trunk with a diameter of 3 mm. The radial pressure in the cuff should be below the pressure of 2.66 kPa (20 mm Hg) which could induce an interference with intra-neural blood flow.

To maintain a constant temperature of 37 °C, a water bath circulator (Boehringer, Labor Manheim GmbH für Labortechnik, Perfectherm PFV, 20–65 °C, 220 V, 1000 W, Fixed Temperatures: (25/30/37/56) °C, Waterbath (36 × 14 × 13) cm, Capacity: 6,5 L), which controls a temperature within the range of ±0.003 °C, is used. For precise measurement and recording of a temperature just below the site where the cuff is mounted onto the nerve, the micro-BetaCHIP temperature probe (Part Number: 10K3MCD1), which is actually the smallest semi-conductive packaged thermistor device, was used. Namely, the probe is produced for applications where space is limited. The probes are extremely small (Diameter 0.457 mm, Nominal Length 3.18 mm) and fragile.

Results and discussion

In Figure 3, a fabricated ninety-nine electrode spiral cuff, actually installed into the cell, is presented. It could be seen that the nominal length of the cuff is 44 mm, external diameter is 5 mm and internal diameter is 2.5 mm.
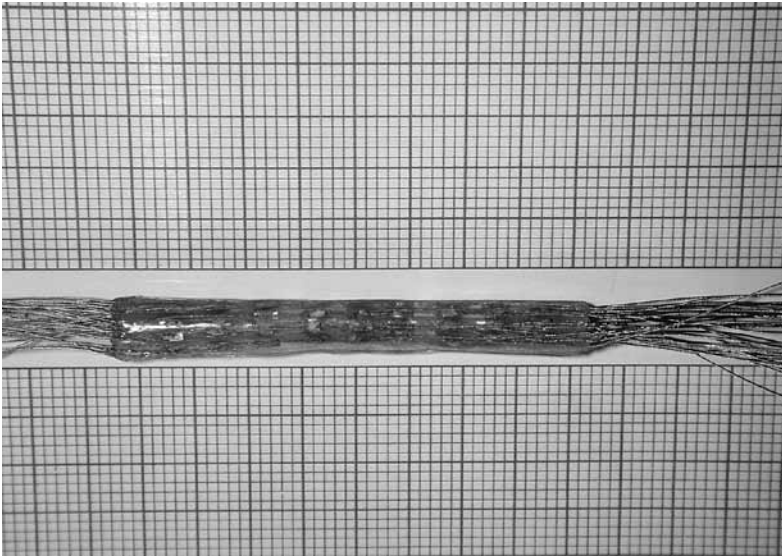
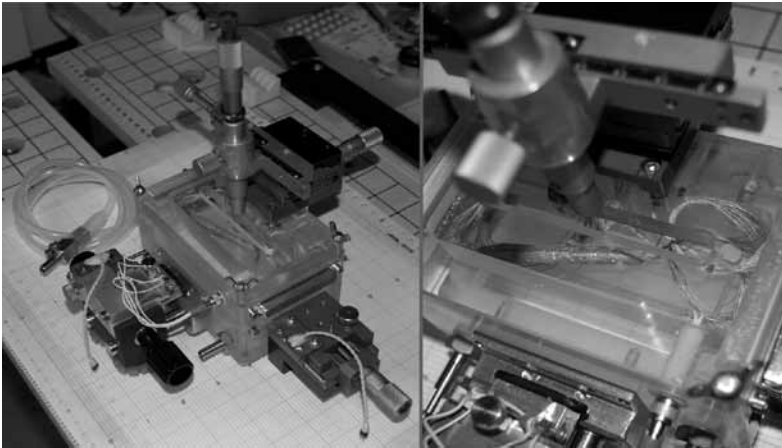**Figure 3.** Fabricated ninety-nine-electrode spiral cuff

Figure 4. Completed cell for electrochemical and electrophysiological measurements in peripheral nerves

In Figure 4 however, a completed cell enabling electrochemical and basic electrophysiological measurements that could be performed in functional peripheral nerve segment under simulated physiological environment, is presented.

In the lower left part of the figure, the micrometer mechanisms enabling precise measurements of stretching of the nerve and radial pressure are shown. In the upper right part of the figure however, a 3D micro-manipulator position-

ing system, enabling for the intra-neural micro-electrode used in the method of voltage clamp measurements to be positioned into the neural cell.

Our work contributed to the development of models and multi-electrode spiral cuffs to be used for efficient and safe selective stimulation of autonomous peripheral nerves and for selective recording of compound action potentials at the same time.

One weakness of a multi-electrode cuff manufacture however, is a technically demanding and a time consuming process. The technical solutions described in our study could be used in various animal and human basic studies concerning neurophysiology of internal organs, and their relation to bodily changes and diseases.

Conclusions

The cell enables for the electrophysiological technique of compound action potential measurement to be used in testing the proposed model under realistic conditions, using insulated functional left vagus nerve of a pig. Besides, the electrochemical technique of cyclic voltammetry could be used to delineate a safe operational potential window of platinum stimulating electrodes also under realistic conditions, using functional left vagus nerve of a pig. This

design has strong potential for applications in neuro-prosthetic technology in the future. For instance, it would be very desirable to control different internal organs for instance cardio-vascular system in patients with heart failure or atrial fibrillation by only one implanted system, e.g. on the vagus nerve.

Acknowledgements

References

[1]   Setty, A. B., Vaughn, B. V., Quint, S. R., Robertson, K. R., Messenheimer, J. A. (1998): Heart period variability during vagal nerve stimulation. *Seizure*, Vol. 7, pp. 213–217.

[2]   Zamotrinsky, A. V., Kondratiev, B., De Jong, J. W. (2001): Vagal neurostimulation in patients with coronary artery disease. Auton. *Neurosci*, Vol. 88, pp. 109–116.

[3]   Ali, I. I., Pirzada, N. A., Kanjwal, Y., Wannamaker, B., Medhkour, A., Koltz, M. T., Vaughn, B. V. (2004): Complete Heart Block with Ventricular Asystole During Left Vagus Nerve Stimulation for Epilepsy. *Epilepsy and Behavior*, Vol. 5, No. 5, pp. 768–71.

[4]   Agnew, W. F., McCreery, D. B. (1990): Considerations for safety with chronically implanted nerve electrodes. *Epilepsia* 31 Suppl 2, pp. S27–32.

[5]   De Ferrari, G. M., Sanzo, A., Schwartz, P. J. (2009): Chronic vagal stimulation in patients with congestive heart failure. Conf Proc IEEE Eng Med Biol Soc., pp. 2037-9

[6]   Labiner, D. M., Ahern, G. L. (2007): Vagus nerve stimulation therapy in depression and epilepsy: therapeutic parameter settings. *Acta Neurol. Scand.*, pp. 23–33.

[7]   Mortimer, J. T. (1981): Motor Prostheses. In Handbook of Physiology, Section 1. J. B. Brookhart and V. B. Mountcastle, (section eds.), V. B. Brooks (volume ed.), S. R. Geiger (executive ed.), American Physiological Society, Bethesda, MD., pp. 155–187.

[8]   Mc Neal, D. R., Bowman, B. R. (1985): Selective activation of muscles using peripheral nerve electrodes. *Med. & Biol. Eng. & Comput.*, Vol. 23, pp. 249–253.

[9]   Caldwell, C. (1971): Multielectrode electrical stimulation of nerve. In Development of Orthotic Systems Using Functional Electrical Stimulation and Myoelectric Control. Finnnal Report of Project 19-P-58396-F-01, University of Ljubljana, Yugoslavia, pp. 124–134.

[10]   Ferguson, A. S., Sweeney, J. D., Durand, D., Mortimer, J. T. (1987): Finite difference modeling of nerve cuff electric fields. Proc. 9th Ann. Conf. IEEE Eng. in Med. & Biol. Soc., Boston, pp. 1579–1580.

[11]   Naples, G. G., Mortimer, J. T., Yuen, T. G. H. (1989): Overview of peripheral nerve electrode design and implantation. In Neural Prostheses, Agnew W. F. and McCreery, D. B., Eds. Englewood Cliffs, NJ: Prentice Hall, pp. 108–145.

[12]   Naples, G. G., Sweeny, J. D., Mortimer, J. T. (inventors) (1986): Implantable cuff, Method and manufacture and Method of installation. U. S. Patent #4,602,624, July 29, 1986.

[13]   Sweeney, J. D., Ksienski, D. A., Mortimer, J. T. (1990): A nerve cuff technique for selective excitation of peripheral nerve trunk regions. IEEE Trans. BME-37, pp. 706–715.

[14]   Robblee, L. S., Rose, T. L. (1990): The electrochemistry of electrical stimulation. Proc. 12th Ann. Conf. IEEE Eng. in Med. & Biol. Soc., Philadelphia, pp. 1479–1480.

[15]   Scheiner, A., Mortimer, J. T., Kicher, T. P. (1991): A study of the fatigue properties of small diameter wires used in intramuscular electrodes. *Journal of Biomedical Materials Research*, Vol. 25, No. 5, pp. 589–608.

Assessment of heavy metal contamination in paddy soils from Kočani Field (Republic of Macedonia): part II

Ocena onesnaženja s težkimi kovinami v tleh riževih polj iz Kočanskega polja (Republika Makedonija): 2. del

Nastja Rogan Šmuc[1], *

[1]University of Ljubljana, Faculty of Natural Sciences and Engineering, Department of Geology, Aškerčeva cesta 12, SI-1000 Ljubljana, Slovenia

*Corresponding author. E-mail: nastja.rogan@guest.arnes.si

Abstract: The identification of heavy metals (Ag, As, Cd, Cu, Mo, Ni, Pb, Sb and Zn) mobility and availability in Kočani paddy soils was evaluated by sequential extraction procedure. According to the sum of the water soluble and exchangeable fractions for Ag, As, Cd, Cu, Mo, Ni, Pb, Sb and Zn measured in the paddy soils at Kočani Field, the mobility and bioavailability potential of the heavy metals studied declined in the following order: Cd > Mo > Sb > Zn > Cu > As > Pb > Ni > Ag. Cd was consistently bound to bioavailable and leachable fractions, as were Mo and Sb, which were also significantly present in the oxidisable fraction. Cu and As were mostly linked to the oxidisable fraction, indicating relative mobility under oxidising conditions. The reducible and reducible / residual fractions prevailed for Zn, Pb, Ni, and Ag, signifying a relatively low mobility capacity.

Izvleček: Po postopku zaporednega izluževanja sem ocenila mobilnost in biodostopnost težkih kovin (Ag, As, Cd, Cu, Mo, Ni, Pb, Sb in Zn) v tleh riževih polj na Kočanskem polju. Glede na vrednosti težkih kovin v vodotopni in izmenljivi frakciji se le-te kot najbolj mobilne in biodostopne pojavljajo v naslednjem vrstnem redu: Cd > Mo > Sb > Zn > Cu > As > Pb > Ni > Ag. Kadmij (Cd) je močno povezan z obema najbolj biodostopnima frakcijama, prav tako molibden (Mo) in antimon (Sb), ki v zmernih deležih nastopata tudi v oksidacijski

Original scientific paper

frakciji. Cu in As sta najmočneje povezana z oksidacijsko frakcijo in tako relativno mobilna v oksidacijskih razmerah. V redukcijski in redukcijsko-finalni frakciji pa prevladujejo naslednje šibko mobilne težke kovine: cink (Zn), svinec (Pb), nikelj (Ni) in srebro (Ag).

Key words: assessment of contamination, heavy metals, paddy soil, sequential extraction procedure, Kočani Field, Republic of Macedonia

Ključne besede: ocena onesnaženja, težke kovine, tla riževih polj, postopek zaporednega izluževanja, Kočansko polje, Republika Makedonija

Introduction

Compared with other compartments of the biosphere, the persistence of contaminants in soil is very long and the contamination of soil, especially by heavy metals, seems to be virtually permanent. The excessive accumulation of heavy metals in agricultural soils around mining areas is a great concern affecting the following situations:
- entrance of metals into the food chain, presenting a potential health risk to local inhabitants;
- loss of vegetation cover induced through phytotoxicity; and
- cycling of metals to surface soil horizons by tolerant plants to induce toxic effects on flora and fauna (Adriano, 2001; Kachenko & Singh, 2006; Liu et al., 2005; McLaughlin et al., 1999; Pruvot et al., 2006; Zhuang et al., 2008).

To evaluate the true short- and long-term environmental impact of heavy metals in soils, the most crucial factors to consider are their mobility and bioavailability through soil-plant systems. But only the soluble, exchangeable and chelated metal species in the soils are bioavailable in individual soil plant system (Kabata-Pendias & Pendias, 2001). Therefore, assessing the environmental risks requires the measurement of the total amount of heavy metals in soils and the total amount of heavy metals detected in the available fractions, also. A widely used modified method for the identification and evaluation of the availability or binding forms of heavy metals in soils is the sequential extraction procedure proposed by Tessier et al. (1979).

All previous investigations have shown and confirm the heavy metal contamination of paddy soils from Kočani Field (Republic of Macedonia) as a result of irrigation with riverine water which is affected by the inflow of acid mine and untreated effluents from the ore pro-

cessing facilities (Zletovo-Kratovo and Sasa-Toranica ore district) (DOLENEC et al., 2007; ROGAN et al., 2009; ROGAN ŠMUC, 2010; ROGAN ŠMUC, 2010). Consequently, the objective of this study was to apply the sequential extraction method (leaching procedure) in order to determine the bioavailability of heavy metals in the soil samples studied and to evaluate the environmental risk in the Kočani soil system area.

(ROGAN ŠMUC, 2010) were selected for the chemical partitioning analysis (binding forms) of Ag, As, Cd, Cu, Mo, Ni, Pb, Sb, and Zn by employing a sequential extraction procedure (LI et al., 1995; TESSIER et al., 1979) in a certified commercial Canadian laboratory (Acme Analytical Laboratories, Vancouver, B. C., Canada).

MATERIALS AND METHODS

Sequential extraction procedure

Kočani paddy soil samples (I-3, II-6, III-5, VI-4 and VII-2, Figure 1) with the highest heavy metal concentrations

The paddy soil samples, weighing 1 g, were placed in screw-top test tubes. To each sample 10 ml of leaching solution was added. Afterwards, the caps were screwed on and the tubes were subjected to the appropriate extraction procedure depending on the stage of the leach. For the sequential leaching, the sample was leached, centrifuged,
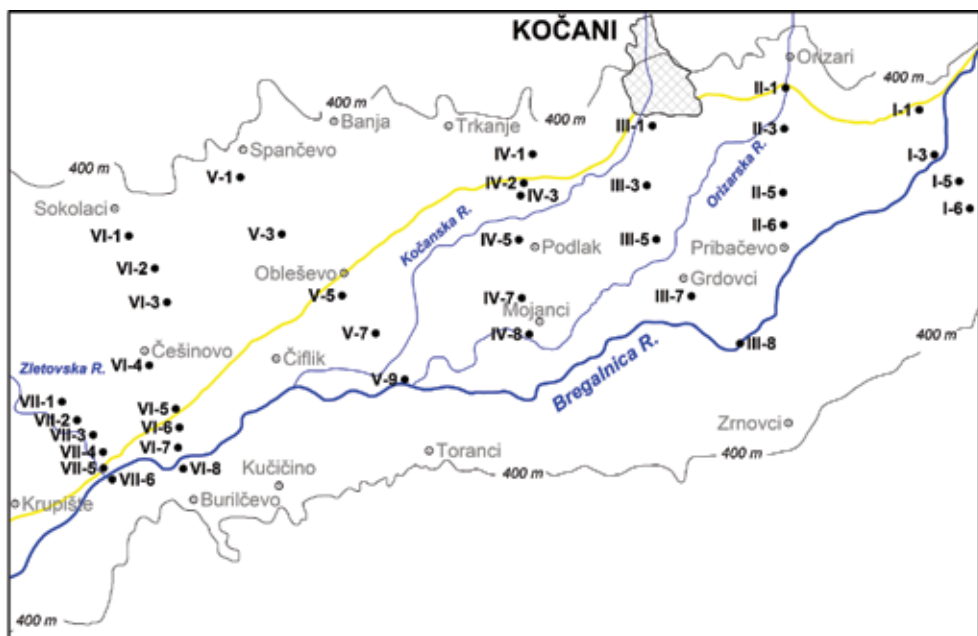

Figure 1. Paddy soil sample locations (sequential extraction procedure).

Table 1. Sequential extraction procedure (fractions and chemical reagents).

Step	Fraction	Chemical reagents
1	Water soluble	Distilled water
2	Exchangeable and carbonate bound	1 m ammonium acetate
3	Organic (oxidisable)	0.1 m sodium pyrophosphate
4	Reducible	Cold 0.1 m hydroxylamine hydrochloride
5	Reducible plus residual	Hot 0.25 m hydroxylamine hydrochloride

decanted and washed and then the residue was leached again in a five-step process from the weakest to strongest solution or chemical reagent. The procedure is presented in Table 1.

After the sequential extraction procedure, the concentration of the analysed elements in the solution was measured using a Perkin Elan 6000 ICP-MS for the determination of 60 or more elements. A QA/QC protocol incorporated a sample duplicate to monitor the analytical precision, a reagent blanks measured background and an aliquot of in-house reference material was used to monitor appropriate accuracy.

Results

The mobility and bioavailability of heavy metals in paddy soils mostly depend on their types of binding forms. Figure 2 represents the results of the sequential extraction procedure (heavy metal binding forms).
The water soluble fraction (1) constitutes the most mobile and potentially

the most available metal species easily released into the surrounding environment (Filgueiras et al., 2002).

The exchangeable fraction (2) includes metals weakly retained on the solid surface by relatively weak electrostatic interaction, metals that can be released by ion-exchange processes and metals that can be coprecipitated with carbonates. Changes in ionic composition, which influence the adsorption/desorption reactions or lower the pH, can cause the remobilisation of metals from this fraction (Filgueiras et al., 2002). Exchangeable metal ions are treated as those that are released most readily into the environment (Filgueiras et al., 2002).

The oxidisable fraction (3) corresponds to elements occurring as oxidisable minerals and organically bound metals. They are assumed to remain in the soil for longer periods but can be mobilised by decomposition processes. The degradation of organic matter under oxidising conditions (Filgueiras et al., 2002) can lead to a release of soluble heavy metals bound to this component.

The reducible fraction (4) comprises unstable metal forms connected with amorphous Mn hydroxides. The metals strongly bound to these oxides are thermodynamically unstable under reducing conditions (FILGUEIRAS et al., 2002).

In the reducible + residual fraction (5) the metals linked to amorphous Fe hydroxides (reducible part) under reducing conditions are expected to be released in nature. By contrast, the residual fraction contains naturally occurring crystalline Mn hydroxide minerals that can hold heavy metals within their crystalline matrix. Heavy metals in residual are not likely to be discharged under normal environmental conditions. Therefore, the metals associated with this fraction can only be mobilised as a result of chemical weathering (DEAN, 2007; FILGUEIRAS et al., 2002; FUENTES et al., 2004; KAZI et al., 2002).

In all paddy soil samples, Ag was dominantly associated with the reducible + residual fraction (5) and then, in minority, with the reducible fraction (4) (Figure 2a). This agrees with KABATA-PENDIAS & PENDIAS (2001), who demonstrated that despite several mobile complexes Ag is immobile in soils if the pH is above 4. The percentage of Ag present in the fractions followed the order: water soluble fraction (1) < exchangeable fraction (2) < oxidisable fraction (3) < reducible fraction (4) < reducible + residual fraction (5).

The highly relevant fraction of As in the paddy soil samples was bound to the oxidisable (3) and reducible + residual fraction (5). The association of As with the reducible fraction (4) was also highly significant (Figure 2b). This is confirms the general finding that although As compounds are readily soluble, As migration is greatly limited due to the strong sorption by organic matter, hydroxides and clays (KABATA-PENDIAS & PENDIAS, 2001). The percentage of As in the sequential extraction fractions followed the order: water soluble fraction (1) < exchangeable fraction (2) < reducible fraction (4) < oxidisable fraction (3) < reducible + residual fraction (5).

The chemical partitioning of Cd in the investigated samples indicated that Cd was mainly linked to the exchangeable fraction (2) and reducible fraction (4) (Figure 2c). The association of Cd with the two most labile fractions, exchangeable and reducible, is in agreement that Cd is most mobile in acidic soils within the range pH 4.5–5.5 (KABATA-PENDIAS & PENDIAS, 2001) (average pH in the paddy soils from Kočani Field: 5.5). The percentage of Cd in the determined fractions was in the order: water soluble fraction (1) < reducible + residual fraction (5) < oxidisable fraction (3) < reducible fraction (4) < exchangeable fraction (2).

The highest content of Cu was associated with the oxidisable fraction (3), followed by the reducible + residual fraction (5) (Figure 2d). Consequently, Cu forms highly stable complexes with the organic matter and its mobility and bioavailability can be controlled by binding with soluble organic matter (ADRIANO, 1986; LI et al., 2001; MBILA et al., 2001). The percentage of Cu in extraction fractions was in the following order: water soluble fraction (1) < exchangeable fraction (2) < reducible fraction (4) < reducible + residual fraction (5) < oxidisable fraction (3).

The most abundant fraction for Mo was the oxidisable fraction (3). Other important fractions for Mo were residual and water-soluble fractions (Figure 2e). This is supported by findings of KABATA-PENDIAS & PENDIAS (2001), that a great proportion of soil Mo is associated with organic matter and Fe hydrous oxides. The percentage of Mo present in the fractions followed the order: exchangeable fraction (2) < reducible fraction (4) < water soluble fraction (1) < reducible + residual fraction (5) < oxidisable fraction (3).

The reducible fraction (4) was the highest for Ni (Figure 2f) and the percentage of Ni in the fractions increases in the order: water soluble fraction (1) < exchangeable fraction (2) < oxidis-able fraction (3) < reducible + residual fraction (5) < reducible fraction (4). In soils, Ni is usually related to either organic matter or amorphous oxides, and at soil pH < 6 is easily available (KABATA-PENDIAS & PENDIAS, 2001). Results in this study are confirming this statement.

In the paddy soil samples, a large proportion of Pb was bound to the reducible + residual fraction (5), and the second most important fraction was the reducible (4) (Figure 2g). Results given by RIFFALDI et al. (1976) and KABATA-PENDIAS & PENDIAS (2001) also indicate that Pb is mainly associated with organic matter, Mn oxides and Fe and Al hydroxides. The percentage of Pb in the fractions followed the order: water soluble fraction (1) < exchangeable fraction (2) < oxidisable fraction (3) < reducible fraction (4) < reducible + residual fraction (5).

Sb was significantly connected with the oxidisable fraction (3) (Figure 2h). On the contrary, KABATA-PENDIAS & PENDIAS (2001) reported about strong association of Sb with Fe and Mn hydroxides. The percentage of Sb in other fractions was low and followed the order: water soluble fraction (1) < reducible fraction (4) < exchangeable fraction (2) < reducible + residual fraction (5) < oxidisable fraction (3).

Figure 2i shows that Zn in the paddy soils was dominantly associated with the reducible fraction (4) and the reducible + residual fraction (5). The association of Zn with Fe and Mn hydroxides in soils has been similarly widely recognised by KUO et al. (1983) and GONZALEZ et al. (1994). The less important associations of Zn with the water soluble and exchangeable fractions might indicate the influence of flooding in the paddy soils, because Zn migrates downwards readily in soil profiles (KABATA-PENDIAS & PENDIAS, 2001). The percentage of Zn determined in the fractions followed the order: water soluble fraction (1) < exchangeable fraction (2) < oxidisable fraction (3) < residual fraction (5) < reducible fraction (4).

The amounts of water soluble (1) and exchangeable (2) fractions are considered the most mobile and bioavailable fractions. Very high proportions of heavy metals in bioavailable fractions could indicate a strong contribution of anthropogenic metals in studied soils (WONG et al., 2002). According to the sum of water soluble (1) and exchangeable (2) fractions for the Ag, As, Cd, Cu, Mo, Ni, Pb, Sb and Zn detected in paddy soils in Kočani Field, the mobility and bioavailability of the heavy metals studied decline in the following order: Cd > Mo > Sb > Zn > Cu > As > Pb > Ni > Ag.

Cd was consistently bound to bioavailable and leachable fractions (1 and 2), as were Mo and Sb, which were also significantly present in the oxidisable fraction (3). Cu and As were mostly linked to the oxidisable fraction (3), indicating relative mobility under oxidising conditions. The reducible (4) and reducible + residual (5) fractions prevailed for Zn, Pb, Ni, and Ag, signifying a relatively low mobility capacity.

Rice cultivation in paddy fields generally requires moderate flooding. Different flooding conditions have various influences on the mobility and bioavailability of heavy metals. Fe and Mn oxides are important adsorbents of heavy metals in soils under oxidising conditions (LEE, 2006). However, under reducing conditions (flooding), a relatively high concentration of heavy metals is found in the exchangeable fraction because of the dissolution of heavy metals adsorbed on the Fe and Mn oxides (CHARLATCHKA & CAMBIER, 2000; LEE, 2006). We collected paddy soil samples in the oxidising conditions and from our study it is evident that Zn, Pb, Ni and Ag are mainly associated with the reducible (4) and reducible + residual (5) fractions and consequently less mobile.

Measured and calculated heavy metal impact on the Kočani paddy soils revealed the following order of the heavy
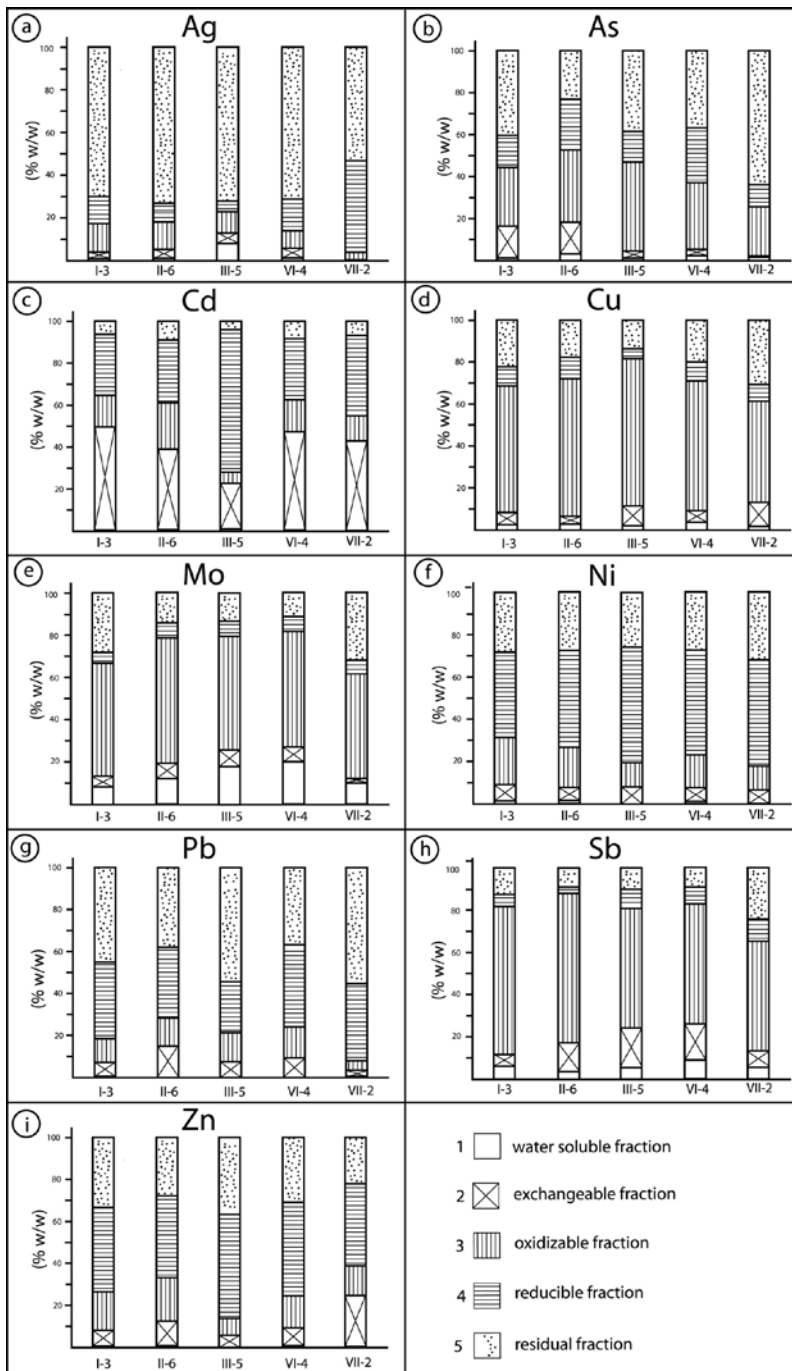
Figure 2. Heavy metal binding forms in paddy soil samples from sampling locations I-3, II-6, III-5, VI-4 and VII-2.

metals studied: Cd > As > Ag > Pb > Sb > Zn > Cu > Ni > Mo (Rogan Šmuc, 2010). However, the sequential extraction results are upgrading the previous mentioned study results (Rogan Šmuc, 2010), showing the mobility and bioavailability characteristics of heavy metals from soils to plants. According to the sequential leaching procedure results, Cd, Mo and Sb were consistently bound to bioavailable and leachable fractions and thus, they are treated as the most bioavailable to the surrounding ecosystems (plants). Therefore, a systematic study on heavy metal transfer from soils to crops and estimated daily intake for the local inhabitants of Kočani Field are essential.

Conclusions

Taking into account the sum of the water soluble (1) and exchangeable (2) fractions for Ag, As, Cd, Cu, Mo, Ni, Pb, Sb and Zn detected in the paddy soils at Kočani Field, the mobility and bioavailability of the heavy metals studied declined in the following order: Cd > Mo > Sb > Zn > Cu > As > Pb > Ni > Ag.

Cd was consistently bound to bioavailable and leachable fractions (1 and 2), as were Mo and Sb, which were also significantly present in the oxidisable fraction (3). Cu and As were mostly linked to the oxidisable fraction (3), indicating relative mobility under oxidising conditions. The reducible (4) and reducible + residual (5) fractions prevailed for Zn, Pb, Ni, and Ag, signifying a relatively low mobility capacity.

Systematic study on heavy metal transfer from soils to crops, estimated daily intake for the local inhabitants of Kočani Field and project for diminishing heavy metal content in contaminated soils are essential.

Acknowledgements

References

Adriano, D. C. (2001): *Trace elements in terrestrial environments: biogeochemistry, bioavailability and risks of metals* (2nd edition). New York: Springer-Verlag.

Charlatchka, R. & Cambier, P. (2000): Influence of reducing conditions on solubility of trace metals in contaminated soils. *Water Air and Soil Pollution*, 118, 143–167.

Dean, J. R. (2007): *Bioavailability, Bioaccessibility and Mobility of Environmental Contaminants*. England: John Wiley and Sons Ltd.

Dolenec, T., Serafimovski, T., Tasev, G.,

DOBNIKAR, M., DOLENEC, M., ROGAN, N. (2007): Major and trace elements in paddy soil contaminated by Pb–Zn mining: a case study of Kočani Field, Macedonia. *Environmental Geochemistry and Health*, 29, 21–32.

FILGUEIRAS, A.V., LAVILLA, I. & BENDICHO, C. (2002): Chemical sequential extraction for metal partitioning in environmental solid samples. *Journal of Environmental Monitoring*, 4, 823–857.

FUENTES, A., LLORENS, M., SAEZ, J., SOLER, M., ORTUNO, J. & MESEGUER, V. (2004): Simple and sequential extraction of heavy metals from different sewage sludges. *Chemosphere*, 54, 1039–1047.

KABATA-PENDIAS, A. & PENDIAS, H. (2001): *Trace Elements in Soils and Plants (3rd ed.)*. Boca Raton: CRC Press.

KACHENKO, A.G. & SINGH, B. (2006): Heavy metals contamination in vegetables grown in urban and metal smelter contaminated sites in Australia. *Water Air and Soil Pollution*, 169, 101–23.

KAZI, T., JAMALI, G., KAZI, G., ARAIN, M., AFRIDI, H. & SIDDIQUI, A. (2002): Evaluating the mobility of toxic metals in untreated industrial wastewater sludge using a BCR sequential procedure and a leaching test. *Anal. Bioanal. Chem.*, 374, 255–261.

LEE, S. (2006): Geochemistry and partitioning of trace metals in paddy soils affected by metal mine tailings in Korea. *Geoderma*, 135, 26–37.

LI, X. D., COLES, B. J., RAMSEY, M. H., THORNTON, I. (1995): Sequential extraction of soils for multielement analysis by ICP-AES. *Chemical Geology*, 124, 109–123.

LI, X. D., SHEN, Z. G., WAI, O. W. H. & LI, Y. S. (2001): Chemical forms of Pb, Zn and Cu in the sediment profiles of the Pearl River Estuary. *Marine Pollution Bulletin*, 42, 215–223.

LIU, H., PROBST, A., LIAO, B. (2005): Metal contamination of soils and crops affected by the Chenzhou lead/zinc mine spill (Hunan, China). *Science of the Total Environment*, 339, 153–166.

MBILA, M. O., THOMPSON, M. L., MBAGWU, J. S. C. & LAIRD, D. A. (2001): Distribution and movement of sludge derived trace metals in selected Nigerian soils. *Journal of Environment Quality*, 30, 1667–1674.

McLAUGHLIN, M. J., PARKER, D. R. & CLARKE, J. M.(1999): Metals and micronutrients – food safety issues. *Field Crops Res*, 60, 143–63.

PRUVOT, C., DOUAY, F., HERVE, F. & WATERLOT, C. (2006): Heavy metals in soil, crops and grass as a source of human exposure in the former mining areas. *Journal of soils and sediments*, 6, 215–220.

RIFFALDI, R., LEVI-MINZI, R. & SOLDATINI, G.E. (1976): Pb absorption by soils. *Water, Air and Soil Pollution*, 6, 119.

ROGAN, N., SERAFIMOVSKI, T., DOLENEC, M., TASEV, G., DOLENEC, T. (2009): Heavy metal contamination of paddy soils and rice (*Oryza sativa* L.) from Kočani field (Macedonia). *Environmental Geochemistry and Health*, 31, 439–451.

ROGAN ŠMUC, N., DOLENEC, T., SERAFI-

MOVSKI, T., TASEV, G., DOLENEC, M. (2010): Distribution and mobility of heavy metals in paddy soils of the Kočani Field in Macedonia. *Environmental earth sciences*, 61, 899–907.

ROGAN ŠMUC, N. (2010): *Heavy metal contamination of soils and crops in teriary basins: a case study of Kočani Field (Macedonia)*. Phd thesis, 108 pp.

TESSIER, A., CAMPBELL, P. G. C., BISSON, M. (1979): Sequential extraction procedure for the speciation of particulate trace metals. *Analytical Chemistry*, 51, 844–851.

ZHUANG, P., MCBRIDE, M. B., XIA, H., LI, N. & LI, Z. (2009): Health risk from heavy metals via consumption of food crops in the vicinity of Dabaoshan mine, South China. *Science of the Total Environment*, 407, 1551–1561.

WONG, S. C., LI, X. D., ZHANG, G., QI, S. H., MIN, Y. S. (2002): Heavy metals in agricultural soils of the Pearl River Delta, South China. *Environmental Pollution*, 119, 33–44.

Investigations of carbide precipitates in modified 9 % Cr steel using different electron spectroscopy techniques

Preiskava karbidnih izločkov v modificiranem jeklu z 9 % Cr z uporabo različnih elektronskih spektroskopskih metod

Aleš Nagode[1, *], Matjaž Godec[2], Gorazd Kosec[3], Ladislav Kosec[1]

[1]University of Ljubljana, Faculty of Natural Sciences and Engineering, Aškerčeva cesta 12, SI-1000 Ljubljana, Slovenia
[2]Institute of Metals and Technology, Lepi pot 11, SI-1000 Ljubljana, Slovenia
[3]Acroni, d. o. o., Cesta Borisa Kidriča 44, SI-4270 Jesenice, Slovenia

*Corresponding author. E-mail: ales.nagode@omm.ntf.uni-lj.si

Abstract: For characterization of carbide precipitates in modified 9 % Cr steel we used a multitechnique approach based on electron beam, combining field emission scanning electron microscopy (FE-SEM), Auger electron microscopy (AES) and energy dispersive X-ray spectroscopy (EDXS). In this paper the principles of the analytical methods are explained and their complementarity is demonstrated.

Izvleček: Za preiskavo karbidnih izločkov v modificiranem jeklu z 9 % Cr smo uporabili različne metode na osnovi elektronskega curka. Kombinirali smo vrstično elektronsko mikroskopijo na poljsko emisijo (FE-SEM), Augerjevo elektronsko mikroskopijo (AES) ter energijskodisperzijsko spektroskopijo rentgenskih žarkov (EDXS). V tem prispevku smo skušali prikazati osnove analitičnih metod in njihovo komplementarnost.

Professional Paper

INTRODUCTION

Electron spectroscopy techniques are techniques that use the interaction of high energy electrons with a sample to perform an analysis. For the characterization of the microstructure we used a multi-technique approach based on electron beam, combining field emission scanning electron microscopy (FE SEM), Auger electron microscopy (AES) and energy dispersive x-ray spectroscopy (EDXS). Auger electron spectroscopy (AES) and energy dispersive x-ray spectroscopy (EDXS) are both analytical techniques used for the elemental analysis or chemical characterization of samples. However, AES is a surface sensitive technique, while EDXS is not. The aim of the present work was to demonstrate the carbide precipitates investigation in vanadium and niobium modified creep-resistant 9 % Cr steel by using FE SEM, AES and EDXS, and especially, to explain the principles, specialities as well as the advantages and disadvantages of particular technique.

The microstructure of modified 9 % Cr steel consisted of tempered martensite containing $M_{23}C_6$ carbide particles formed during a final normalizing and tempering heat treatment. The thermal stability of $M_{23}C_6$ is relatively high, which produce the basic creep strength by precipitating on subgrain boundaries during tempering. The $M_{23}C_6$ carbides

increase creep strain in these alloys by retarding subgrain growth, which is a major source of creep strain. In modified 9 % Cr steel there are also MX precipitates present i.e. VN and Nb(C, N). During the creep exposure, the precipitation of Laves phase and additional precipitation of VN and Nb(C, N) take place. The introduction of MX precipitates in modified 9 % Cr steel by alloying with V, Nb and N can improve creep rupture strength by approximately 50 % at 600 °C. A fine distribution and high thermal stability of the carbide and nitride particle is a key to high creep strength. It is well known that microstructural evolution of steels determines the life and long time behavior of the material To evaluate service time of the components it is very important to characterize the microstructure.[1–6]

THEORETICAL BACKGROUND

Electron bombardment of a sample produces a large number of effects in a sample because the incident electrons interact with specimen atoms in a variety of ways (Figure 1). These effects allow us to use different electron spectroscopy techniques in analysing sample.

In the present work we have been focused only on the secondary electrons used for imaging and characteristic x-rays and Auger electrons used for the analysis.
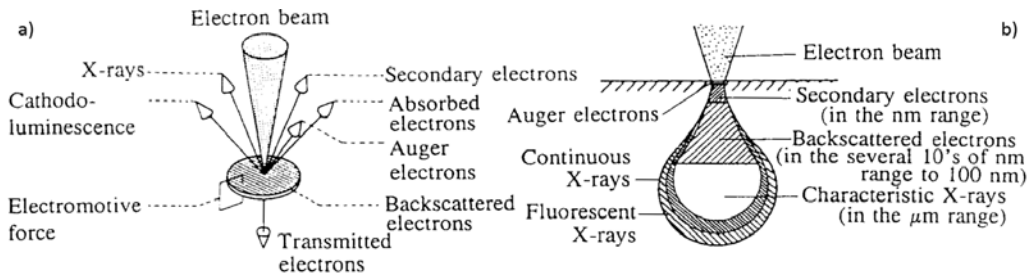
Figure 1. The effects produced by electron bombardment of the material:
a) shows the different type of information obtained; b) shows the regions
from which the information is generated.

Secondary electron imaging (SEI)
The incident electrons cause electrons to be emitted from the sample due to elastic and inelastic scattering events within the sample's surface and near-surface material. Emitted lower-energy electrons resulting from inelastic scattering are called secondary electrons.

To create an image, the incident electron beam is scanned in a raster pattern across the sample's surface. The emitted secondary electrons are detected for each position in the scanned area by an electron detector. The topography of surface features influences the number of electrons that reach the secondary electron detector from any point on the scanned surface. This local variation in electron intensity creates the image contrast that reveals the surface morphology. Therefore, secondary electrons provide high-resolution imaging of fine surface morphology.

Auger electron spectroscopy (AES)
AES is one of the most commonly used techniques for surface analysis and it is used to determine the atoms present at a surface, their concentrations and also their chemistry. Auger electrons with a characteristic kinetic energy can only escape from the outer 0.5–5 nm of a solid surface. This effect makes AES an extremely surface sensitive technique. Auger electron emission (Fig. 2) is one of the two possible relaxation mechanisms for an excited atom with a vacancy in a core level.

The ground state of the system is shown in Figure 2a). In Figure 2b) an incident electron has created a hole in the core level K by ionization. The hole in the K shell is filled by an electron from L_2, releasing an amount of energy $(E_K - E_{L2})$ which can be given to another electron. In this example the other electron is in the L_3 shell, and it is then ejected with energy $(E_K - E_{L2} - E^*_{L3})$. E^*_{L3} is the binding energy not of L_3 in its ground state, but in the presence of a hole in L_2. The doubly ionised final state is shown in Figure 2c).
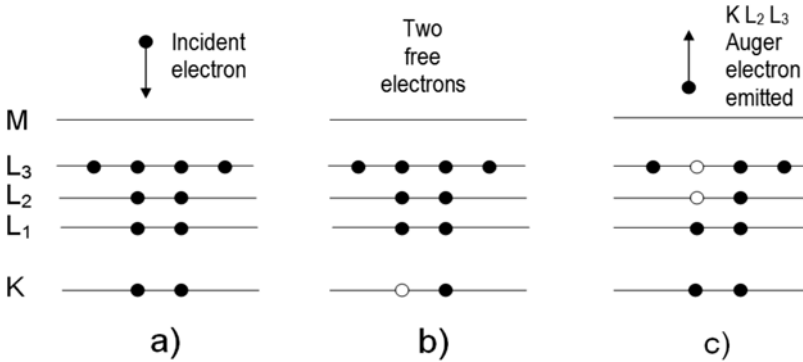
Figure 2. Schematic diagram of the process of Auger emission in a solid.
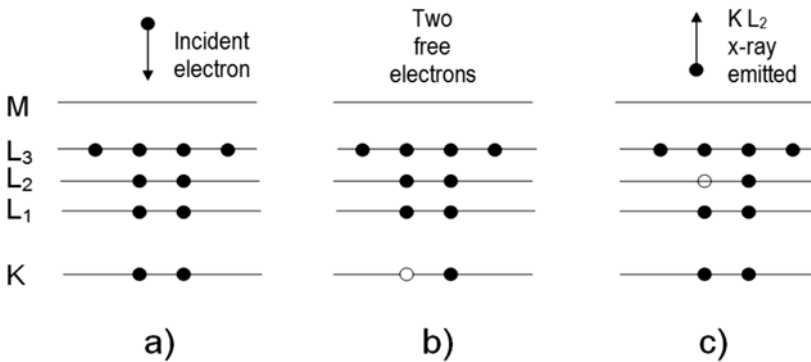

Figure 3. Schematic diagram of X-ray emission.

Energy dispersive X-ray spectroscopy (EDXS)

The other relaxation mechanism is x-ray fluorescence, in which an x-ray is emitted instead of an Auger electron (Figure 3). The x-ray emission is generated by beam of energetic electrons when it impinges on a specimen. As it has already been explained in the process of Auger electron emission an incident electron (Figure 3a) has created a hole in the core level K by ionization (Figure 3b). The hole in the K shell is then filled by an electron from the L_2, releasing an amount of energy $(E_K - E_{L2})$. Instead of giving the energy to another electron as in the case of Auger electron emission (Figure 2c), this energy can appear as an x-ray of energy $hv = (E_K - E_{L2})$ (Figure 3c). With heavier elements, x-ray emission is more likely, while with lighter elements, the probability of Auger emission increases and x-ray emission decreases.

Energy dispersive x-ray spectroscopy (EDXS) is thus, an investigative meth-

od which exploits x-ray emission and is commonly used in an SEM for the elemental identification and quantification of sample chemical composition. The x-rays depending on accelerating voltage and material density are generated in a region about 1–3 μm in depth, and therefore EDXS is not a surface science technique.

Experimental procedure

The investigated material is a section of steam pipe made of modified 9 % Cr steel which has been in service for 10 000 h at about 550 °C. Samples were matallographically prepared for microstructural characterization by grinding, polishing and etching in a water solution of ferric chloride with addition of HCl (5 %). AES investigations were carried out in a Microlab 310F VG-Scientific instrument. A primary electron beam of 10 keV was used. FE AES studies were performed after removing amorphous C and O by Ar$^+$ ion sputtering. EDXS analyses were carried out on a FE-SEM (Jeol JSM-6500F) equipped with INCA Energy 400 ED spectrometer. EDXS analyses were performed at several spots using two different accelerating voltages, namely 10 kV and 20 kV. After EDXS points analyses also EDXS maps were done using accelerating voltage of 10 kV to show the elemental distribution.

Results and discussion

Auger electron spectroscopy (AES)

As it has already been mentioned, the AES analysis was performed in several spots (Figure 4) after removing adsorbed amorphous C and O by Ar$^+$ ion sputtering.
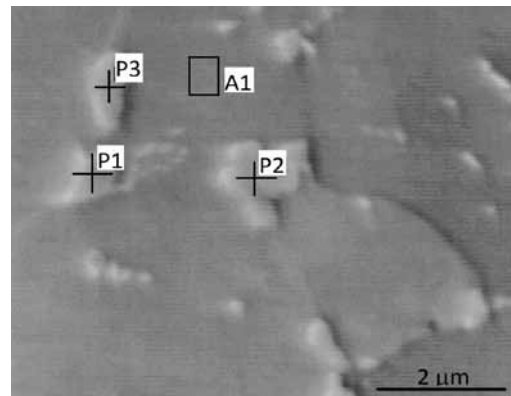

Figure 4. SE image of the microstructure of modified 9 % Cr steel where AES analyses were performed.

The AES analyses of the precipitates (P1, P2 and P3 in Figure 5) reveal the presence of Fe, Cr, Mo and C (Figure 5). However, AES analysis of the matrix (A1 in Figure 5) shows no Auger peaks from Mo or Cr because their concentration in the matrix is below the detection limit for the AES. The oxygen Auger peaks can be seen on AES spectra are due to contamination because of a longer duration of the analysis. Despite UHV conditions inside the vacuum chamber of the SEM/AES apparatus there are

still present molecules of oxygen which adsorbed on the surface after sputtering.

An enlarged detail of carbon peak obtained by AES analysis of the precipitates (Figure 6) shows a typical carbidic shape. That means that the investigated precipitates are carbides.

AES point analyses made on the carbide precipitate and matrix (Figure 7) indicate that the carbides are not homogenous but are mixed iron-chromium-molybdenum carbides (Figure 8). The oxygen peak is, again, because of contamination of the surface of specimen in the vacuum chamber because of longer duration of the analyses.
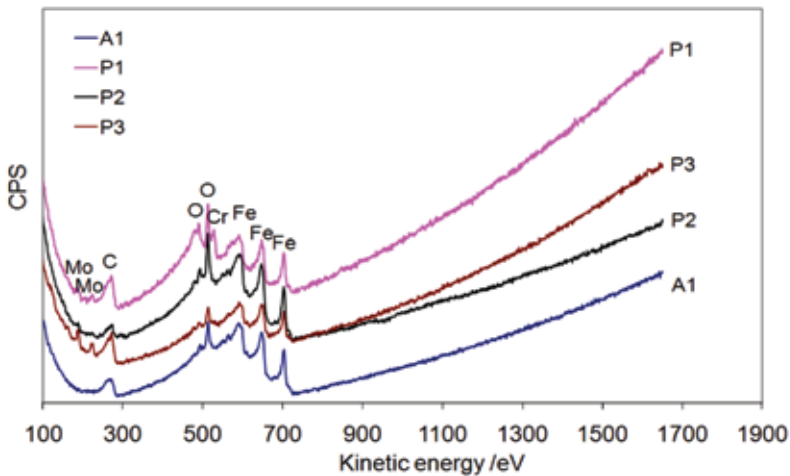
Figure 5. Auger spectra in P1, P2, P3 and A1
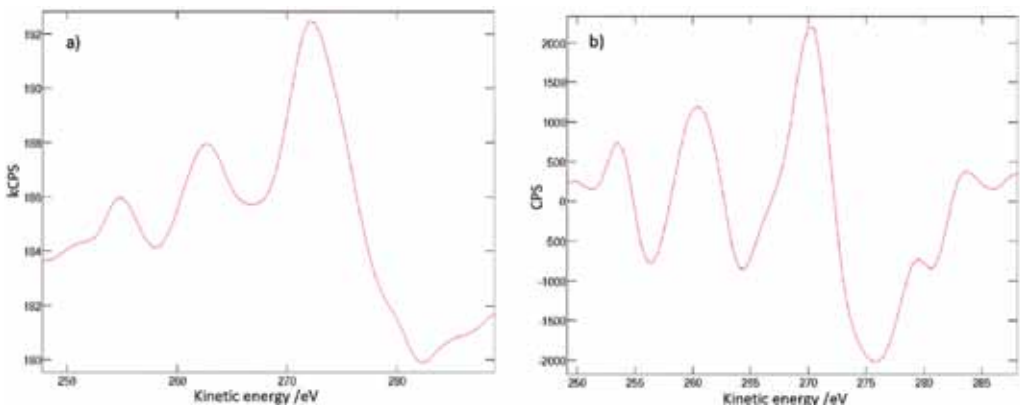
Figure 6. Auger spectra from carbide: a) direct spectra; b) derivative spectra
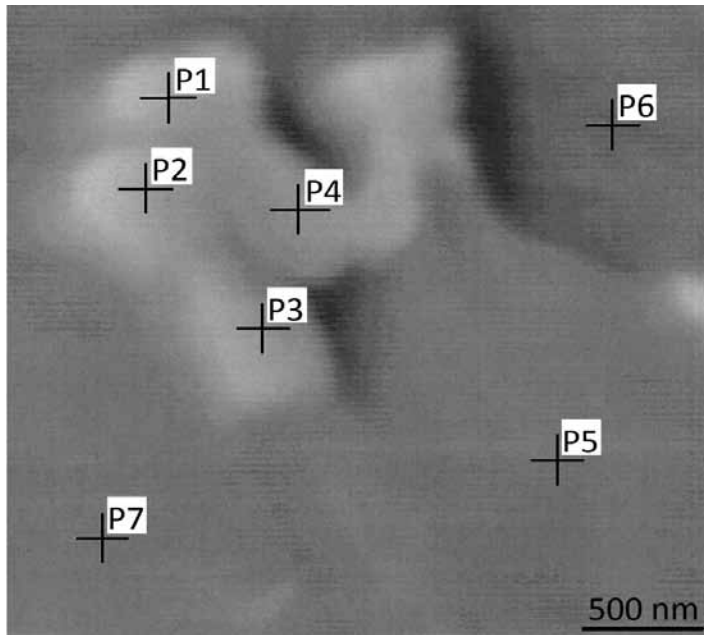
Figure 7. SE image of the area where AES point analyses were performed
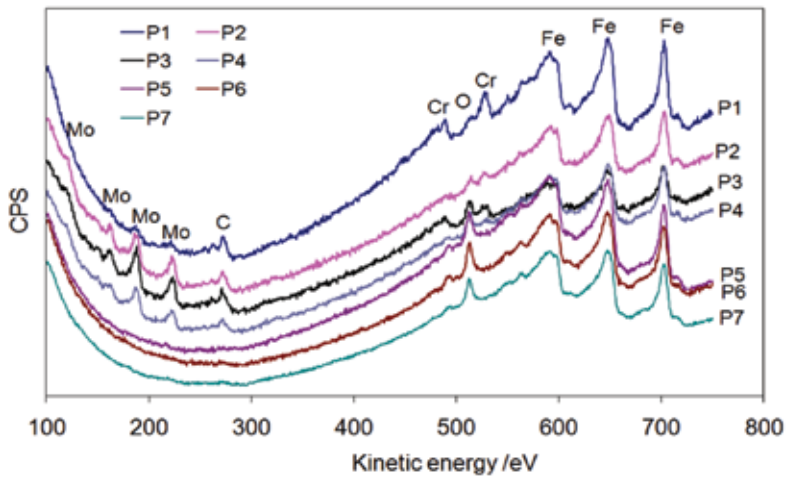

Figure 8. Auger spectra in P1, P2, P3, P4, P5, P6 and P7

Energy dispersive X-ray spectroscopy (EDXS)

The EDXS analyses of carbide precipitates (Figure 9) were performed at different accelerating voltages of incident electron beam, namely 10 kV and 20 kV, respectively.

The results of EDXS analyses performed with the accelerating voltage of 20 kV show smaller concentrations of Cr, Mo, C and Si in precipitates than at 10 kV (Table 1). The reason for this lies in different size of analysed volume. The smaller the accel-
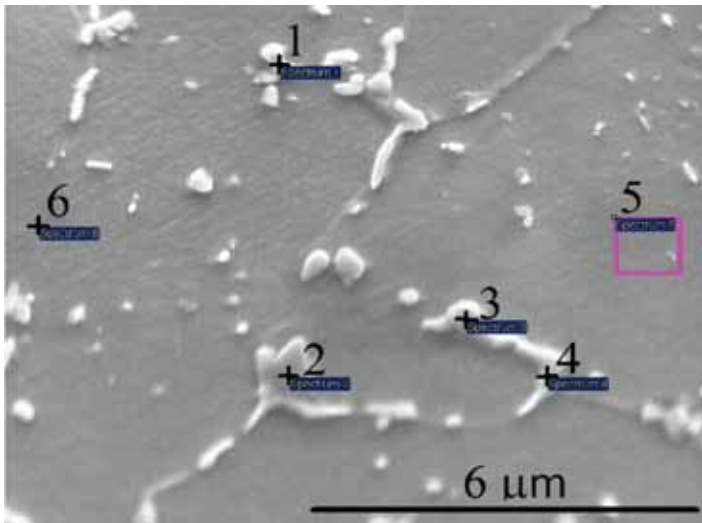

Figure 9. SE image of microstructure of modified 9 % Cr steel where EDXS analysis was made

Table 1. Material composition of different elements at several spots using different accelerating voltages of incident electron beam.

AC = 20 kV	Concentration in mole fractions, x/%					
	C	Si	Cr	Fe	Ni	Mo
Spectrum 1	19.51	0.63	11.22	65.94	1.16	1.53
Spectrum 2	13.43	1.36	7.11	72.88	3.00	2.22
Spectrum 3	13.57	1.39	6.52	73.19	2.85	2.49
Spectrum 4	16.45	1.86	7.67	66.84	3.16	4.02
Spectrum 5	7.57	0.40	3.56	86.14	1.99	0.35
Spectrum 6	7.29	0.42	4.81	85.74	1.74	0.00
AC = 10 kV	Concentration in mole fractions, x/%					
	C	Si	Cr	Fe	Ni	Mo
Spectrum 1	20.88	0.48	22.17	53.19	0.56	2.71
Spectrum 2	14.10	1.59	6.04	72.85	1.45	3.97
Spectrum 3	14.64	1.76	10.11	67.15	2.03	4.31
Spectrum 4	22.47	3.02	14.56	48.92	2.20	8.83
Spectrum 5	7.72	0.19	4.42	86.50	0.80	0.36
Spectrum 6	5.68	0.15	2.36	90.28	1.52	0.00

erating voltage is the smaller is ana-lysed volume. Thus, the characteristic x-rays at accelerating voltage of in-cident electron beam of 20 kV come not only from the carbide precipitates but also from a larger region of sur-rounding matrix, which consists of lower concentrations of Mo, Cr and C than precipitates.

Although the analysed volume is smaller in the case of using 10 kV, some part of x-rays during EDXS analysis of precipitates still comes from the matrix. Therefore, Ni and Si were obtained by the analyses of the carbides and the content of Fe is higher than it should be. The EDXS analysis of carbon is problematic as well. Since the applied scanning electron microscope is not equipped with cold trap that would absorb the residual gases, the carbon present in vacuum chamber is baked on the specimen surface by electron beam. Thus, a content of C, especially in the matrix is too high.

Since better EDXS quantitative re-sults were obtained at lower accel-erating voltage of incident electron beam also EDXS maps were record-ed at 10 kV (Figure 10). EDXS maps which show the elemental distribu-tions confirm that the precipitates are richer in C, Mo and Cr than the matrix. As well as EDXS point analy-ses also EDXS map of Si shows an increased concentration of Si in the carbide precipitates according to the matrix. It has been suggested that this is not due to the presence of Si in the precipitates but because of the en-richment of Si close to $M_{23}C_6$/matrix interface, since the solubility of Si in these carbides is very low.[4]

Because AES is a surface sensitive technique and EDXS is not, the spatial resolution of AES and EDXS differ significantly. The advantage of AES is the information about the chemi-cal state of the present element which can be obtained from AES spectrum. AES of the precipitates showed that carbon line shape was typical for car-bide and thus, it can be concluded that carbon in the precipitates was present as carbide. However, the quantitative AES analysis is not as precise as in the case of EDXS analysis and, thus, it was not even performed. The first reason lies in the sensitivity factors for AES quantitative analysis which are not well determined for com-pounds, while the second is signal-to-noise ratio which is much better in the case of EDXS.[7] However, none of these two techniques are the most proper for the determination of type of the carbides. For that purpose diffrac-tion techniques, for instance trans-mission electron microscope (TEM), X-ray diffraction (XRD) or electron backscatter (EBSD) are much better choice.
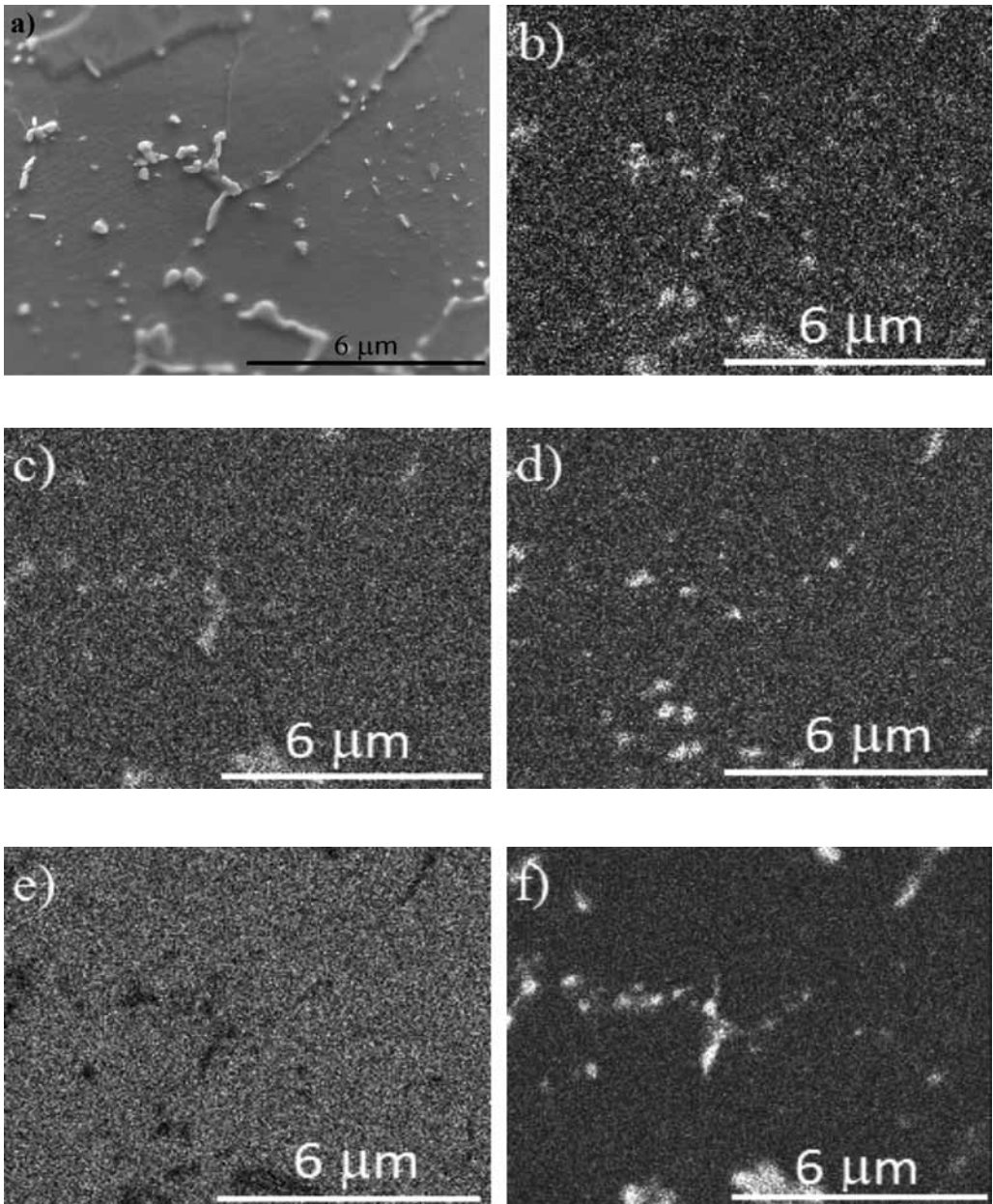
Figure 10. Element distribution from EDXS: a) SE Image, b) C, Kα; c) Si, Kα; d) Cr, Kα; e) Fe, Kα; f) Mo, Lα.

Conclusions

In this paper the application of Auger electron spectroscopy (AES) and energy dispersive x-ray spectroscopy (EDXS) were presented for characterization of carbide precipitates in modified 9 % Cr steel. AES is a surface sensitive technique, while EDXS is not. The Auger electrons come from the top few atomic layers of the surface (0.5–5 nm), while characteristic x-rays from 1–3 µm, depends on the accelerating voltage of incident electron beam and material density. AES showed that the precipitates contain C, Fe, Cr and Mo which was also confirmed by EDXS analyses. AES measurement of C line shape showed that the carbon in the precipitates was present as carbide. Carbide precipitates were not homogeneous but were mixed iron-chromium-molybdenum carbides. Silicon enrichment close to the carbide precipitate/matrix interfaces was also observed. In the case of EDXS analysis of the precipitates the results obtained by lower accelerating voltage of incident beam (10 kV) were much better since less x-rays come from the matrix. However, for the determination of the types of carbides other techniques, such as diffraction techniques (TEM, XRD, EBSD) should be used.

References

[1] FOLDYNA,V., KUBON, Z., FILIP, M., MAYER, K. H., BERGER, C. (1996): Evaluation of structural stability and creep resistance of 9–12 % Cr steels. *Steel Research*, Vol. 67, No. 9, pp. 375–381.

[2] HALD, J. (1996): Metallurgy and creep properties of new 9–12 % Cr steels. *Steel Research*, Vol. 67, No. 9, pp. 369–374.

[3] EGGELER, G., NILSVANG, N., ILSCHNER, B. (1987): Microstructural changes in a 12 % chromium steel during creep. *Steel research*, Vol. 58, No. 2, pp. 97–103.

[4] LUNDIN, L. M., HÄTTESTRAND, M., ANDREN, H. O. (2000): *Redistribution of Elements during Ageing and CreepTtesting of 9–12 % Chromium Steels,* Advanced Materials for 21st Century Turbines and Power Plant", Proc. 5th Int. Charles Parsons Turbine Conf., EDS. A. Strang, WM Banks, R.D. Conroy, GM McColvin, J.C. Neal and S. Simpson, Book 736, IOM Communications, London, pp. 603–617.

[5] HÄTTESTRAND, M. (2000): *Precipitation Reactions at High Temperatures in 9–12 % Chromium Steels,* PhD Thesis. Department of Experimental Physics, Chalmers university of Technology and Göteborg university, Göteborg, Sweden, 2000, pp. 1–19.

[6] KANEKO, K., MATSUMURA, S., SADAKATA, A., FUJITA, K., MOON, W. J., OZAKI, S., NISHIMURA, N., TOMO-

KIYO, Y. (2004): Characterization of carbides at different boundaries of 9Cr-steel*, Material Science and Engineering*, Vol. 374, A, pp. 82–89.

[7]   GODEC M., ŠETINA BATIČ, B., MANDRI- NO, DJ., NAGODE, A., LESKOVŠEK, V., ŠKAPIN, S. D, JENKO, M. (2010): Characterization of the carbides and martensite phase in powder-metallurgy highspeed steel. *Materials characterization*, Volume 61, Issue 4, pp. 452–458.

Reconstruction of two road tunnels

Rekonstrukcija dveh cestnih predorov

Jakob Likar[1, *], Melanija Huis[2], Andrej Likar[2]

[1]University of Ljubljana, Faculty of Natural Sciences and Engineering, Aškerčeva cesta 12, SI-1000
Ljubljana, Slovenia
[2]Geoportal, d. o. o., Slovenia

*Corresponding author. E-mail: jakob.likar@ntf.uni-lj.si

Abstract: Reconstruction of road tunnels in so far, as shown in this article, in the Republic of Slovenia has not yet been performed. In the Tunnel Ljubno and the Tunnel below Ljubljana Castle is determined the stable situation. Here we are focusing mainly on the primary lining of tunnel tube, even a fifty or many years to function. For the purpose of the reconstruction have been made more detailed analysis of several important parameters in terms of providing long-term stability of the wider area and the normal function of the tunnel. The project provided technical solutions to the reconstruction which has been successfully performed and to consider a valid technical standards used in the Republic of Slovenia. The final arrangement of the external parts of the reconstructed tunnel tube no changes involved in pre-planned architectural designs. The time course of reconstruction of the Tunnel below Ljubljana Castle corresponded to the time schedule of Municipality of Ljubljana. All participants who collaborated in the reconstruction process were satisfied, because all executed works were done properly with valid technical standards.

Izvleček: Vsebina prispevka se nanaša na opis načrtovanja in rekonstrukcije dveh cestnih predorov v Sloveniji. Prvi je na avtocesti A2 Karavanke–Obrežje, drugi v Ljubljani pod Ljubljanskim gradom. Oba sta bila zgrajena po drugi svetovni vojni. Metoda gradnje predorov je bila tedaj prilagojena vgradnji toge in debele nearmirane primarne obloge brez talnega oboka. Načrtovanje in izvajanje obeh rekon-

---

strukcij je potekalo v skladu z veljavnimi predpisi in smernicami, ki določajo dimenzije in varnostne pogoje pri gradnji sodobnih predorov. V prvi vrsti je bilo ugotovljeno, da profila predorov ne izpolnjujeta osnovnih zahtev. Pri načrtovanju različnih faz rekonstrukcije, vključno z odstranitvijo notranjih oblog, predvsem v predoru Ljubno, so bile upoštevane geološke in geotehnične lastnosti hribin ter geomehanske meritve pri gradnji sosednje predorske cevi. Posebna pozornost je bila namenjena načinu načrtovanja tehnologije gradnje z upoštevanjem meritev nabrekalnih tlakov v sosednji na novo zgrajeni cevi predora Ljubno. Rekonstrukcija predora pod Ljubljanskim gradom, ki je posebej prikazana v tem prispevku, je bila načrtovana in izvedena iz varnostnih razlogov, saj je bila notranja obloga razpokana in dotrajana. Ta je bila v celoti odstranjena, drenažni sistem za hribinsko vodo pa izdelan na novo. Prav tako sta bila na novo vgrajena betonska temelja, hidroizolacija z notranjo oblogo ter vozišče. Temu je sledila vgradnja sodobne elektrostrojne opreme. Obe rekonstrukciji predorov, ki sta prvi tovrstni v Sloveniji, sta potekali hitro in učinkovito. Projekta sta bila tehnično zahtevna tako glede geotehničnih razmer, kar velja za predor Ljubno, kot tudi glede izvajanja zaporednih faz rekonstrukcije glede na izjemno kratek rok izvedbe, saj je zapora prometa v predoru pod Ljubljanskim gradom povzročala velike zastoje na širšem območju centra Ljubljane.

Key words: Road tunnel, Reconstruction old tunnel, Numerical method, Geostatical 3D analysis, Primary shotcrete lining, Inner concrete lining

Ključne besede: cestni predor, rekonstrukcija starega predora, numerične metode, geostatična 3D-analiza, primarna obloga iz brizganega betona, notranja betonska obloga

Introduction

When assessing the technological progress of the construction of tunnels, it is necessary to ask what technical conditions were present before 60 or more years ago. Although the technical capabilities at the time of construction of underground structures significantly worse than today, most of the tunnels that were built, operated relatively well. Particularly the static stability should be appointed because it was maintained in the different rock environments. It also appeared that the installed concrete inner lining which were exposed to the negative effects of aggressive atmosphere, which is often

found in road tunnels, kept accepted working conditions.

In planning phase of reconstruction the tunnels which were built in between 50. and 60. years of a past century required special expert assessment which included the knowledge about techniques and technologies that were used during construction. It was found that global stability of Tunnel Ljubno and Tunnel below Ljubljana Castle is relatively adequate with a few expected uncertainties.

Important requirements of both reconstructions are adaptations to technical and transport requirements which as for new built tunnels as for reconstructions of tunnels include all geometric elements relating to structural and electrical-mechanical conditions. In this case the provided quality drainage has were included waterproofing, stability, requirements for inner lining, pavements and all necessary safety devices.

Taking into account the conditions which were present after the Second World War, the construction of the two tunnels were of high quality without real stability problems until today, according to that time available technological capabilities. More detailed analyses of conditions in the tunnels before reconstruction reveal the stability problems of the invert in Tun-

nel Ljubno, which was built without it. Another outstanding problem to ensure safety in the Tunnel below Ljubljana Castle was in derogation of cracked and partially deteriorated inner lining and ineffective water drainage (Figure 10). In both cases the technical solutions which proposed tunnel designer Geoportal, d. o. o., were accepted and successfully realized.

RECONSTRUCTION OF THE RIGHT TUBE IN TUNNEL LJUBNO

In the northern part of motorway section A2 Karavanke – Obrežje, the old right tube (part of old regional road) close to the new built Tunnel Ljubno left tube, is planned for reconstruction which has included motorway section too. The existing alignment run continue from the west side of the Viaduct Peračica, right tunnel tube and continue to the Viaduct Ljubno in the Jesenice direction – Austrian border.

Reconstruction of the tunnel tube includes extension of the current clearance profile to the standard which allows two lanes 3.75 m width, one intervention lane width 3.20 m and two intervention corridors 0.5 m width. The amount of excavated material in the profile is approximately 86 m² per running meter of tunnel. On Figure 1 the location and the old existing cross section of the right tunnel tube is shown.
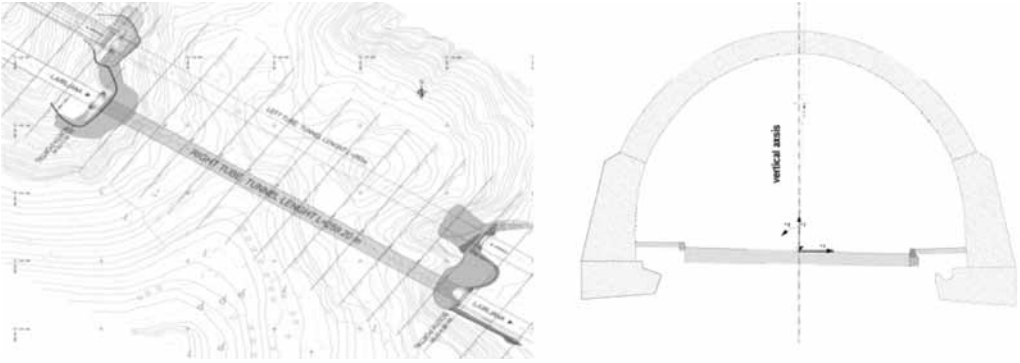
Figure 1. Location of the reconstructed right tunnel tube and cross-section of the right tunnel tube before reconstruction.

Geological and geotechnical conditions

In order to design reconstruction right tunnel tube optimally there were carried out extensive field and laboratory investigations and explorations of characteristic ground materials present in the tunnel area. All mentioned investigations were carried out before the design of new left tunnel tube was done. Special attention was paid relating to investigating the hard clay (Sivica) in which almost full excavation process was expected. Design of excavation and primary support lining was done in an appropriate way because the geological and geotechnical field investigations were carried out in extensive amount. Field's research comprised geological mapping, boreholes drilling, Standard Penetration Tests (SPT) and Pressuremeter Tests. Laboratory tests were included measurements of moisture content, UCS, Triaxial Shear Tests and measurements of swelling potential and deformability of hard clay (Sivica). Changing the rheological conditions shown significant differences in results of performed tests on hard clay (Sivica).

It was found that in a dry environment hard clay (Sivica) has solid strength properties, while contacts with water causes the relatively high presence of swelling potential.

The results revealed the presence of swelling potential, not clear demonstrate the unique possibilities of activation swelling process during reconstruction. This important fact was not measured because the applied ground load on primary lining was smaller against the load calculated from laboratory swelling tests.

The results of monitoring measurements in pressure cells (and extensometers), which were built during the con-
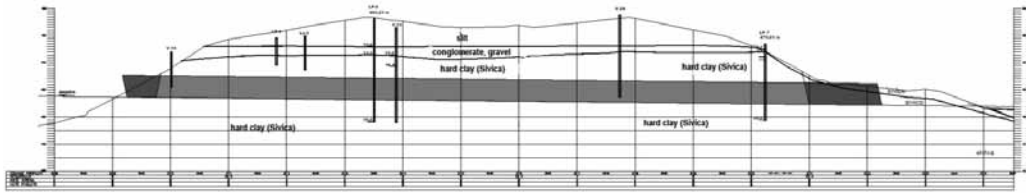
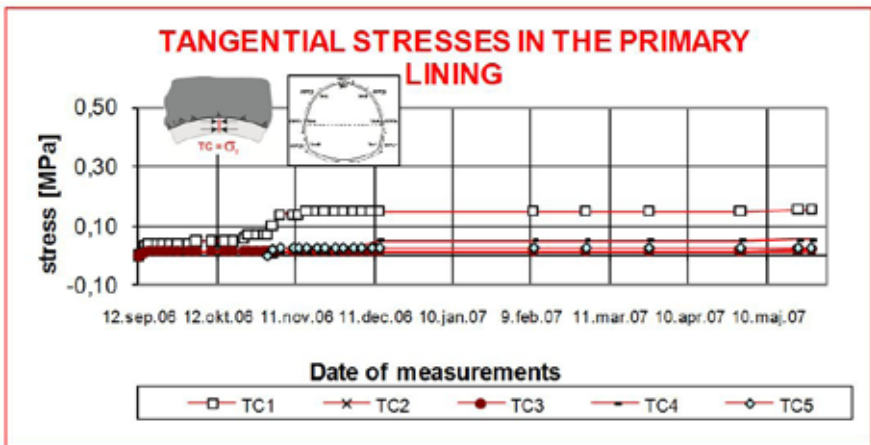**Figure 2.** Longitudinal profile of the right tunnel tube.

Figure 3. Measurement results of circular (tangential) stress in the primary lining in left tunnel tube
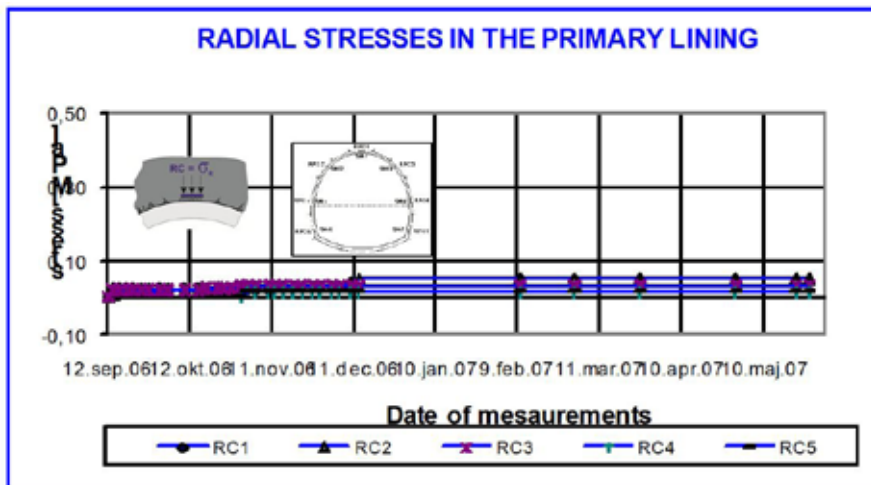

Figure 4. The results of measurements of radial stress on the contact between the primary lining and surrounding rock in the left tunnel tube.

struction of the left tunnel tube in the same geological geotechnical conditions did not show additional increases in circular (tangential) and radial stress (see Figures 3 and 4). In the future the swelling potential will not produce additional stresses on the inner lining, because the primary lining has enough loading capacity. The process which explain swelling pressure increasing in investigating ground shows that the closure of cracks depends of ground water isolation.

This is consistent with the results of extensive research by various swelling rocks (Wittke, 2000, 2002), which have rheological properties similar to hard clay (Sivica). It has been proven that naturally developed swelling pressures are much lower or minimum than those which are obtained from laboratory investigations.

Due to the fact that the rock in contact with ground water expose to effect of self sealing, the potential ability is to reduce swelling by the pores closed. In reality the swelling pressure was reduced with smaller water permeability of rocks. Based on the above observations and interpretations the calculation of bearing capacity of primary lining were taken into account.

Technical characteristics of the existing right tunnel tube

Professional assessment of the situation before reconstruction demonstrated that the existing tunnel lining was in a good condition, exception of portals where a lot of water was flowing since the drainage was not working properly.

Spaced contacts between the tunnel lining and portal structures and some working stitches inside the tunnel allowed flowing water into the tunnel. Road surface was in worse condition, mostly due to excessive traffic loads, and additionally because of the invert was missing.
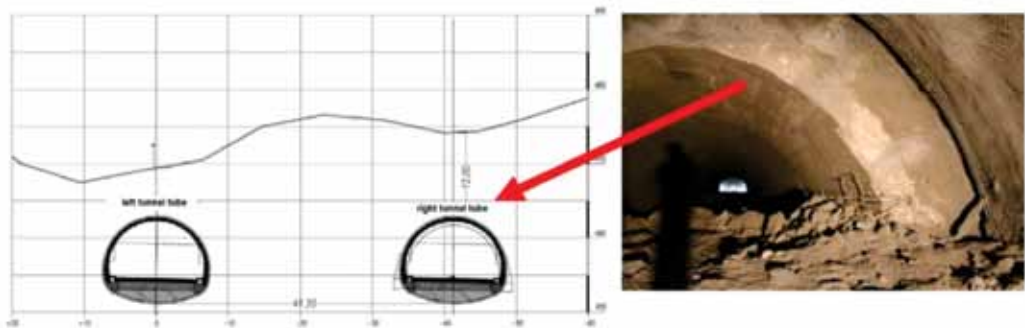

Figure 5. Cross-sections of the left tunnel tube and right tunnel tube which was reconstructed.

The main elements of the existing tunnel layout are:
- total length of tunnel tube: 232.24 m
- longitudinal slope: –1.14 % (in the direction of Ljubljana)
- the transverse slope of pavement: –2.5 %
- maximum overburden: 25 m

Total length of the right tunnel tube after reconstruction with cut and cover sections is 257.20 m. Spacing between tunnel tubes axis is 41.2 m, as shown in Figure 5.

Geostatic analyses and technical solutions of reconstruction

For the purposes of determining the amount of the primary support measures for the excavation profiles several 2D and 3D geostatic finite element analyses were done. To provide sufficient load capacity of support (ULS - ultimate limit states) the primary lining was dimensioned according to the corresponding steps and phases of excavation and primary lining installation.

When planning the excavation steps, special attention was paid to the level of serviceability (SLS – serviceability limit states) where the extension of the influence area was determined.
The steps and stages were designed in a way to prevent additional displacements in the left tunnel tube, caused by reconstruction of old tube.

Figure 6 shows the size of the radial displacements in the direction into the excavation area after re-profiling top heading, bench and invert. Results of analyses showed that the excavation process in right tube has not influence on the area around existing left tunnel tube.

Geotechnical assessments were taken into account the characteristics of hard clay (Sivica) and all necessary measures to reduce the risk of water and air which could affect on the stability of excavation profile.
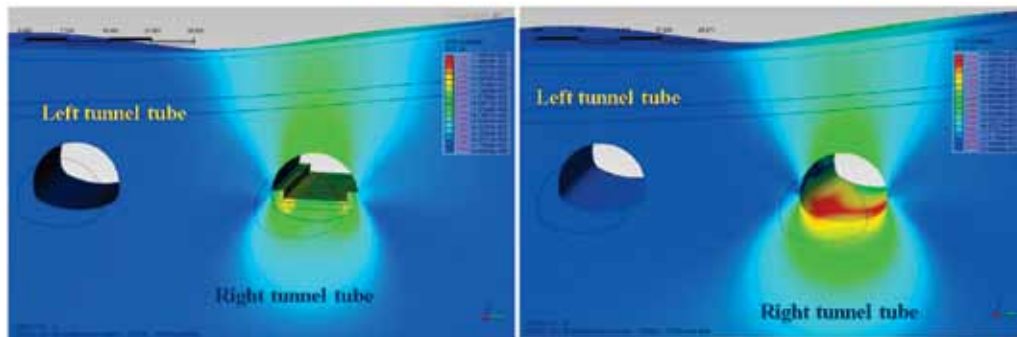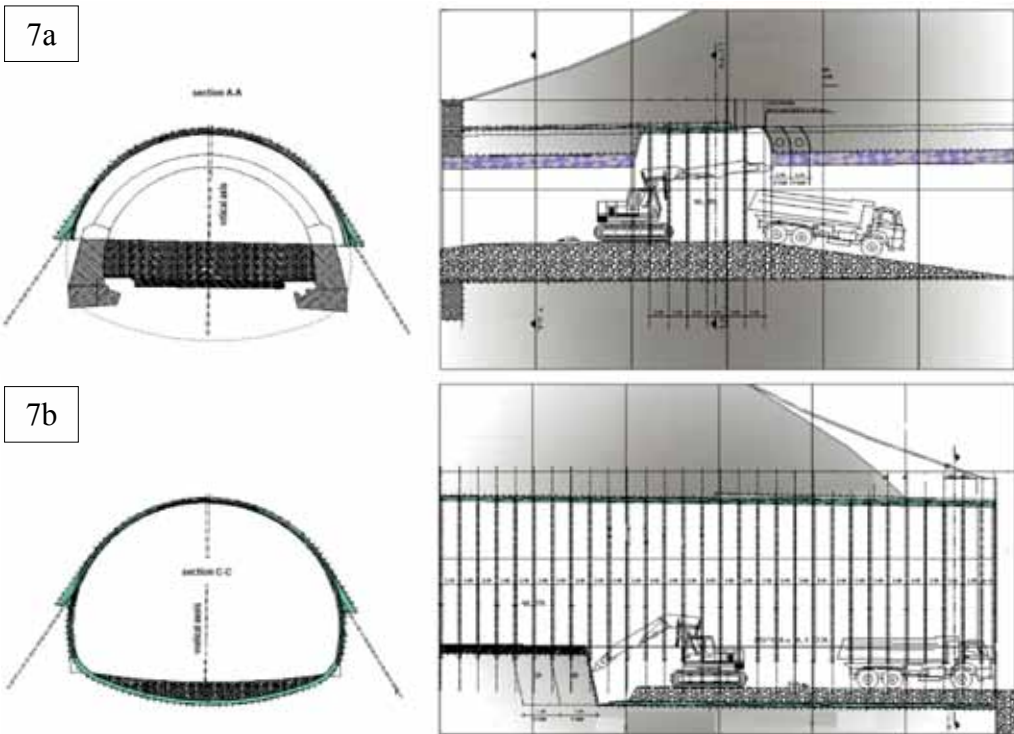

Figure 6. Radial displacements around the excavation and installation of primary support after excavation of top heading bench and invert

Figures 7a and 7b Method of excavation and installation of primary lining after excavation of top heading, bench and invert.

Project covered the operations of drilling and rock bolting if it is necessary, but without use water in terms of swelling limited.

Reconstruction of the right tunnel tube took place in five phases successively one to another:

- excavation of top heading and installation of primary support (Figure 7a.),
- excavation of bench and invert and installation of primary support (Figure 7b.),
- construction of portal structures (Figure 7b.),

- installation of abutments and waterproofing membrane and inner lining (Figure 7b.),
- final civil works (Figure 7b.).

RECONSTRUCTION OF THE TUNNEL BELOW LJUBLJANA CASTLE

Municipality of Ljubljana started the activities for the reconstruction of the Tunnel below Ljubljana Castle in the month of July 2009. The primary purpose of reconstruction is elimination and replacement of ceramic linings,
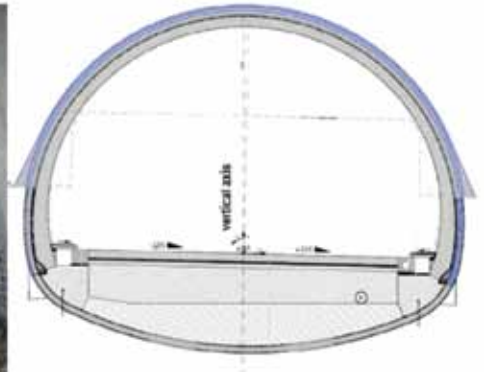
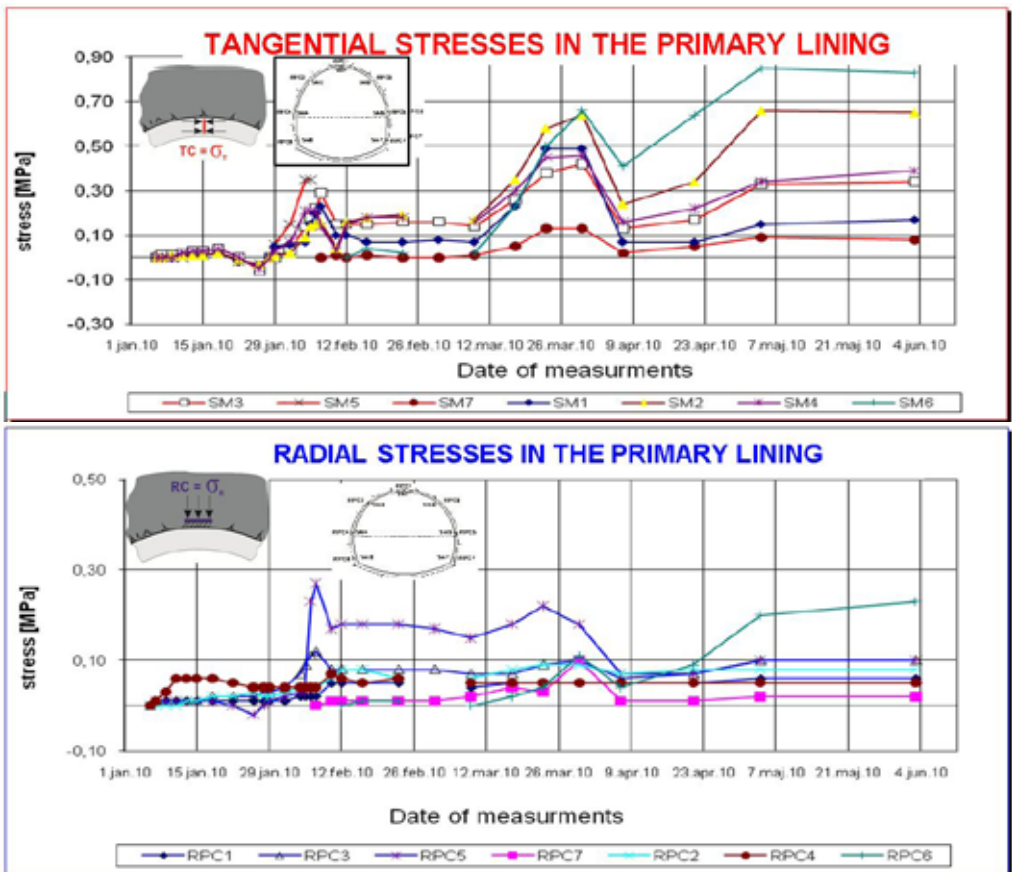**Figure 8.** The final cross-section of right tunnel tube after reconstruction.

Figure 9. The measurement results of circular (tangential) and radial stress in primary lining of left tunnel tube during reconstruction of right tunnel tube.
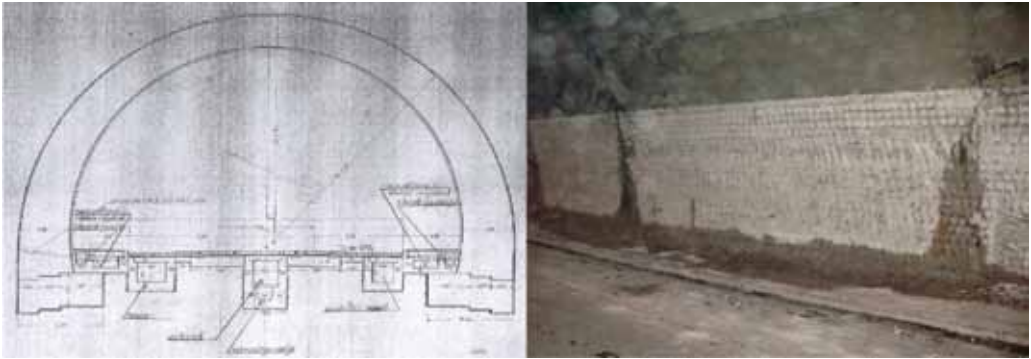
Figure 10. Transverse profile of the tunnel below Ljubljana Castle was dedicated to traffic in 1959. The damages were identified in 2009.

prevention seepage of water into tunnel, reconstruction of cracks in the concrete, painting the tunnel and partial reconstruction of electro-mehanical installations.

Introduction

The Tunnel below Ljubljana Castle was built in the fifties of last century and was constructed by so called old construction method of several smaller audits, which were allowed the gradual concreting of supporting arch, which was 1 m thick or more. To the supporting arch was installed bitumen insulation and at the final stage was installed a thin inner lining due to draining water. The drainage has been resolved by precast lining. The water has drain through channels in the longitudinal system which was blockade over the years.

The tunnel was dedicated to a transport in 1959 as a direct connection between the Poljanska road in Karlovška road. It was built as a two-way tunnel in according with the standards force at that time. It has function without majors interventions or repairs since opening until today. In the last period, the inner tunnel lining began to appear cracks and consequently smaller inflows, which were result of dilapidation of inner lining. ZRMK was conducted research in order to establish the internal structure of the tunnel and concluded that inner lining is 3 cm to 15 cm thick, non-uniformity built in the (axis of the tunnel tube) tunnel and partially cracked. In addition to the reduced static stability of the inner lining was influenced by blocked drainage system. This was a potentional cause of increased hydrostatic water pressure to the inner lining. Well-know example is the Tunnel Ljubelj, there occurred years ago a defect from inner concrete lining due to increasing water pressure, this causing a serious accident. In all this it cannot be excluded neither affect of aggressive tunnel atmosphere and frostiness.

Route of the tunnel and geological conditions of the area

Rout of the road in the tunnel running from the junction with Karlovška road at the south tunnel portal (chainage km. 0+000) to Kopitar road at the south tunnel portal (chainage km. 0+487.73). Surveyable tunnel situation is shown in Figure 11.

Geological structure of the area where the tunnel was built relatively stable with the exception of the last third of the tunnel tube on the south side. This fact is confirmed by research wells that were drilled in the primary lining and the surrounding area before reconstruction was performed. The surrounding soil consisted by mostly sandstones, partially siltstones, extremely minor part of slate. At several places, the present phenom-enon of a ground water which infiltrates into the tunnel with the wider area of the Castle hill. All the springs are channelled in a drainage system so the normal stress conditions are provided in the lining around the tunnel tube.

The main elements of tunnel alignments are:
- total lenght of tunnel tube: 487.73 m
- maximum height above sea level: 298.25 m (South Portal)
- longitudinal bend varies from 0.2 % to 1.3 % and decreasing in the direction of chainage increasing (direction Vodnik Market)
- the pavement superlevation: pavement is performed in the roof slope and decrease from the axis of pavement, left – right +2.0 % to –1.3 %
- maximum overburden: 65 m.

Figure 11. A synotropic situation the Tunnel below Ljubljana Castle.

The technical solution to a permanent tunnel rehabilitation mostly includes:

- removal of the inner lining layer and preparation for drainage of water including drilling of drainage wells,
- making of waterproofing with PVC foil
- making longitudinal drainage with cross drainage
- concreting new inner lining with a special tunnel panelling,
- to settle pavements by using installation cable ducts
- colouring the tunnel up to a height 4 m.

Tunnel rehabilitation technology

To ensure prescribed bright pavement profile and having regard to the Regulation on technical standards and conditions for the design of road tunnels in the Republic Slovenia. The reconstruction of the tunnel included removal of existing inner lining to a depth up to 25 cm in the crown, then followed excavation for foundations and concreting foundations in excavation round in the length of 12 m.

At places where caused a major damages in the lining such, the gaps were stabilized local by wired nets Q189 and shotcrete C20/25 to equalization. Reinforcing nets were fixed to the primary liner with anchors RA $\phi = 28$ mm length $L = 30$ cm. The drainage of pit water from behind the primary lining is regulated by the drainage boreholes $\phi = 48$mm layer tunnel tube length of $L = 1.5$ m in span 1 borehole/2.25 m².

On sections with higher inflows are on those tunnel points drilled lining drainage wells $\phi = 100$ mm and install perforated drainage pipes $\phi = 75$ mm length $L = 1$m. After installing the drainage system has been performed layer of shotcrete C20/25 to equalization ruggedness in the thickness of approximately 3 cm,
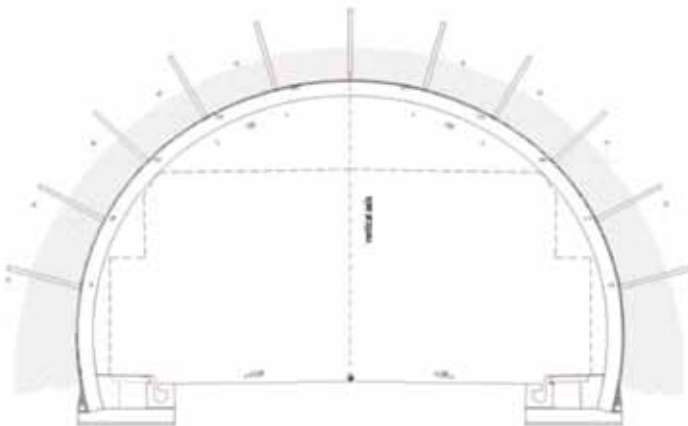

Figure 12. The measure of controlled collection and drainage of background water by drainage bore holes.
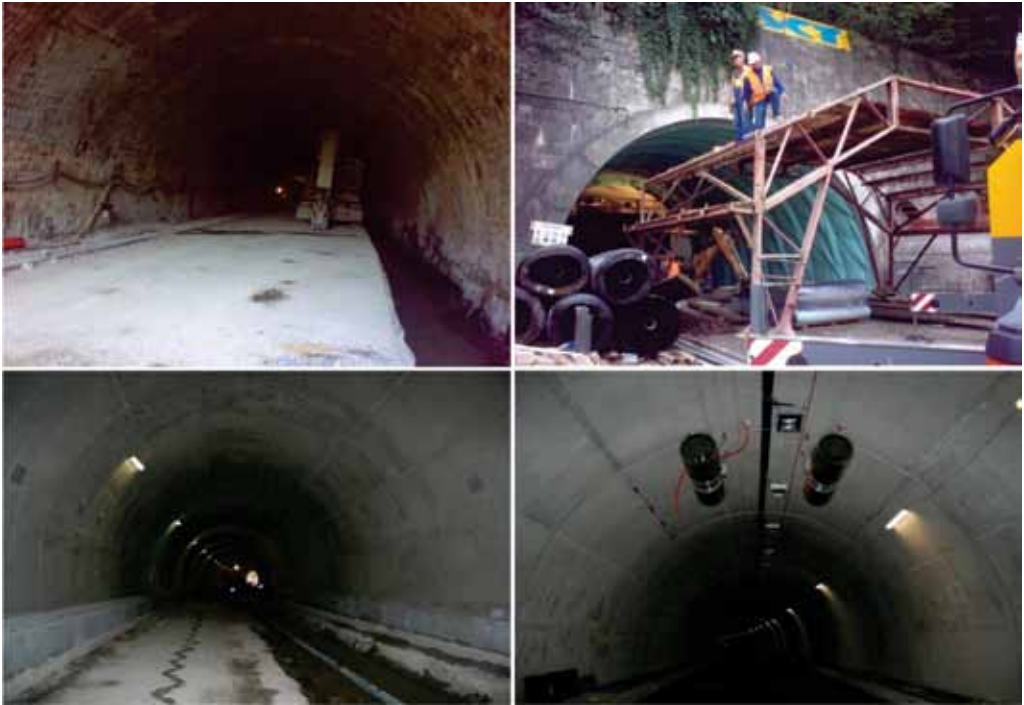
Figure 13. View an excavation for the installation of a new foundation and preparation for the installation of inner lining in the substructure roads and laying asphalt pavement and installation of electrical equipment in the reconstruction of the tunnel.

Figure 14. The final appearance of the tunnel when it was re-dedicated to a traffic 11. 11. 2009.

then follows the stage of installing waterproof layer including the installation of three-dimensional nets layer of polyamide fibbers and non-flammable waterproofing layer foil across the tunnel tubes. The last phase include excavation round concreting ($L_k = 12$ m) reinforced concrete inner lining 30 cm in thickness. Figure 13 shows the reconstruction of certain procedures tunnel.

Conclusions

- Successful reconstruction and rehabilitation of 50 years and older road tunnels was made on the basis of relevant applied researches and project documentation.
- Surprisingly the primary lining of cast concrete were in good condition even after 50 or more years, although at the time of installation technology was not on such a level as it is today.
- Those considerations are stimulative in the context of verification of long-term stability of the tunnel. In recent years it has been built many such objects in Slovenia and abroad.
- Although some of the technological reconstruction phases are similar to construction of the new tunnels which were performed, but it is necessary to consider the specific conditions of execution.
- Using the results of laboratory studies swelling properties of hard clay (Sivica) is conditionally justified.

Intensity of swelling pressures was able to reduce in the Tunnel Ljubno due to consideration of a self-protective effect.
- 3D geostatic analyses were performed in the context of checking a compliance of primary and inner linings and they proved to be useful in terms of rational construction planning.
- Consideration of the spatial effect is essential for high quality design of structural tunnel elements. All works were performed quality in the prescribed time limit at rehabilitating the Tunnel below Ljubljana Castle so that is a legitimate case of a good practise in the rehabilitation of tunnels in the urban environment.

References

[1]   GEOPORTAL, d. o. o. (2009), "Predor LJUBNO – desna cev na AC A2 Karavanke – Obrežje; odsek Brezje–Podtabor km 28+780 do km 30+300", faza PGD, Ljubljana.

[2]   SIST EN 1990, SIST EN 1991, SIST 1992-1-1, SIST EN 1997-1.

[3]   TNO D. (2008), "Midas GTS" in 2.5.1. Netherlands.

[4]   GEOPORTAL, d. o. o. (2009), "Sanacija predora pod Ljubljanskim gradom", faza PZI. Ljubljana.

[5]   Uredba o tehničnih normativih in pogojih za projektiranje cestnih predorov v Republiki Sloveniji, Uradni list RS, št. 48, 11. 5. 2006.

Author`s Index, Vol. 58, No. 1

INSTRUCTIONS TO AUTHORS

RMZ-MATERIALS & GEOENVIRONMENT (RMZ- Materiali in geookolje) is a periodical publication with four issues per year (established 1952 and renamed to RMZ-M&G in 1998). The main topics of contents are Mining and Geotechnology, Metallurgy and Materials, Geology and Geoenvironment.

RMZ-M&G publishes original Scientific articles, Review papers, Preliminary notes, Professional papers **in English**. In addition, evaluations of other publications (books, monographs,...), In memoriam, Professional remarks and reviews are welcome. The Title, Abstract and Key words in Slovene will be included by the author(s) or will be provided by the referee or the Editorial Office.

* Additional information and remarks for Slovenian authors:
Only Professional papers, Publications notes, Events notes, Discussion of papers and In memoriam, will be exceptionally published in the Slovenian language.

Authorship and originality of the contributions. Authors are responsible for originality of presented data, ideas and conclusions as well as for correct citation of data adopted from other sources. The publication in RMZ-M&G obligate authors that the article will not be published anywhere else in the same form.

Specification of Contributions

RMZ-M&G will publish papers of the following categories:

<u>Full papers</u> *(optimal number of pages is 7 to 15, longer articles should be discussed with Editor prior to submission). An abstract is required.*
- **Original scientific papers** represent unpublished results of original research.
- **Review papers** summarize previously published scientific, research and/or expertise articles on the new scientific level and can contain also other cited sources, which are not mainly result of author(s).

- **Preliminary notes** represent preliminary research findings, which should be published rapidly.
- **Professional paper**s are the result of technological research achievements, application research results and information about achievements in practice and industry.

Short papers (the number of pages is limited to 1 for Discussion of papers and 2 pages for Publication note, Event note and In Memoriam). No abstract is required for short papers.

- **Publication notes** contain author's opinion on new published books, monographs, textbooks, or other published material. A figure of cover page is expected.
- **Event notes** in which descriptions of a scientific or professional event are given.
- **Discussion of papers (Comments)** where only professional disagreements can be discussed. Normally the source author(s) reply the remarks in the same issue.
- **In memoriam** (a photo is expected).

Supervision and review of manuscripts. All manuscripts will be supervised. The referees evaluate manuscripts and can ask authors to change particular segments, and propose to the Editor the acceptability of submitted articles. Authors can suggest the referee but Editor has a right to choose another. **The name of the referee remains anonymous.** The technical corrections will be done too and authors can be asked to correct missing items. The final decision whether the manuscript will be published is made by the Editor in Chief.

The Form of the Manuscript

The manuscript should be submitted as a complete hard copy including figures and tables. The figures should also be enclosed separately, both charts and photos in the original version. In addition, all material should also be provided in electronic form on a diskette or a CD. The necessary information can conveniently also be delivered by E-mail.

Composition of manuscript is defined in the attached Template

The original file of Template is available on RMZ-Materials and Geoenvironment Home page address:

http://www.rmz-mg.com

References - can be arranged in two ways:
- first possibility: alphabetic arrangement of first authors - in text: (Borgne, 1955), or
- second possibility: [1] numerated in the same order as cited in the text: example[1]

Format of papers in journals:

> LE BORGNE, E. (1955): Susceptibilite magnetic anomale du sol superficiel. *Annales de Geophysique*, 11, pp. 399–419.

Format of books:

> ROBERTS, J. L. (1989): Geological structures, *MacMillan*, *London*, 250 p.

Text on the hard print copy can be prepared with any text-processor. The electronic version on the diskette, CD or E-mail transfer should be in MS Word or ASCII format.
Captions of figures and tables should be enclosed separately.
Figures (graphs and photos) and tables should be original and sent separately in addition to text. They can be prepared on paper or computer designed (MSExcel, Corel, Acad).
Format. Electronic figures are recommended to be in CDR, Al, EPS, TIF or JPG formats. Resolution of bitmap graphics (TIF, JPG) should be at least 300 dpi. Text in vector graphics (CDR, Al, EPS) must be in MSWord Times typography or converted in curves.
Color prints. Authors will be charged for color prints of figures and photos.
Labeling of the additionally provided material for the manuscript should be very clear and must contain at least the lead author's name, address, the beginning of the title and the date of delivery of the manuscript. In case of an E-mail transfer the exact message with above asked data must accompany the attachment with the file containing the manuscript.

Information about RMZ-M&G:
Editor in Chief prof. dr. Peter Fajfar (phone: ++386 1 4250-316) or
Secretary Barbara Bohar Bobnar, univ. dipl. ing. geol. (phone: ++386 1 4704-630),
Aškerčeva 12, 1000 Ljubljana, Slovenia
or at E-mail addresses:
peter.fajfar@ntf.uni-lj.si,
barbara.bohar@ntf.uni-lj.si

Sending of manuscripts. Manuscripts can be sent by mail to the **Editorial Office** address:
- RMZ-Materials & Geoenvironment
  Aškerčeva 12,
  1000 Ljubljana, Slovenia
or delivered to:
- **Reception** of the Faculty of Natural Science and Engineering (for RMZ-M&G)
  Aškerčeva 12,
  1000 Ljubljana, Slovenia
- E-mail - addresses of Editor and Secretary
- You can also contact them on their phone numbers.

These instructions are valid from August 2009

NAVODILA AVTORJEM

RMZ-MATERIALS AND GEOENVIRONMENT (RMZ- Materiali in geookolje) – kratica RMZ-M&G - je revija (ustanovljena kot zbornik 1952 in preimenovana v revijo RMZ-M&G 1998), ki izhaja vsako leto v štirih zvezkih. V reviji objavljamo prispevke s področja rudarstva, geotehnologije, materialov, metalurgije, geologije in geookolja.

RMZ- M&G objavlja izvirne znanstvene, pregledne in strokovne članke ter predhodne objave samo v angleškem jeziku. Strokovni članki so lahko izjemoma napisani v slovenskem jeziku. Kot dodatek so zaželene recenzije drugih publikacij (knjig, monografij …), nekrologi In Memoriam, predstavitve znanstvenih in strokovnih dogodkov, kratke objave in strokovne replike na članke objavljene v RMZ-M&G v slovenskem ali angleškem jeziku. Prispevki naj bodo kratki in jasni.

Avtorstvo in izvirnost prispevkov. Avtorji so odgovorni za izvirnost podatkov, idej in sklepov v predloženem prispevku oziroma za pravilno citiranje privzetih podatkov. Z objavo v RMZ-M&G se tudi obvežejo, da ne bodo nikjer drugje objavili enakega prispevka.

Vrste prispevkov

Optimalno število strani je 7 do 15, za daljše članke je potrebno soglasje glavnega urednika.
Izvirni znanstveni članki opisujejo še neobjavljene rezultate lastnih raziskav.
Pregledni članki povzemajo že objavljene znanstvene, raziskovalne ali strokovne dosežke na novem znanstvenem nivoju in lahko vsebujejo tudi druge (citirane) vire, ki niso večinsko rezultat dela avtorjev.
Predhodna objava povzema izsledke raziskave, ki je v teku in zahteva hitro objavo.
Strokovni članki vsebujejo rezultate tehnoloških dosežkov, razvojnih projektov in druge informacije iz prakse.
Recenzije publikacij zajemajo ocene novih knjig, monografij, učbenikov, razstav …(do dve strani; zaželena slika naslovnice in kratka navedba osnovnih podatkov - izkaznica).

In memoriam (do dve strani, zaželena slika).

Strokovne pripombe na objavljene članke ne smejo presegati ene strani in opozarjajo izključno na strokovne nedoslednosti objavljenih člankov v prejšnjih številkah RMZ-M&G. Praviloma že v isti številki avtorji prvotnega članka napišejo odgovor na pripombe.

Poljudni članki, ki povzemajo znanstvene in strokovne dogodke (do dve strani).

Recenzije. Vsi prispevki bodo predloženi v recenzijo. Recenzent oceni primernost prispevka za objavo in lahko predlaga kot pogoj za objavo dopolnilo k prispevku. Recenzenta izbere Uredništvo med strokovnjaki, ki so dejavni na sorodnih področjih, kot jih obravnava prispevek. Avtorji lahko sami predlagajo recenzenta, vendar si uredništvo pridržuje pravico, da izbere drugega recenzenta. **Recenzent ostane anonimen**. Prispevki bodo tudi tehnično ocenjeni in avtorji so dolžni popraviti pomanjkljivosti. Končno odločitev za objavo da glavni in odgovorni urednik.

Oblika prispevka

Prispevek predložite v tiskanem oštevilčenem izvodu (po možnosti z vključenimi slikami in tabelami) ter na disketi ali CD, lahko pa ga pošljete tudi prek E-maila. Slike in grafe je možno poslati tudi risane na papirju, fotografije naj bodo originalne.

Razčlenitev prispevka:

Predloga za pisanje članka se nahaja na spletni strani:

http://www.rmz-mg.com/predloga.htm

Seznam literature je lahko urejen na dva načina:
-po abecednem zaporedju prvih avtorjev ali
-po [1]vrstnem zaporedju citiranosti v prispevku.

Oblika je za oba načina enaka:
Članki:

> Le Borgne, E. (1955): Susceptibilite magnetic anomale du sol superficiel. *Annales de Geophysique*; Vol. 11, pp. 399–419.

Knjige:

    Roberts, J. L. (1989): Geological structures, *MacMillan*, *London*, 250 p.

Tekst izpisanega izvoda je lahko pripravljen v kateremkoli urejevalniku. Na disketi, CD ali v elektronskem prenosu pa mora biti v MS Word ali v ASCII obliki.

Naslovi slik in tabel naj bodo priloženi posebej. Naslove slik, tabel in celotno besedilo, ki se pojavlja na slikah in tabelah, je potrebno navesti v angleškem in slovenskem jeziku.

Slike (ilustracije in fotografije) in tabele morajo biti izvirne in priložene posebej. Njihov položaj v besedilu mora biti jasen iz priloženega kompletnega izvoda. Narejene so lahko na papirju ali pa v računalniški obliki (MS Excel, Corel, Acad).

Format elektronskih slik naj bo v EPS, TIF ali JPG obliki z ločljivostjo okrog 300 dpi. Tekst v grafiki naj bo v Times tipografiji.

Barvne slike. Objavo barvnih slik sofinancirajo avtorji

Označenost poslanega materiala. Izpisan izvod, disketa ali CD morajo biti jasno označeni – vsaj z imenom prvega avtorja, začetkom naslova in datumom izročitve uredništvu RMZ-M&G. Elektronski prenos mora biti pospremljen z jasnim sporočilom in z enakimi podatki kot velja za ostale načine posredovanja.

Informacije o RMZ-M&G: urednik prof. dr. Peter Fajfar, univ. dipl. ing. metal. (tel. ++386 1 4250316) ali tajnica Barbara Bohar Bobnar, univ. dipl. ing. geol. (tel. ++386 1 4704630), Aškerčeva 12, 1000 Ljubljana
ali na E-mail naslovih:
peter.fajfar@ntf.uni-lj.si
barbara.bohar@ntf.uni-lj.si

Pošiljanje prispevkov. Prispevke pošljite priporočeno na naslov **Uredništva:**
- RMZ-Materials and Geoenvironment
  Aškerčeva 12,
  1000 Ljubljana, Slovenija
oziroma jih oddajte v
- **Recepciji** Naravoslovnotehniške fakultete (pritličje) (za RMZ-M&G)
  Aškerčeva 12,
  1000 Ljubljana, Slovenija
- Možna je tudi oddaja pri uredniku oziroma pri tajnici.

Navodila veljajo od avgusta 2009.

TEMPLATE

The title of the manuscript should be written in bold letters (Times New Roman, 14, Center)

Naslov članka (Times New Roman, 14, Center)

Name Surname[1], …. , & Name Surname[x] (Times New Roman, 12, Center)

[x] University of ..., Faculty of ..., Address…, Country ... (Times New Roman, 11, Center)

*Corresponding author. E-mail: ... (Times New Roman, 11, Center)

Abstract (Times New Roman, Normal, 11): The abstract should be concise and should present the aim of the work, essential results and conclusion. It should be typed in font size 11, single-spaced. Except for the first line, the text should be indented from the left margin by 10 mm. The length should not exceed fifteen (15) lines (10 are recommended).

Izvleček (Times New Roman, navadno, 11): Kratek izvleček namena članka ter ključnih rezultatov in ugotovitev. Razen prve vrstice naj bo tekst zamaknjen z levega roba za 10 mm. Dolžina naj ne presega petnajst (15) vrstic (10 je priporočeno).

Key words: a list of up to 5 key words (3 to 5) that will be useful for indexing or searching. Use the same styling as for abstract.

Ključne besede: seznam največ 5 ključnih besed (3–5) za pomoč pri indeksiranju ali iskanju. Uporabite enako obliko kot za izvleček.

INTRODUCTION (TIMES NEW ROMAN, BOLD, 12)

Two lines below the keywords begin the introduction. Use Times New Roman, font size 12, Justify alignment.

There are two (2) admissible methods of citing references in text:

1. by stating the first author and the year of publication of the reference in the parenthesis at the appropriate place in the text and arranging the reference list in the alphabetic order of first authors; e.g.:
   "Detailed information about geohistorical development of this zone can be found in: ANTONIJEVIĆ (1957), GRUBIĆ (1962), ..."
   "… the method was described previously (HOEFS, 1996)"
2. by consecutive Arabic numerals in square brackets, superscripted at the appropriate place in the text and arranging the reference list at the end of the text in the like manner; e.g.:
   "... while the portal was made in Zope environment. [3]"

MATERIALS AND METHODS (TIMES NEW ROMAN, BOLD, 12)

This section describes the available data and procedure of work and therefore provides enough information to allow the interpretation of the results, obtained by the used methods.

RESULTS AND DISCUSSION (TIMES NEW ROMAN, BOLD, 12)

Tables, figures, pictures, and schemes should be incorporated in the text at the appropriate place and should fit on one page. Break larger schemes and tables into smaller parts to prevent extending over more than one page.

CONCLUSIONS (TIMES NEW ROMAN, BOLD, 12)

This paragraph summarizes the results and draws conclusions.

Acknowledgements (Times New Roman, Bold, 12, Center - optional)

This work was supported by the ****.

References (Times New Roman, Bold, 12)

In regard to the method used in the text, the styling, punctuation and capitalization should conform to the following:

FIRST OPTION - in alphabetical order

Casati, P., Jadoul, F., Nicora, A., Marinelli, M., Fantini-Sestini, N. & Fois, E. (1981): Geologia della Valle del'Anisici e dei gruppi M. Popera - Tre Cime di Lavaredo (Dolomiti Orientali). *Riv. Ital. Paleont.*; Vol. 87, No. 3, pp. 391–400, Milano.

Folk, R. L. (1959): Practical petrographic classification of limestones. *Amer. Ass. Petrol. Geol. Bull.;* Vol. 43, No. 1, pp. 1–38, Tulsa.

SECOND OPTION - in numerical order

[1] Trček, B. (2001): *Solute transport monitoring in the unsaturated zone of the karst aquifer by natural tracers.* Ph. D. Thesis. Ljubljana: University of Ljubljana 2001; 125 p.

[2] Higashitani, K., Iseri, H., Okuhara, K., Hatade, S. (1995): Magnetic Effects on Zeta Potential and Diffusivity of Nonmagnetic Particles. *Journal of Colloid and Interface Science, 172*, pp. 383–388.

Citing the Internet site:

CASREACT-Chemical reactions database [online]. Chemical Abstracts Service, 2000, updated 2. 2. 2000 [cited 3. 2. 2000]. Accessible on Internet: http://www.cas.org/CASFILES/casreact.html.

Texts in Slovene (title, abstract and key words) can be written by the author(s) or will be provided by the referee or by the Editorial Board.

PREDLOGA ZA SLOVENSKE ČLANKE

Naslov članka (Times New Roman, 14, Na sredino)

The title of the manuscript should be written in bold letters (Times New Roman, 14, Center)

Ime Priimek[1], …, Ime Priimek[X] (Times New Roman, 12, Na sredino)

[X]Univerza…, Fakulteta…, Naslov…, Država… (Times New Roman, 11, Center)

*Korespondenčni avtor. E-mail: ... (Times New Roman, 11, Center)

Izvleček (Times New Roman, Navadno, 11): Kratek izvleček namena članka ter ključnih rezultatov in ugotovitev. Razen prve j bo tekst zamaknjen z levega roba za 10 mm. Dolžina naj ne presega petnajst (15) vrstic (10 je priporočeno).

Abstract (Times New Roman, Normal, 11): The abstract should be concise and should present the aim of the work, essential results and conclusion. It should be typed in font size 11, single-spaced. Except for the first line, the text should be indented from the left margin by 10 mm. The length should not exceed fifteen (15) lines (10 are recommended).

Ključne besede: seznam največ 5 ključnih besed (3–5) za pomoč pri indeksiranju ali iskanju. Uporabite enako obliko kot za izvleček.
Key words: a list of up to 5 key words (3 to 5) that will be useful for indexing or searching. Use the same styling as for abstract.

Uvod (Times New Roman, Krepko, 12)

Dve vrstici pod ključnimi besedami se začne Uvod. Uporabite pisavo Times New Roman, velikost črk 12, z obojestransko poravnavo. Naslovi slik in tabel (vključno z besedilom v slikah) morajo biti v slovenskem jeziku.

Slika (Tabela) X. Pripadajoče besedilo k sliki (tabeli)

Obstajata dve sprejemljivi metodi navajanja referenc:

1. z navedbo prvega avtorja in letnice objave reference v oklepaju na ustreznem mestu v tekstu in z ureditvijo seznama referenc po abecednem zaporedju prvih avtorjev; npr.:

   "Detailed information about geohistorical development of this zone can be found in: Antonijević (1957), Grubić (1962), ..."

   "… the method was described previously (Hoefs, 1996)"

ali

2. z zaporednimi arabskimi številkami v oglatih oklepajih na ustreznem mestu v tekstu in z ureditvijo seznama referenc v številčnem zaporedju navajanja; npr.;

   "... while the portal was made in Zope[3] environment."

Materiali in metode (Times New Roman, Krepko, 12)

Ta del opisuje razpoložljive podatke, metode in način dela ter omogoča zadostno količino informacij, da lahko z opisanimi metodami delo ponovimo.

Rezultati in razprava (Times New Roman, Krepko, 12)

Tabele, sheme in slike je treba vnesti (z ukazom Insert, ne Paste) v tekst na ustreznem mestu. Večje sheme in tabele je po treba ločiti na manjše dele, da ne presegajo ene strani.

Sklepi (Times New Roman, Krepko, 12)

Povzetek rezultatov in sklepi.

Zahvale (Times New Roman, Krepko, 12, Na sredino - opcija)

Izvedbo tega dela je omogočilo ………

VIRI (TIMES NEW ROMAN, KREPKO, 12)

Glede na uporabljeno metodo citiranja referenc v tekstu upoštevajte eno od naslednjih oblik:

PRVA MOŽNOST (priporočena) - v abecednem zaporedju

CASATI, P., JADOUL, F., NICORA, A., MARINELLI, M., FANTINI-SESTINI, N. & FOIS, E. (1981): Geologia della Valle del'Anisici e dei gruppi M. Popera – Tre Cime di Lavaredo (Dolomiti Orientali). *Riv. Ital. Paleont.*; Vol. 87, No. 3, pp. 391–400, Milano.

FOLK, R. L. (1959): Practical petrographic classification of limestones. *Amer. Ass. Petrol. Geol. Bull.;* Vol. 43, No. 1, pp. 1–38, Tulsa.

DRUGA MOŽNOST - v numeričnem zaporedju

[1] TRČEK, B. (2001): *Solute transport monitoring in the unsaturated zone of the karst aquifer by natural tracers.* Ph. D. Thesis. Ljubljana: University of Ljubljana 2001; 125 p.

[2] HIGASHITANI, K., ISERI, H., OKUHARA, K., HATADE, S. (1995): Magnetic Effects on Zeta Potential and Diffusivity of Nonmagnetic Particles. *Journal of Colloid and Interface Science, 172*, pp. 383–388.

Citiranje spletne strani:
CASREACT-Chemical reactions database [online]. Chemical Abstracts Service, 2000, obnovljeno 2. 2. 2000 [citirano 3. 2. 2000]. Dostopno na svetovnem spletu: http://www.cas.org/CASFILES/casreact.html.

Znanstveni, pregledni in strokovni članki ter predhodne objave se objavijo v angleškem jeziku. Izjemoma se strokovni članek objavi v slovenskem jeziku.

Skupina hse

PREMOGOVNIK VELENJE
V E L E N J E

PREMOGOVNIK VELENJE
je pomemben in zanesljiv člen
v oskrbi Slovenije
z električno energijo.

Zavedamo se odgovornosti do
lastnikov, zaposlenih in okolja.

ČUT ZA PRIHODNOST

IRGO

Inženirska geologija
Hidrogeologija
Geomehanika
Projektiranje
Tehnologije za okolje
Svetovanje in nadzor